Technical university of Liberec

Faculty of Textile Engineering

DIPLOMA THESIS

2012 **PAUL SICELO NGCOBO**

Technical University of Liberec

Faculty of Textile Engineering

Department of Textile Chemistry

Effects of temperature on sorption process using nanofibrous membrane

Paul S. Ngcobo

Supervisor: Assoc. prof. Jakub Wiener, MSc. PhD.

Consultant: Jana Šašková, MSc.

Number of pages: 104

Number of figures: 23

Number of tables: 24

Number of graphs: 30

Number of Appendices: 2

Statement

I have been informed that my thesis is fully applicable to the Act No. 121/2000 Coll. about copyright, especially §60 - school work.

I acknowledge that Technical University of Liberec (TUL) does not breach my copyright when using my thesis for internal need of TUL.

Shall I use my thesis or shall I award a licence for its utilisation, I acknowledge that I am obliged to inform TUL about this. TUL has right to claim expenses incurred for this thesis up to amount of actual full expenses.

I have elaborated the thesis alone utilising listed literature and on the basis of consultations with supervisor.

Date: 09 May 2012

Signature:

Acknowledgements

I would first like to sincerely acknowledge and thank my supervisor Prof. Jakub Wiener with his technical skills and experience, none of this work would have been possible without him, and also like to thank Ing. Jana Šašková for her support in this project. I would also like to thank God for giving me oxygen and enough strength to overcome Izinxushunxushu and problems. My family has been a great inspiration to me, especially my son uSelesele and not to forget my wonderful parents, Pastor. M.A Ngcobo and Ms T.S Ntshangase, and the rest of the family.

I would also like to acknowledge the Kwa-Zulu Natal Department of Economic Development for funding my studies (namabhanoyi), lastly, to thank the Technical University of Liberec academic staff to share their valuable information and skills to make me a better person……..

Abstract

The release of dyes into the environment only contributes a small proportion of water pollution but due to dye brilliance, they are visible even in very small quantities such that the control of water pollution has become of high importance nowadays. Government legislations are therefore forcing dye using industries to treat their effluent to high standards. Colour removal by conventional treatment methods such as ozonation, bleaching, hydrogen peroxide/UV, electrochemical techniques are not adequate due to the fact that most textile dyes have complex aromatic molecular structures that resist degradation. The research has shown that the use of membrane filtration can be an alternative for low cost treatment methods. In this study membrane made of electrospun polyamide 6 nanofibres is used in order to investigate the effects of increasing temperature on dye removal (sorption) using sorption filtration method. C.I Acid blue 41, C.I Acid yellow 42 and C.I Acid blue 78 were used to determine the accumulated mass of each on the electrospun polyamide 6 nanofibre membrane, using the temperatures of between 20 ^{0}C and 60 ^{0}C. The accumulated mass could decrease with the increase in temperature till the glass transition temperature of the membrane such that above this temperature the accumulation of dye was increased. All the results were based on spectrophotometric analysis and also the SEM was used for image analysis in order to analyze the effects of increasing temperature on the surface of the membrane. All the dyes tested could follow the Langmuir isotherm such that the curves for the experiments and the ones for Langmuir isotherm were comparable with very small differences. The results also show that C.I Acid Blue 41 had the highest values of sorption capacity compared to Acid Blue 78 and Acid Yellow 42, this was because of the highest saturation value (S) compared to the other two. Determination of sorption capacity at equilibrium was tested after a period of 10 days with increasing mass of fibre from 1 piece up to 10 pieces of 30mm x 30mm nanofibrous membrane with constant concentration and volume of solutions used.

Table of contents

List of tables

List of Figures

List of Abbreviations

T_g: Glass transition temperature (^0C)
C : Concentration (mg/L) Or (g/L)
m : Mass
V : Volume
C_L: Concentration of the liquor (filtrate)
C_{L0}: Original concentration of before filtration (0.01g/l)
A_t : Absorbance after filtration (or after sorption)
A_0 : Original absorbance of the dye solution before filtration.
m_0 : Original mass before filtration (0.1 mg)
m_L : Mass after filtration = C_L* V
A_f : Area of the funnel
ρ_f : Areal density of fibres
m_f : Mass of fibre
m_d : Mass of dye
%E: Percentage Exhaustion
Cs: Sorption capacity, mass of dye/mass of fibre (mg/g)
D_P : Pore size
γ : Surface tension of mercury
θ : Surface contact angle of mercury on capillary surface
P : Applied pressure
Y : Amount of adsorption
S: Maximum adsorption of dye, saturation (mg/g)
K: Affinity between sorbate and sorbent (L/g)
N(Q): Number of sites
α,*n* : constants
ΔG: Gibbs free energy ($J.mol^{-1}$)
ΔH: Enthalpy ($J.mol^{-1}$)
T : Temperature (K)
ΔS: Entropy ($J.mol^{-1}.K^{-1}$)
D : Diffusion coefficient
J : Penetration Flux

1. Introduction

Industrialization and urbanization have contributed a greater proportion in rapid deterioration of water quality. The scientific evidences and researches prove that the effluents released from different industries e.g. textile, leather, paint, etc. consist of hazardous toxic compounds some of which are known carcinogens and others probable carcinogens [5][2]. Textile industries especially those involved in finishing processes are major water consumers and the source of considerable pollution. The environmental challenge for the textile industry is associated with liquid waste, that results in the domination over air-emissions and solid wastes in terms of the severity of environmental impact [5][1]. A typical textile company or industry generates various types of wastewater that differ in quality and also in magnitude such that the waste water from printing and dyeing units are normally reach in colour, together with the residual of reactive dyes and chemicals, therefore a proper treatment before releasing to the environment is necessary [5][1][2]. Other industries that make use of dyes are paper, printing, plastic, paint, cosmetic food, pharmaceutical and petrochemical [1]. Release of some dyes in water streams results in a serious environmental impacts, many of the dyes cause health problems such as allergic dermatitis, cancer, skin irritation and also mutation in humans [2][1].

In addition, Over and above, dyes absorb sunlight within water media resulting in the prevention of photosynthesis of aquatic plants. For the above mentioned reasons, the removal of dyes from wastewater became of great importance and attracted a large number of research activities [1][2]. Increasing colour concentrations makes the water unfit for domestic or industrial uses, by reducing transmittance, dyes limit plant growth and self-purification processes. In addition they exert an adverse effect on fish life [2]. Colour removal by conventional treatment methods such as ozonation, bleaching, hydrogen peroxide/UV, electrochemical techniques are not adequate due to the fact that most textile dyes have complex aromatic molecular structures that resist degradation [2][1]. These dyes are stable to light, oxidizing agents and aerobic digestion. For these reasons the need for more efficient treatment processes has attracted the attention to pressure-driven membrane techniques. Membrane filtration not only enables high removal efficiencies, but also allows reuse of water and some of the valuable waste constituents (specifically dyes). Ultrafiltration has been successfully applied for recycling of high molecular weight and insoluble dyes (e.g disperse), auxiliary chemicals (polyvinyl alcohol) and water [2].

However, ultrafiltration does not remove low molecular weight and soluble dyes (acid, direct, reactive and basic) but efficient colour removal has been achieved by nanofiltration. Because of the sensitivity of membranes to fouling, adsorption finds application in tertiary wastewater treatment as a polishing step before the final discharge [2]. The nanofiltration

(NF) membrane is a pressure-driven membrane with properties in between reverse osmosis (RO) and ultrafiltration (UF) membranes. There are several advantages associated with the use of NF such as high flux, high retention of molecules, low operational pressure, low investment and low maintenance costs [5].

The membranes that will be in use during the investigation will be the polyamide 6 electrospun nanofibers, there are a number of reasons as to why one should use these electrospun membranes. Firstly, one of the most significant characteristic of nanofibers is the enormous availability of surface area per unit mass or rather large surface area-to-volume ratio up to 10^5 compared to the standard fibers [9][8]. The electrospun nanofibrous membrane reflects controlled liquid evaporation, excellent oxygen permeability and promoted fluid drainage capacity at the same time inhibiting oxygenous microorganism invasion because it possesses ultrafine pores, to mention a few [9].

Furthermore, in this study the principles of sorption filtration are applied, this incorporates both the adsorption and the diffusion of dye particles through the nanofibrous membrane. The changes in temperature have major effects on adsorption and dye retention during nanofiltration. An increase in temperature results in a decrease in the retention until a critical temperature of the membrane is exceeded. As a result after this temperature the flux decreases and the retention is increased [24]. The aim of the study was to investigate this behaviour for nylon 6 nanofibrous membrane.

2. Literature review

Polyamide 6 nanofiber production from caprolactam monomer

2.1 Basic information about nylon (polyamide)

The introduction of nylon opened the door for all kinds of the novel products this is because of its unprecedented material properties, it was the world's first synthetic fiber and engineering plastic. It can be considered as the first synthetic semi-crystalline polymer that is not temperature sensitive compared to the other polymers [25]. The most noticeable feature of most polyamides is that over a large temperature range and chemically hash environments, they withstand high loads and tension for extended periods of time. The well-known examples of the first nylon products were toothbrushes, parachutes and panties, and the latter is well witnessed by the fact that the panties are also called nylons which reflects the impact of the nylon on the society. At the beginning, the term nylon only covered linear, aliphatic chains with regular repeating amide functionalities, -C(=O)-NH-, nowadays the term nylon is applied when referring to aliphatic and semi-aromatic polyamides [25]. Polyamides can be divided into two major groups, namely AB- or AABB-type depending on the monomer used. AB-type polyamides are homopolymers with only one amide bond per repeating unit whereas AABB-type polymers are alternating copolymers with two amide bonds per repeating unit, the major representative for AB-type is Nylon 6 and Nylon 6,6 is a major representative of the AABB-type polyamides. Nylon 6 was developed by Dr. Paul Schlack at I.G. Farben on 28 January 1938 and Nylon 6,6 by Wallace Carrothers at DuPont. Together, Nylon 6 and Nylon 6,6 account for more than 95 % of the total amount of nylon used in the world in which Nylon 6 is responsible for 59% of this quantity [32]. The future survival of nylons is determined by the continuous innovation of properties, improvements of the quality, reduction of environmental impact of both monomer and polymer synthesis and lastly, the reduction of production costs [25][32].

2.2 Production of polyamide 6 from caprolactam

Hydrolytic ring opening polymerization of caprolactam

The production of nylon 6 results from the use of the monomer called 6-aminocaproic acid also known as ε-caprolactam or just caprolactam. Caprolactam (CL) is itself produced by the chemical reaction called Beckman rearrangement after heating cyclohexanonoxim in sulfuric acid[32]. There are several polymerization techniques for the polymerization of caprolactam that exist but the most commonly used method is the *hydrolytic ring opening polymerization* of caprolactam and this will be discussed in details in this review. The process makes the use of the VK tube (abbreviation for the German expression "vereinfacht kontinuierlich" which is interpreted as "simplified continuous", a vertical flow pipe that is

heated. The hydrolytic ring opening polymerization consists of three equilibrium reactions. First in the Initiation of polymerization that proceeds by the hydrolysis of small amount of present caprolactam, the molten caprolactum consisting of 0.3-5% of water is used. The figure below shows the initiation of polymerization and the electron transfer between water and caprolactam to produce the first equilibrium that results in a ring opening of the caprolactam.

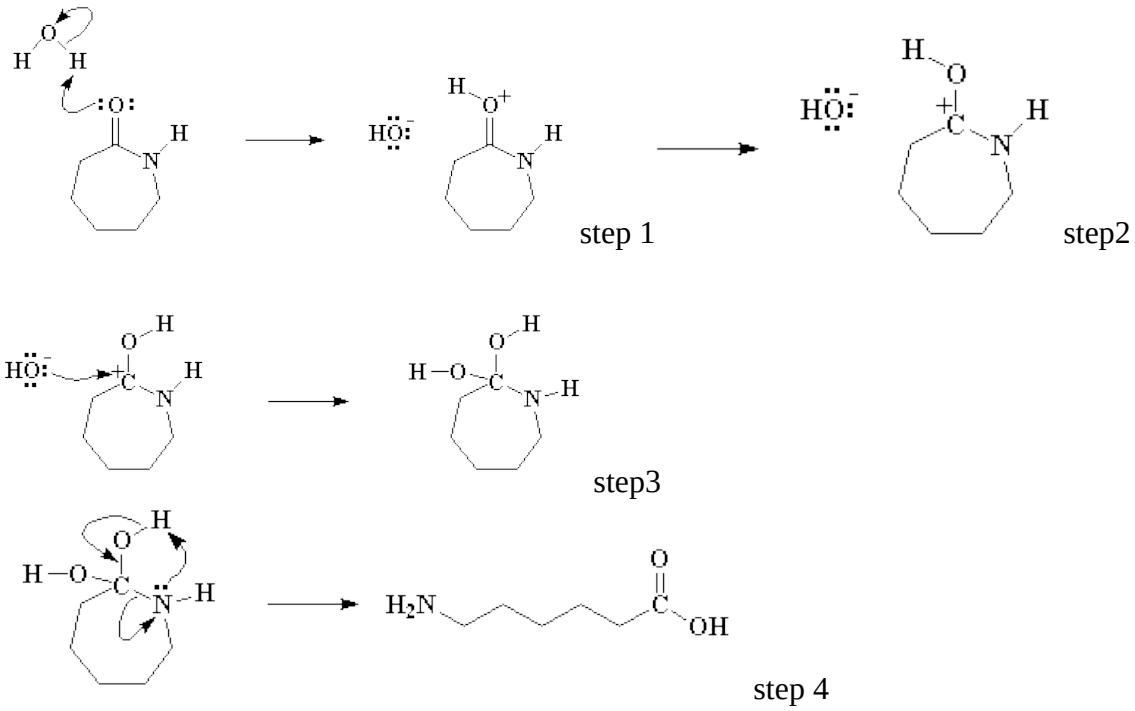

Figure 1: The rearrangement of molecules during the reaction [32][13].

In the first step of the reaction the carbonyl extracts a proton from nearby water molecule resulting in a protonated carbonyl and a free hydroxyl group. The positively charged carbonyl is not stable therefore swipes a pair of electrons from the carbonyl double bond, leaving the positive charge on the carbonyl carbon atom (carbocation) in step 2 above. In the third step the hydroxyl ion attacks the carbocation resulting in an unstable diol. In the fourth step, because of the instability of the diol, the O-H bond is destroyed and relocated to form a carbonyl and the C-N bond replaces the pair of electrons that are used to form the N-H bond and this rearrangement results in a ring opening of the caprolactam resulting in a linear amino acid [32][13].

The second equilibrium is the direct addition of the caprolactam to the amine end-group of a growing chain and this increases the molar mass which also implies a ring opening polymerization of caprolactam. Consider the figure below that shows the second equilibrium resulting showing the reaction of the linear amino acid and the caprolactam. In the fifth step the caprolactam reacts in the same manner as it did with the water molecule, this time

leaving the anionic amino acid and the caprolactam itself with a positive carbonyl, this can further rearrange to form a carbocation like in step 2 above. The carbocation now reacts with the amino acid that is negatively charged to form a complex in step 6. The structure can now rearrange itself such that the oxygen atom bonds with the hydrogen, the double bond is now formed between C and O atom and the new bond between the C and H atom thus the structure produced is now stable (step 7 below) [25][13]. (refer to the figure below)

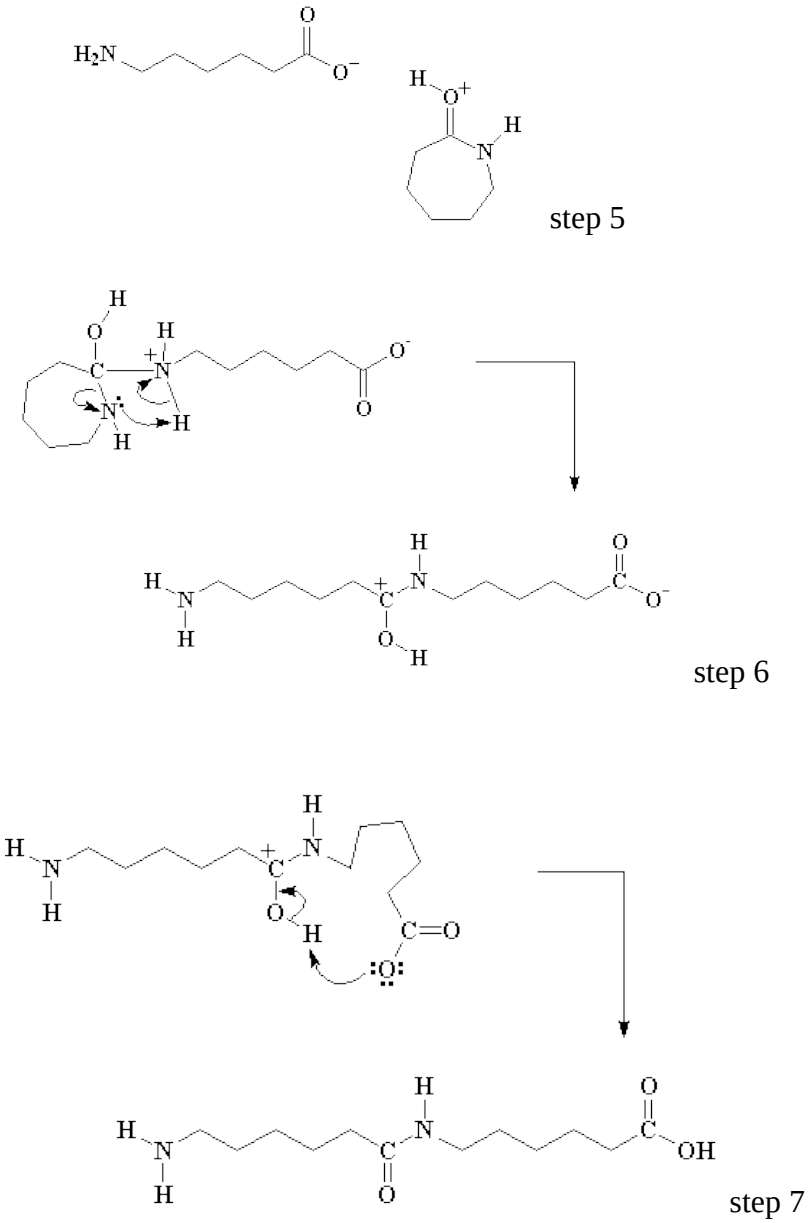

Figure 2: shows rearrangement of atoms during production of nylon 6 [25].

The third equilibrium is the condensation of two linear molecules that also results in an increase in molar mass this is shown in the figure below. A substantial availability of water is advantageous for the ring opening of caprolastam, but the removal of the same amount of water is required to promote the higher molar mass during the polycondensation [25].

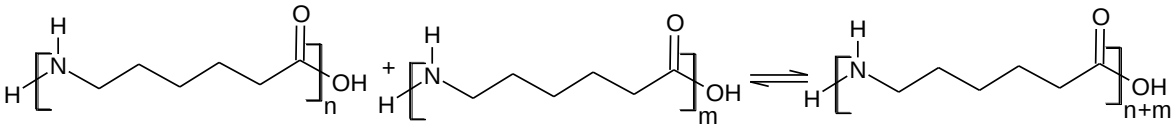

Figure 3: shows the overall reaction of nylon 6 production [25]

A minimum weight average molar mass of 15.000 – 20.000 g/mol is required in order to obtain nylon 6 with good properties and also that the conversion should be larger than 99.25% with complete selectivity for the condensation product starting with a pure monomer of 100% [25][32].
The synthesis of nylon 6 is accompanied by the production of the cyclic oligomers in the secoequilibrium shown by step 6 and 7 above, such that the amount of oligomers can increase to more than 10 wt% in the polymerization temperature of 280 °C resulting in a sticky product with inferior properties. As a result the nylon 6 has to be purified always by extraction after polymerization resulting in the space consumed by extraction unit being larger than the polymerization unit itself and thus higher operational costs are involved [25][32]. Therefore the commercial production of nylon 6 involves a two-step continuous process such that in the first step a small amount of the caprolactam is hydrolytically ring-opened followed by the direct ring opening polymerization of caprolactam whereby 85% of the monomer is converted into pre-polymer. The vertical reactor is used for further condensation in which the polymer moves slowly down under temperatures between 250 ^{0}C and 270 ^{0}C resulting in an increase of viscosity. The polymer strand is crystallized (cooled down) in water and cut into chips that are finally sent to warm water extractor that removes the low molecular weight products and monomer from the final product [25].

2.3 Electrospinning Process

The chips of nylon 6 that are produced from caprolactam by hydrolytic ring opening polymerization are further processed to nanofibers by the process called electrospinning. This process will be discussed in details below.

2.3.1 What is electrospinning?

The electrospinning process was introduced by Formhals in 1934 wherein electrostatic force was used in an experimental setup for the production of polymer filaments. When fibers are spun this way, the process is termed electrospinning. Or this can be simplified as a process that creates nanofibers through an electrically charged jet of polymer solution or polymer melt [7]. Electrospinning can be considered as the cheapest and the most straight forward method of producing nanomaterials since the electrospun nanofibers are of indispensable importance for the economic and scientific revival of developing countries [9]. A good example to illustrate this is a pore structured electrospun nanofibrous membrane that is used as a wound dressing, promotes the exudation of fluid from the wound thus preventing wound desiccation or the build-up under the covering. The electrospun nanofibrous membrane reflects controlled liquid evaporation, excellent oxygen permeability and promotes fluid drainage capacity at the same time inhibiting oxygenous microorganism invasion because it possesses ultrafine pores [9].

2.3.2 Applications of electospun fibres

These materials can be used in nonwoven fabrics, reinforced fibres, support for enzymes, drug delivery systems, in the conduction of polymers and composites, fuel cells, photonics, wound dressing, sensorics, medicine, filtration, tissue engineering catalyst support, to mention just a few [9].

2.3.3 Electrospinning unit and creation of fibers during the process

The process is more or less the same as the process of producing polymer fibers of large diameter where by the molten polymer is drawn from the die and the polymer melt is dried to form individual strand of fiber. Electrospinning involves the drawing of polymer either in the form of polymer solution or molten polymer, in our case for the production of nylon 6, the latter will be discussed. Electospinning makes use of charges that are applied to the fluid to provide a stretching force to a collector where there is a potential gradient [7]. Normally the melt is kept in the syringe and the metal needle is charged with DC high voltage generator, creating the positive charge on the melt or polymer solution [9]. When sufficient high voltage is applied, polymer solution jet will erupt from a polymer solution droplet but the polymer chain entanglements within the melt will prevent the electrospinning jet from breaking up [7]. At this moment in time the fibers form what is so called the Taylor cone caused by the equilibrium between the electrostatic force of the charged surface and the surface tension such that a higher applied voltage leads to an elongated cone. The fibers cool down as they as travel though the atmosphere and approach the collector that is oppositely charged (see figure below) [7][9].

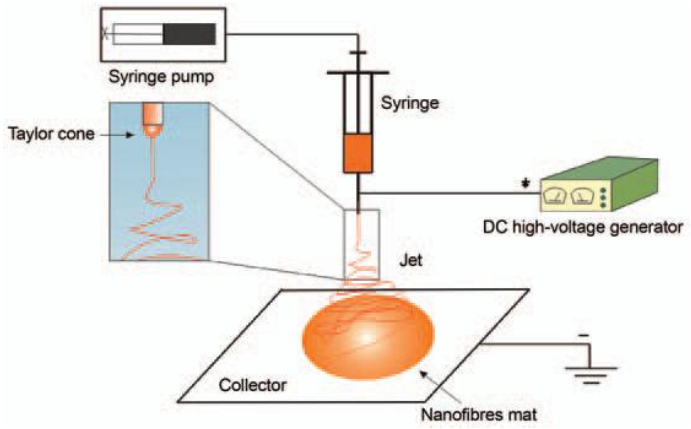

Figure 4: The electrospinning set-up that is mostly used with the Taylor cone

2.3.4 Important features of electrospinning

- The vapor pressure of the solvent should be suitable such that it evaporates quickly enough for the fiber to maintain its integrity when it reaches the target but should not be too quickly to allow the fiber to harden before it reaches the nanometer range [7].
- Suitable solvent should be available to dissolve the polymer.
- The viscosity and surface tension of the solvent must neither be too large to prevent the jet from forming nor be too small to allow the polymer solution to drain freely from the pipette.
- The power supply should be able to overcome the viscosity and surface tension of the polymer solution and sustain the jet from the pipette.
- The gap between the pipette and grounded surface should not be too small to create sparks between the electrodes but should be large enough for the solvent to be evaporated in time for the fibers to form [7].

2.3.5 Process conditions for electrospinning process

Various external factors exerting on the electrospinning jet are important parameters that affect the electrospinning process. The voltage supplied, the feed rate, the temperature of the solution, type of collector, the diameter of the needle and the distance between the needle tip and the collector are the most important factors that will be discussed in details in the following discussion [7][3].

- ***Voltage***

The application of the high voltage to the solution is a crucial element in electospinning process. The necessary charges on the solution are induced by high voltage together with the electric field that results in the initiation of the electrospinning process when the electrostatic force in the solution overcomes the surface tension of the solution [7]. In general, both high

negative or positive voltage of more than 6 kV is capable of causing solution drop at the tip of the needle for the distortion into a shape of a Taylor Cone during jet initiation. Higher voltage of the solution is also subjected to the feed rate of the solution in order to stabilize the Taylor Cone. The Columbic repulsive forces in the jet will then stretch the viscoelastic solution such that the higher amount of applied voltage results in the greater amount of charges that will cause faster acceleration of the jet, more volume of solution will be drawn to the tip of the needle, which may result in a smaller and less stable cone [7]. When the drawing to the collection plate is much faster than the supply from the source, the Taylor Cone may recede into the needle. Both the voltage supplied and the resultant electric field have an influence in the stretching and acceleration of the jet, they result in a greater influence on the morphology of the fibers obtained. For example, the use of the higher voltage causes the greater stretching of the solution due to the Columbic forces in the jet as well as electric field, thus a great effect in the reduction of fiber diameter [7][3].

- ***Feedrate***

The feedrate is the determination of the amount of solution available for electrospinning. For every given voltage there exists a corresponding federate for maintaining a stable Taylor cone [7]. There is a corresponding increase in the fiber diameter or beads size due to the increase in feedrate and a greater volume of solution that is drawn away from the needle tip, but this is also subjected to the certain limit. If the federate is the same as the flow rate of the solution carried away by the electrospinning jet, there must also be a corresponding increase in charges due to the increase in feedrate. Thus a corresponding increase in the stretching of the solution which encounters the increased diameter due to increased volume [7][3]. The jet will then take a longer time to dry due to the greater volume of solution drawn from the needle tip. As a result, the solvent in the deposited fibers may not have enough time to evaporate given the same flight time. Fussing together of fibers where they make contact forming webs results from the residual solvents [7][3]. As a result, a lower feedrate is more preferable as the solvent will have enough time to evaporate.

- ***Temperature***

The temperature has two major effects, namely increasing the evaporation rate and reduction of the polymer solution viscosity. At higher temperature the fibers produced have more uniform diameter due to the lower viscosity of the solution and greater solubility of the polymer in the solvent allowing an extended stretching of the solution [7][3]. The Columbic forces are able to exert a greater stretching force on the solution resulting in fibers of smaller diameter due to the lower viscosity of the solution [7][3]. The further stretching of the solution by the Columbic forces is also due to increased temperature that increases polymer molecules mobility. However, in cases where biological substances such as enzymes and

proteins are added to the solution for electrospinnig, the use of high temperatures may result in the loss of functionality of added biological substances [7][3].

- ***Effect of collector***

There electric field between the collector and the source is the minimum requirement for the electrospinning to initiate. In most electrospinning setup, the collector plate is made up of a conductive material such as aluminum foil which is electrically grounded in order to maintain a stable potential difference between the source and the collector [7]. In the case when the nonconducting material is used as a collector, charges on the jet accumulate quickly on the collector which results in fewer fibers deposited. Fibers collected on the non-conducting material usually possess a lower packing density compared to the ones collected on a conductive surface. This is the result of the repulsive forces of the accumulated charges on the collector as the number of deposited fibers is increased [7][3]. Charges on the fibers are dissipated for a conducting collector thus allowing more fibers to be attracted to the collector, the fibers therefore pack closely together as a result.

For a non-conductive collector, 3D fiber structures may result because of the accumulation of the charges due to the repulsive forces of like charges. If there is sufficient density of charges on the fiber mesh formed initially, the repulsion on the subsequent fibers my result in the formation of honeycomb structures [7][3]. This can however be the case even for the conductive collector when the deposition rate is high and the fiber mesh is thick enough resulting in a high accumulation of residual charges on the fiber mesh since polymer nanofibers are non-conductive in general. As a result, there is a formation of dimples on the fiber mesh as seen in the figure below.

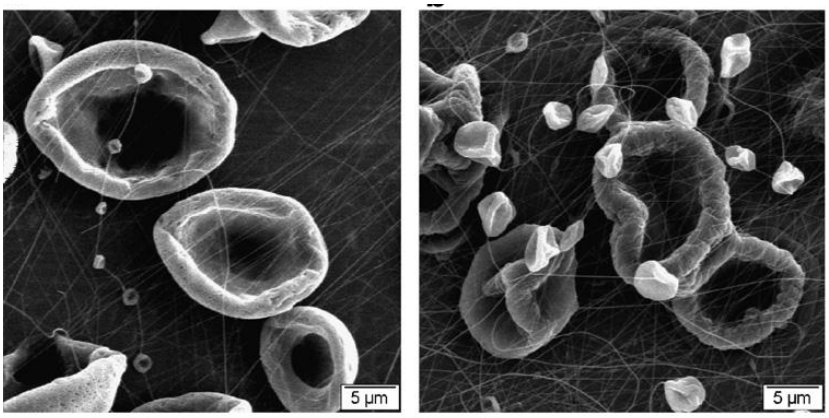

Figure 5: shows the images of the dimples [6]

The porosity of the collector also has an effect of the deposition of fibers. The experiments have shown that collectors that are porous like paper and metal mesh result in a collection of fiber mesh with lower packing density that the fiber collected using smooth surfaces such as metal foils [7][3]. In a porous target there is a faster evaporation of residual fibers because of

the higher surface area whereas smooth surfaces may cause an accumulation of solvents around the fibers due to slow evaporation rate. Therefore, due to the diffusion and wicking of the residual solvents on the fibers, the fibers are therefore pulled together to give a more densely packed structure [7]. As the fibers dry faster on a porous collector, it is more likely that the charges remain on the fibers which then repel subsequent fibers. However, in a smooth surface the delay of the solvent encourages the residual charges to be conducted away to the collector [7][3].

- ***Diameter of pipette orifice/needle***

The internal diameter of the needle or the pipette orifice has a certain effect on the electrospinning process. A smaller diameter reduces the clogging as well as the amount of beads on the electrospun fibers [7][3]. The reduction in clogging could be due to the less exposure to the atmosphere of the solution during the process. The decrease of the internal diameter of the orifice also results in the decrease of the diameter of the electrospun fibers. When the size of the droplet at the tip of the orifice is decreased, the surface tension of the droplet increases [7][3]. For the same applied voltage, a much greater Columbic force is required to cause jet initiation, and this results in the decrease of the jet acceleration and this allows more time for the solution to be stretched and elongated before the collection. However, if the diameter of the orifice is too small, it may not be possible to extrude a droplet of the solution from the tip of the orifice [7][3].

- ***Distance between tip and collector***

Varying the distance between the tip and the collector results in a direct influence in both the electric field strength and flight time. For the formation of independent fibers, the jet must be allowed time for most of the solvents to be evaporated. When the distance between the collector and the tip is reduced the jet will have a shorter distance to travel before reaching the collector plate, the electric field strength will also increase at the same time thus increasing the acceleration of the jet to the collector [7][3]. If the distance is too low, excess solvent may cause the fibers to merge where they contact to form junctions resulting in inter and intra layer bonding. The effects of varying the distance depend on the solution properties, it may or may not have a significant effect on the fiber morphology. The formation of beads may result if the distance is too low because of the increased field strength between the needle tip and the collector [7][3]. Decreasing the distance has the same effects as increasing the voltage supplied, both resulting in increased field strength. However, on the other hand increasing the distance results in the decrease of the average fiber diameter, the longer the distance results in a longer flight time for the solution to be stretched before it is deposited on the collector. If the distance is too large, there are no fibers that are deposited on the collector [7][3].

2.4 Pore size and porosity

Pores play a major role in the determination of the physical and the chemical properties of porous substrates and also have a deterministic effect on the performance of the membranes, therefore for the designation of the membrane's analysis of the pore size and distribution is vital [7][3]. In electrospun nanofibrous substrates there are two types of pores that are identified, namely, pores on or within each fiber and pores between fibers on a nanofibrous membrane. Pore size can be determined by the use of direct or indirect methods, direct methods includes the use of techniques such as electron microscope (SEM and TEM) or atomic force microscope (AFM). Indirect methods include bubble point measurements, solute retention challenge, extrusion porosimetry, molecular resolution porosimetry and intrusion porosimetry [7][3].

2.4.1 Pores on electrospun nanofibrous membrane

Consider the figure below, it shows the spaces between fibers that are possessed by the electrospun nanofibrous membrane. Through electrospinning a highly porous membrane is generated such that in separation technology, the knowledge of porosity and pore size is critical in the determination of the membranes performance. The importance of pore size is that it discriminates between the type (size or molecular weight) of species that can penetrate through and the ones that will be retained whereas the porosity determines the flux or flow across the membrane [7][3].

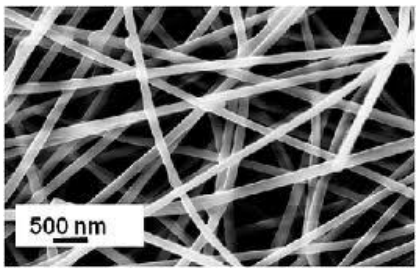

Figure 6: The pores on electospun nanofibrous membrane [7]

SEM can be used for the determination of the pore size of electrospun nanofibrous membranes but cannot be used for the determination of porosity. Further disadvantage is that only pores on the top surface can be analyzed while pores beneath the membrane surface cannot be directly determined [7][3]. Mercury porosimetry is the mostly adopted methodology used for membrane pore characterization.

2.4.2 Mercury porosimetry (intrusion porosimetry)

A sample is placed inside the cell that is then filled with mercury from a capillary, because mercury is a non-wetting liquid, there is no instantaneous filling of the sample pores. Due to

the application of pressure, the mercury penetrates into pores of a sample such that the largest pores get filled first and smaller pores are filled as a result of increasing pressure [7]. The figure bellow shows the mercury intrusion porosimeter apparatus.

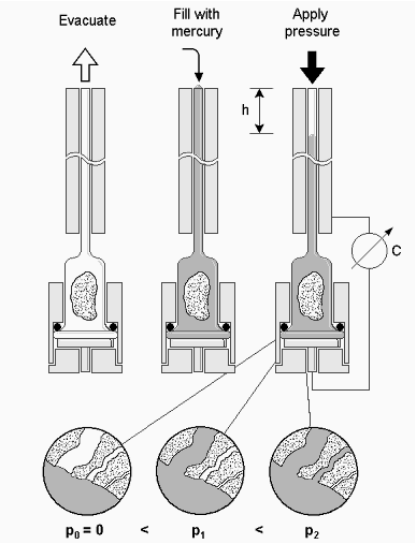

Figure 7: The principle of Mercury intrusion porosimetry [21]

Pore size (D_p) is calculated using the following equation:

$$D_p = -4\gamma\cos\theta/P \quad (1)$$

Where γ is the surface tension of mercury, θ is the surface contact angle of mercury on capillary surface and P is the applied pressure.

The biggest advantage of using the above method is that the total pore volume and the total pore area can also be determined in addition to the pore size and its distribution [7]. However a major drawback of using mercury is that it makes use of high pressures as the pore size diminishes and this can result in the membrane being destroyed, especially for the electrospun membranes the pores are dynamic in nature and are not rigid pores with self-supporting structures [7]. Therefore, for the successful analysis, thick samples are necessary such that if samples of less than 100nm are used they are destroyed by the pressure. In addition, the other drawbacks of using mercury are its cost and toxicity. Therefore it is possible to use any lower surface tension liquid in place of mercury, in principle any liquid that does not wet the membrane spontaneously can be used and should obey the abovementioned equation [7].

2.4.3 Extrusion porosimetry

Alternatively, instead of intrusion porosimetry, extrusion porosimetry can be employed, whereby the sample pores are filled with a wetting liquid. The differential pressure of a non-reacting gas is increased on the sample in order to displace the liquid from the pores, thereafter, the liquid is displaced from the pores and the sample is weighed. The above mentioned equation is also used to determine the pore diameter [7].

2.4.4 Structure of electrospun membranes

Using the electrospinning process it was demonstrated the ability to fabricate nanofibers of organic polymers with diameters as small as 3 nm. These molecular bundles, assembly themselves during electrospinning with only 6 or 7 molecules across the diameter of the fiber, and half of the 40 or so parallel molecules in the fiber are on the surface [8].

2.4.5 Tensile properties of electrospun nylon 6 single nanofibers

Electrospun nyon 6 nanofiber mats are found to exhibit:

- Tensile strength of 10.45 MPa
- Strain at break of 250%
- A 2% offset yield stress of 6.7 MPa
- Yield strain of 48%
- Young's modulus of 19.4 MPa, 56 times lower than that of an undrawn single nylon 6 filament, and 770 times lower than that of a conventional nylon 6 fiber.

The possible reasons for the low mechanical properties are because the molecular chains inside the electrospun fibers are not in good orientation along the fiber axis and due to the weak entanglement inside the nanofibrous mat [4].

2.4.6 Thermal properties and density of nylon 6

- Glass transition temperature: 47 ^{0}C
- Melting temperature: 220 ^{0}C
- Amorphous density at 25 ^{0}C: 1.084 g/cm^3
- Crystalline density at 25 ^{0}C: 1.23 g/cm^3
- Molecular weight of repeat unit: 113.16 g/mol

2.5 Introduction to nanotechnology

2.5.1 Background and definition of nanofibers

Nanofibers are solid state linear nanomaterials that are characterized by flexibility and also possess an aspect ratio greater than 1000:1. According to the National Science Foundation (NSF), nanomaterials are defined as matters that have at least one dimension equal to or less

than 100 nanometers which implies that nanofibers are fibers that have diameters equal to or less than 100 nm [8][7][9].

Thus, 1 nanometre = 1nm = 10^{-9} metre = 10^{-9} m, a single human hair is around 80,000 nm in width [7][8].

Materials that are in the fiber form are of great practical and fundamental importance because of the combination of high specific surface area, flexibility and superior directional strength that makes fibers a preferred material form for many applications ranging from reinforcement for aerospace to clothing [8]. Materials in nanometer scale with a fibrous structure are the fundamental building blocks of living systems. From the 1.5 nm double helix strands of DNA molecules to cytoskeleton filaments with diameters around 30 nm, to sensory cells and rod cells of the eyes nanoscale fibers form the extra-cellular matrices or the multifunctional structural backbone for tissues and organs. As a result, specific junctions between these cells conduct electrical and chemical signals that result from various kinds of stimulations. The signals function is to direct normal functions of the cells such as energy storage, tissue generation, sensing and information storage and retrieval [8].

2.5.2 Categories of nanotechnology

This sub-topic will try to classify nanofibers into one or more sub-category of nanotechnology, to do so it is wise to view each of the different common sub-fields of the nanotechnology itself. As far as "nanostructures" are concerned, they can be viewed as objects or structures whereby at least one of its dimensions is within nano-scale. A "nanoparticle" can be viewed as a zero-dimensional nano-element which is the simplest form of nanostructure. It follows that a "nanotube" or a "nanorod" can be considered as a one dimensional nano-element from which slightly more complex nanostructures can be constructed from. Following the same logical thought, a "nanoplatelet" or a "nanodisk" is a two-dimensional element which, along with its one-dimensional counterpart, is useful in the construction of nanodevices [7].

2.5.3 Surface area of nanofibers to that of standard fibers

One of the most significant characteristics of nanofibers is the enormous availability of surface area per unit mass or rather large surface area-to-volume ratio [9][8]. To illustrate this we consider a fibre of radius 1 mm and length of 10mm the surface area is:

$S = 2\pi rL = 2\pi x10^{-3}x10^{-2} = 2\pi x10^{-5}$ m^2 (S = surface area of the fiber, r = radius of the fiber and L = length of the fiber)

Now we divide the fibre into nanofibres with radius of 10 nm, the number of nanofibres can be calculated as:

$n = r^2/r_0^2$ (n = number of nanofibres, r = radius of standard fibre and r_0 = radius of nanofibre)

$= (10^{-3})^2/(10x10^{-9})^2$

$= 10^{-6}/10^{-16}$

$= 10^{10}$

So the total area of nanofibers is:

$S_0 = 2\pi n r_0 L = 2\pi x10^{10}x10^{-8}x10^{-2} = 2\pi\ m^2$

Therefore, the volume remains unchanged while the surface is increased by the following factor:

$S_0/S = 2\pi\ m^2/\ 2\pi x10^{-5}\ m^2$

$= 10^5$

For the fiber having the diameters ranging from 5 to 500 nanometers, the surface area per unit mass is around 10,000 to 1,000,000 square meters per kilogram. In nanofibers that are three nanometers in diameter, and which contain about 40 molecules, about half of the molecules are on the surface. The figure below illustrates the effect of the size on the surface area of the fibers, it shows that as the fiber diameter increases, the surface area of the fiber decreases [8].

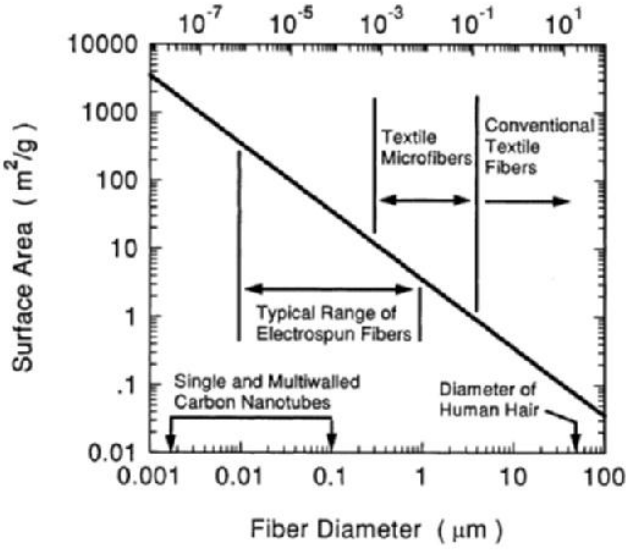

Figure 8: The effect of fiber diameter on the surface area of the fiber [8]

2.5.4 The future of nanotechnology

Future advancements in nanotechnology will be instigated by firstly, the improvements in electrospinning technology and process control to allow consistent production of nanofiber mats with single-digit fiber diameter and secondly, the potential to combine several physical, chemical and biological functionalities into a single fiber to perform multipurpose fiber mats and smart materials a reality [3]. The functionalities that are considered need to move beyond the simple passive effects of biocidal effectiveness (for instance incorporating nanosilver), super hydrophobicity by surface texturing or simple breathable wound dressings. Future nanofibers are predicted to be likely to deliver more advanced multiple functionalities and will likely be active devices that perhaps enable impressive disruptive technology. These are specifically, fabric-based computing/communications capabilities (integration of circuitry and transponders into nanofibers), disposable physiology/ environment monitoring in apparel (disposable sensors, alarms, and on-demand countermeasures integrated into fabric), rapid physiological testing arrays (automated or bedside clinical testing that is on demand) [3]. That was only to mention a few, there is a large room of improvement in the nanotechnology as the newer technologies are developed.

2.6 Acid dyes and their removal

2.6.1 Acid dyes

Acid dyes are anionic dyes along with direct dyes and reactive dyes. Acid dyes are used to dye protein fibers such as wool, silk, ingora, feathers etc and can be used even for dyeing man-made nylon, which is chemically similar to silk, these fibers all consist of proteins with animo groups $–NH_2$ [29][18]. Acid dyes are so called because they possess acidic molecular group such as $–SO_3H$ and work in a low pH environment with a mildly acidic “fixative” like white vinegar or citric acid. The bond between the dye and the fiber occurs between the basic amino groups and acidic groups. Acid dyes are thought to fix to fibers by hydrogen bonding, Van der Waals forces and ionic bonding [18]. The figure below illustrates the typical example of the anionic dye.

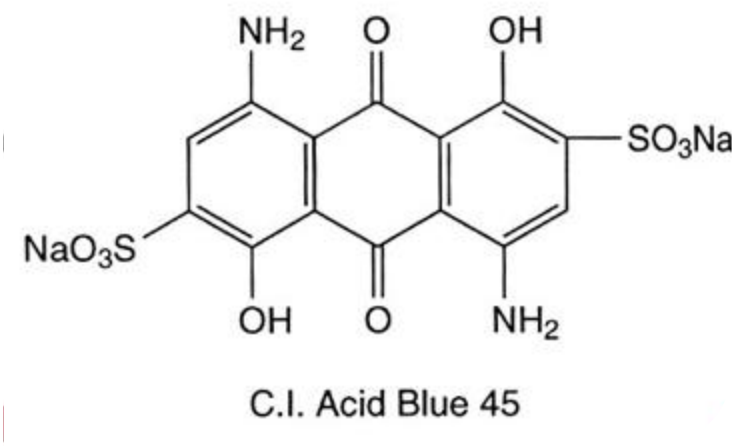

Figure 9: The structure of anionic dye structure of acid blue 45 [18]

These dyes are brightly coloured, and also water soluble making it most problematic to remove as they tend to pass through conventional treatment systems unaffected [29]. The municipal aerobic treatment systems, depend on biological activity, they are also inefficient in the removal of these dyes [29]. The table below shows some of the conventional methods that are used for dye removal and their disadvantages.

Table 1: Shows different methods and their disadvantages [29]

Physical or chemical method	**Disadvantage**
Fontons reagent	Sludge generation
Ozonation	Short half-life (20 min)
Photochemical	Formation of by-product
Activated carbon	Very expensive
Electrochemical destruction	High cost of elelctricity
Silica gel	Side reactions
Iron exchange	Not effective for all dyes

2.6.2 Acid dyes and polyamide

Below is the structure of polyamide 6 (nylon 6), it consists of the amino group of which under acidic conditions it possesses a free amine end group NH_3^+ that can then form the bond with the acid dyes [18][2].

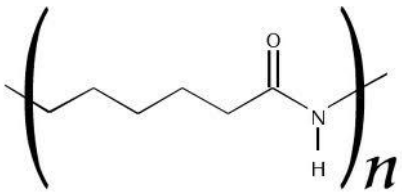

Figure 10: Shows the structure of the polyamide

The dye molecule is structured from two components the dye chromophore and the dye auxochrome. The chromophore includes a double bond (C=C) that is responsible for the colour of the dye due to the oscillation of the structure when the light is absorbed [2]. The second portion of the molecule is responsible for the bond between the fibre and the dye in the present case it is the sulphonic group. The dye is bound to the fibre through covalent and ionic bonding, Van der Waals forces and impregnation of colloidal dye particles into the fibre [2]. If the dye is applied in weakly acid conditions, the reaction with the fibre does not occur and dyeing is then obtained on treatment with the alkali such that reaction with the fibre takes place. Free amino groups in the nylon fibre provide reactive sites, but there is also some evidence that reactions may also occur with amide groups [2]. In the case of membranes, dyes are reactive towards the chemical functions present at the fibre surface, the same chemical functions that are found in the polymer surface used for the preparation of membranes.

2.6.3 Polyamide dye interaction and the isoelectric point

The following equations show the reaction schemes between the polyamide fibres and the acid dyes. Below the isoelectric point polyamide have a positive charge and can react with anionic dyes (acid dyes):

H_3N^+ – Polyamide – COOH + $DyeSO_3^-$ → $DyeSO_3^-$ H_3N^+ – Polyamide – COOH

In the above equation the ionic bond is formed between the dye and the positively charged polyamide.

Above the isoelectric point polyamide have a positive charge and can only react with cationic dyes:

H_2N – Polyamide – COO^- + Dye^+ → H_2N – Polyamide – COO^- Dye^+

In this case the bond is formed between the polyamide and the positively charged dye. At pH of 6 the membrane carries negative charges (COO^-) and positive charges at pH 3 (NH_3^+), this implies that, the interaction with the acid dyes is much lower at high pH because of the repulsion between the dye molecules and the surface of the membrane, whereas at lower pH the interaction is higher because of the attraction between the dye and the surface of the membrane [2].

2.7 Sorption process

Sorption can be described as a physical or chemical process by which one substance becomes attracted to another. This process is made up of two processes known as adsorption and absorption. Adsorption is the physical adherence or bonding of ions and molecules onto the surface of another phase (e.g. reagents adsorbed to a solid catalyst surface). Absorption is the incorporation of a substance in one state into another of a different state (e.g. liquids being absorbed by a solid or rather gases being absorbed by a liquid). Sorbing species is called the sorbate, and the solid media to which the sorbate is attracted to is called the sorbent [15]. The figure below illustrated the difference between adsorption and absorption.

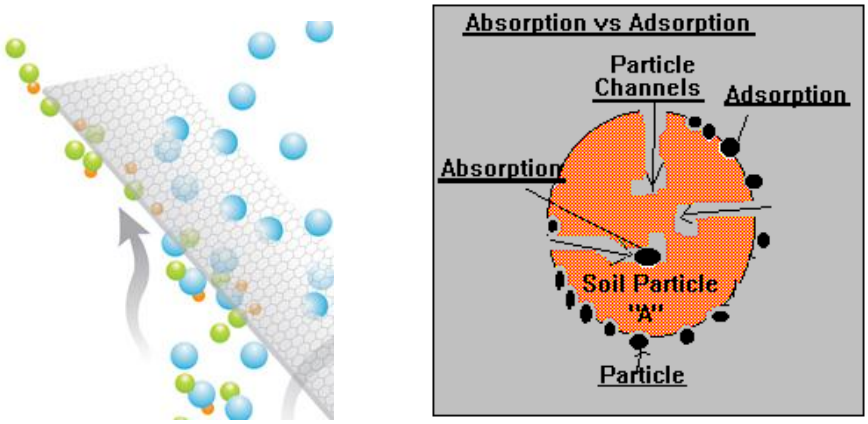

Figure 11: The difference between adsorption and absorption [15]

In the above figure (left) different particles (green, orange and blue) are adsorbed on the surface of the sorbent, but only the blue particles that are absorbed into the inside of the sorbent the rest of the particles just accumulate on the surface of the sorbent, this whole process is better illustrated or better understood by considering the diagram on the right [15].

2.7.1 *Sorption isotherms*

Isotherms can be described as graphical representations of the mass of contaminants adsorbed per unit dry mass of solid or organic matter (S) against the concentration of the contaminant (C). The use of the isotherms is subjected to the fact that the instantaneous equilibrium is reached between the sorbent and the sorbate and also that the isotherms can be considered reversible [15]. There are two main isotherms that are used under the sorption, namely the Langmuir that is based on assumptions and also the Freudlich that is mainly used in real life examples [13]. Each of these isotherms will be described and derived and their graphical presentations will be shown.

2.7.1.1 *Langmuir isotherm*

Irving Langmuir was awarded the Nobel Prize in 1932 for his investigations concerning surface chemistry. His isotherm describes the Adsorption of Adsorbate (A) onto the surface of the Adsorbent (S), used for ionic mechanisms and it requires the use of three assumptions [23]:

- The surface of the adsorbent is in contact with a solution containing an adsorbate which is strongly attached to the surface.
- The surface is assumed to have a specific number of sites where the solute molecules can be adsorbed.
- The adsorption involves the attachment of only layers of molecules to the surface (monolayer of adsorption).

The chemical reaction for monolayer adsorption can be represented as follows:

$$A + S \rightleftharpoons AS \quad (2)$$

AS is the representation of a solute molecule bound to a surface site on S. The equilibrium constant K_{ads} for this reaction is given by:

$$k_{ads} = \frac{[AS]}{[A][S]} \quad (3)$$

[A] is the concentration of A whereas [S][AS] are two-dimensional analogs of concentration and are expressed in units such as mol/cm^2. The principle of chemical equilibrium holds with these terms [23]. The complete form of the Langmuir considers the above equation in terms of surface coverage θ defined as the fraction of the adsorption to which a solute molecule has become attached. The expression for the fraction of the unattached sites is denoted as (1 – θ). Therefore the term [AS]/[S] can be written as.

$$\frac{[AS]}{[S]} = \frac{\theta}{(1-\theta)} \quad (4)$$

[A] is therefore expressed as C and K_{ads} is written as

$$K_{ads} = \frac{\theta}{C(1-\theta)} \quad (5)$$

After rearranging, the final form of Langmuir isotherm is obtained

$$\theta = \frac{K_{ads} * C * S}{(1+K_{ads} * C)} \quad (6)$$

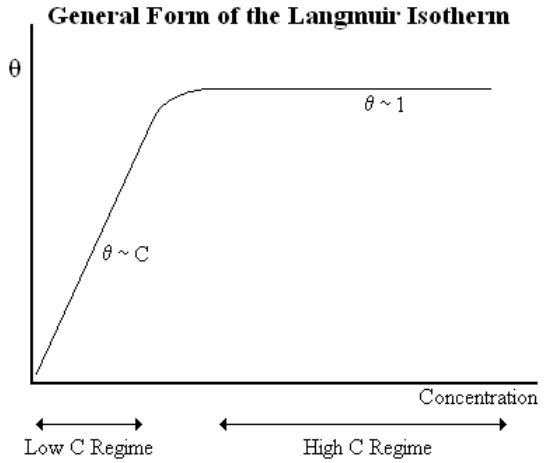

Figure 12: The general form of the Langmuir isotherm.

If *Y* is defined as the amount of adsorption in units of moles adsorbate per mass adsorbent, and Y_{max} as the maximum adsorption, then:

$$\theta = \frac{Y}{Y_{max}} \tag{7}$$

The isotherm can therefore be expressed in the form of a straight line [23]:

$$\frac{C}{Y} = \frac{1}{K_{ads}Y_{max}} + \frac{C}{Y_{max}} \tag{8}$$

2.7.1.2 *Freudlich isotherm*

This isotherm is an equilibrium isotherm that is used most often in real world examples, it is similar to that of monocomponent isotherm which is obtained when an exponential distribution of adsorption energies is assumed, it is used for the substantive mechanisms [30][15].

$$N(Q) = \alpha \exp(\frac{-nQ}{RT}) \tag{9}$$

Where *N(Q)* is the number of sites having adsorption energy *Q* and *α* and *n* are constants. It is therefore further assumed that for each energy level, the coverage θ follows the Langmuir isotherm.

$$\theta = \frac{bC}{(1+bC)} \tag{10}$$

Where C is the sorbate concentration and the adsorption coefficient *b* depends on the adsorption energy in the form:

$$b = b_0 \exp(\frac{Q}{RT}) \quad (11)$$

The fraction of adsorption sites having energy of adsorption between *Q* and *Q* + *dQ* occupied by sorbate is:

$$d\theta_T(Q) = \theta(Q)N(Q)dQ \quad (12)$$

The total coverage by the sorbate is obtained by integration of the above equation over the whole range of adsorption energies and the integral after substitution of θ(*Q)* and *N(Q)* from equation 1 – 3 above yields:

$$\theta_T = \frac{\alpha RT b_0^n}{n} * C^n \quad = AC^n \quad (13)$$

Where *A* is constant under isothermal conditions, if the adsorption is expressed in terms of weight of adsorbate per unit weight of adsorbent q, then the Freudlich isotherm is written in the form [30]:

$$q = KC^n \quad (14)$$

The Freudlich normally results in a curved graph until the logs of both q and C are taken, which yields a straight line making it easier to obtain the slope and the intercept of the line. The slope is 1/n and the intercept is roughly an indicator of sorption capacity and the slope 1/n, of adsorption intensity [31] consider the equation below:

$$log\ q = log\ K + n log\ C \quad (15)$$

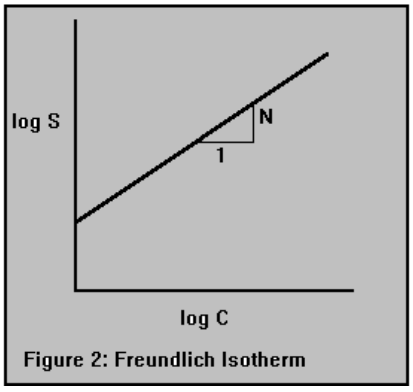

Figure 13: Illustrates the Freudlich isotherm [15][30]

The Freudlich and the Langmuir agree very well at moderate ranges of concentration C. Unlike the Langmuir equation however, it does not reduce to a linear adsorption expression at very low concentrations, nor does it agree well with the Langmuir equation at very high concentrations, since n must reach some limit when the surface is fully covered [31].

2.7.2 *Adsorption ar dye fibre interaction and thermodynamics involved*

During adsorption it is common to distinguish between three types of adsorptions that are involved, the affinity may be predominantly due to:

- Electrical attraction of the solute to the adsorbent this is known as exchange adsorption.
- Van Der Waals attraction, this is known as physical or ideal adsorption.
- Chemical reaction and this is known as chemisorption or chemical adsorption, there are higher energies associated with this kind of adsorption [30].

Adsorption results in the removal of solutes from solution and their concentration at a surface, until the amount of solute remaining in solution is in equilibrium with that of the surface such that the isotherms mentioned above can be applicable.

There are three primary rate steps in the process of adsorption of materials:

A. It is the transport of the adsorbate through a surface film to the exterior of the adsorbent also known as film diffusion.
B. It is the diffusion of the adsorbate within the pores of the adsorbent also known as pore diffusion.
C. It is the adsorption of the solute on the interior surfaces bounding pores and capillary spaces.

For most operating conditions the transport of adsorbate through the surface film or boundary layers is rate-limiting [31][30].

Adsorption reactions are temperature dependent they are normally exothermic, according to the following equation of thermodynamics:

$$\Delta G = \Delta H - T\Delta S \qquad (16)$$

Where ΔG is the Gibbs free energy ($J.mol^{-1}$), ΔH is the enthalpy ($J.mol^{-1}$), T is the temperature (K) and ΔS is the entropy ($J.mol^{-1}.K^{-1}$)

Being exothermic indicates that ΔH has a negative value, thus the extent of adsorption increases with decreasing temperature. Changes in enthalpy for adsorption are usually of the order of those for crystallization or condensation reactions meaning that small variations in temperature tend not to alter the adsorption process to a significant extent [30][31].

2.7.3 Diffusion into the membrane

Diffusion itself can be easily described as the spread of particles from the regions of high concentrations to the regions of lower concentrations. Small diffusive molecules termed penetrants and one of the assumptions assumed is that over a large enough length scales, penetrants follow random paths [10]. This randomness is assuming that penetrants follow the equation below known as Fickian diffusion and thus allowing diffusion to be quantified by a single number, the diffusion coefficient D.

$$J = D\nabla c \quad (17)$$

J is the penetration flux, D is the diffusion coefficient and ∇c, the penetrant concentration gradient. This is one of the ways in which D can be defined. The model is aimed for glassy polymers in which the polymer chains are essentially frozen and the diffusion can take place within the amorphous phase and also between the fibres [10]. Therefore as a result penetrant diffusion is strongly influenced by polymer mobility, which itself is strongly dependent on temperature, density and penetrant concentration (or equivalently, polymer conversion). Lowering temperature, decreasing penetrant concentration or raising density lowers polymer mobility [10].

2.7.4 Previous Models

There are three main types of models for the experiments and computer simulations.[10]

- The dual-mode sorption model, it assumes that penetrants can exist in either of two phases, each with different diffusive properties.
- The Free volume models that assume that the probability of a diffusive jump is proportional to a critical amount of free volume accumulating adjacent to the penetrant for it to jump into.
- Finally there are the molecular modes, they calculate the energy for an assumed specific simplified polymer motion of an energy activated jump of the penetrant.

2.7.5 Existing models for diffusion

2.7.5.1 Free volume model

It is one of the first models for diffusion of molecules in any condensed-phase system and assumes that the ability of molecules to diffuse is dependent on the amount of empty spaces in the system, or spaces between the fibres. This was first attempted by Doolittle in 1951 in simple hydrocarbon liquids and in 1961, Fujita was the first to apply free volume theory to penetrants diffusion in concentrated polymers with suitable modifications. Free volume theories have been found to describe diffusion coefficients above the glass transition, but have been found to break down in the glassy region [10]. The mostly used theory in the free volume is the William-Landel-Ferry equation written bellow:

$$\log\frac{D(T)}{D(T_g)} = \frac{C_1(T-T_g)}{C_2+(T-T_g)} \quad (18)$$

T_g is the glass transition temperature
C_1 and C_2 are constants

2.7.5.2 Dual sorption model

This model was designed specifically for glassy polymers, it is not much a predictive model but rather an explanation of why D's are concentration dependent. The model assumes that the penetrants gas dissolved in the polymer can be divided into two phases. One phase consists of penetrant dissolved in the normal way, with the concentration C_D, related to pressure, *p* by Henry's law, which in the dilute limit is [10]:

$$C_D = K_D P, \quad (19)$$

Where K_D is the Henry's constant.
The second phase consists of penetrants trapped in a fixed number of cavities in the polymer, characteristic of glassy polymers and the concentration for such penetrants is given by a Langmuir isotherm.

2.7.5.3 Activation energy models

These models result in the calculation of the activation energy, *E*, and the pre-exponential factor, D_0, for an assumed molecular process, giving *D* by an Arrhenius expression:

$$D = D_0 \exp(-E/RT) \quad (20)$$

E = activation energy of diffusion
R = gas constant
T = absolute temperature
D_0 = constant.

The model attempts to calculate the energy for two polymer chains, assumed to be parallel but be forced apart, as seen in the figure below, this allows a penetrant to squeeze in-between in a direction perpendicular to the page see the Figure below.

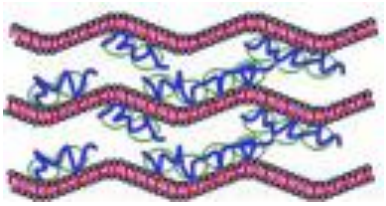

Figure 14: The penetration of the penetrant forcing the polymer chains apart [10]

2.8 Sorption at elevated temperatures

2.8.1 The effects on flux and retention

The changes in temperature have major effects on retention during nanofiltration. An increase in temperature results in a decrease in the retention until a critical temperature of the membrane is exceeded. As a result after this temperature the flux decreases and the retention is increased [24]. There are a number of reasons for this kind of behavior during nanofiltration and these will be discussed. The critical temperature of the polymer in this case is referred to as a glass transition temperature of the polymer (T_g). Below T_g the increase of temperature in the solution filtered results in the decrease of retention this is due to the fact that the kinetic energy of the molecules is increased at elevated temperatures and this provides them with enough energy to pass easily through the membrane [24][26]. T_g for polyamide is 47 ^{0}C, this means that any increase of temperature but below T_g results in the decrease of retention, due to that increase in temperature, there is also an increase in flux as the temperature increases. However, when the operational temperatures are higher than T_g, there is a sharp increased mobility of the molecule segments in the polymer that is observed. Under these conditions the polyamide is now above its glass-transition temperature and it is highly in an elastic state [26]. In this state there is segmental mobility of the macromolecules in the amorphous areas because of this, there is swelling of the fibres within the membrane as a result there is a decrease in fiber pores and also inter-spaces in-between the fibres [24][26]. As a result of swelling, the retention is increased and the flux is decreased making it beneficial to filter at the temperature of 50 ^{0}C or above compared to filtering at 25 ^{0}C [27]. A higher process temperature changes the separation performance due to temperature-dependent changes in the active layer of the membrane, along with the effects of temperature that may be directly or indirectly related to decrease in viscosity, such as reduced pressure drop and increased external mass transfer [27].

Nanofibrous membranes of polyamide are good at withstanding elevated temperatures, but they become more sensitive to pH and pressure and eventually lose their nanofiber properties. A general rule is that the pH values should be 7 ± 2 when operating at temperatures between 50 and 70 °C, and also that the pressure (expressed in bars) multiplied by the temperature (°C) should not exceed 1200 [27]. Generally the water flux increases with temperature by approximately 3% per 1 °C and the membrane transmission typically follows an Arrhenius type relation where the activation energy and permeability coefficient vary for each solute or solvent. Theoretically, from 0 to 100 °C, the density of water decreases by 4% while the dynamic viscosity decreases by 63%, in practice the only temperature dependent variable is the dynamic viscosity, that decreases with increasing temperature resulting in the pressure drop [27]. After swelling, transport through dense films

can be considered as an activated process and can be described by an Arrhenius type equation shown below:

$$P_0 = A_p \exp^{-E_0/RT} \quad (21)$$

In the above equation, the membrane sorption and diffusion are combined and accounted for in the pre-exponential permeability coefficient (A_p) and the activation energy (E_P) [27].

2.8.2 Adsorption as a physical process

In any adsorption process, the material being adsorbed is simply but effectively removed from one phase (wastewater) and transferred to another phase (sorbent). This implies that adsorption process is a physical separation process in which the adsorbed material is not chemically altered because there is no chemical reaction taking place between the sorbent and the sorbate [11][2]. Since the chemical characteristics of the adsorbed material are not altered, the use of adsorption in wastewater treatment is associated with the removal of hazardous material(s) from the wastewater and its transfer to the membrane [11]. This implies that the membrane now contains the hazardous material, therefore appropriate actions must be taken to treat the membrane at the end of the cycle. The membrane can therefore be:

- Regenerated by intensive cleaning using high pressure.
- Disposed of together with the pollutants it contains) in a land fill
- Destroyed together with the pollutants it contains in an incinerator.

2.8.3 Factors affecting adsorption during filtration

There are several factors that affect the adsorption of sorbate on the sorbent surface, but the most important are [11]:

- The surface area of adsorbent, larger size implies a greater adsorption capacity.
- Particle size of adsorbent, smaller particle sizes result in the reduction of internal diffusional and mass transfer limitation to the penetration of the adsorbate inside the adsorbent (i.e equilibrium is more easily achieved and nearly full adsorption capability can be attained).
- Contact time or residence time. The longer the time the more complete the adsorption will be.
- Solubility of solute (adsorbate) on a liquid (wastewater), substances that are slightly soluble in water will be more easily removed from water that the substances with high solubility. Also non-polar substances will be more easily removed that the polar substances since the latter have a greater affinity for water.
- Affinity of the solute for the adsorbent, this depends on the polarity of the membrane surface, the more polar substances will be attracted to the polar membrane and the non-polar will be easily removed by the non-polar membranes.

- Number of carbon atoms, for substances in the same homologous series a larger number of carbon atoms is generally associated with a lower polarity and hence this affects the potential for being adsorbed.
- Size of the molecule with respect to the size of the pores. Larger molecules may be too large to enter small pores and this may reduce adsorption independently of other causes.
- Degree of ionization of adsorbate molecule, More highly ionized molecules are adsorbed to a smaller degree that neutral molecules.
- pH, the degree of ionization in a species is affected by the pH, this in turn affects adsorption [11].

2.9 *Spectrophotometry*

Spectrophotometry is one of the branches of spectroscopy where there are measurements of the absorption of light by molecules that are in a gas or vapor state or dissolved molecules or ions [12]. This technique investigates the absorption of the substances between the wavelengths limits 190 nm and 780 nm, visible spectroscopy is restricted to the wavelength ranges that are only detectable by the human eye, which is above 360 nm, and ultraviolet spectroscopy is used for shorter wavelengths [12]. In this wavelength range the absorption results from the electromagnetic radiation caused by the excitation (transition to higher energy level) of the non-bonding or bonding electrons of the molecule or ions. Spectrophotometry is based on two principles:

- The intensity of colour is a measure of the amount of a material in solution.
- The second principle is that every substance absorbs or transmits certain wavelengths of radiant energy but no other wavelengths, thus the absorption or transmission of specific wavelengths is a characteristic for a substance, and a spectral analysis serves as a "fingerprint" of the compound [12].

2.9.1 Light and the reception of colour

Light is a form of electromagnetic radiation, when incident on a substance three things can happen:

- The light can be reflected by the substance.
- It can be absorbed by the substance.
- Certain wavelengths can be absorbed and the remainder transmitted or reflected.

Reflection of light is of minimal interest in spectrophotometry it is therefore ignored and only transmittance and absorbance can be used [12].

The radiation wavelength is related to its frequency and also with the photon energy according to well-known Plank's relationship [12][14].

$$E = h*f = h(c/\lambda) \quad (22)$$

Where
E is the photon energy
h is the Planks constant ($6.63x10^{-34}$ $J.s^{-1}$)
f is the radiation frequency
c is the light velocity in vacuum ($2.998x10^{8}$ $m.s^{-1}$)
λ is the wavelength of radiation

2.9.2 Transmittance, Absorbance and the BEER-LAMBERT LAW

Transmittance can be defined as the ratio of the amount of light transmitted to the amount of light that initially incident on the surface or solution. Consider the diagram below that shows the transmittance of light though the solution [12].

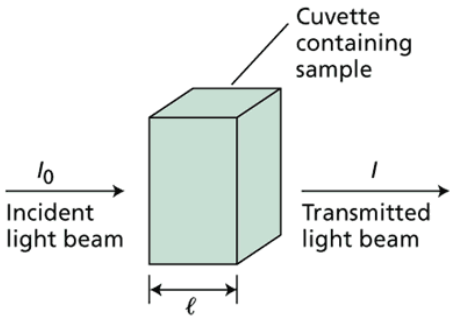

Figure 15: The transmittance of light [12]

Transmittance = I/I_0 = intensity of transmitted light/intensity of incident light.
On the other hand Absorbance can be defined as the negative logarithm of the transmittance, and absorbance and transmittance bear an inverse relationship [12].
Absorbance = -logT = -logI/I_0
From the experimental observations it was deduced that absorbance increases as the concentration increases. It was also deduced that the absorbance is also directly proportional to the path length travelled by the light, it increases as the path length increases [12].

2.9.3 BEER-LAMBERT LAW

The two above mentioned relationships of absorbance, constitute this law.
Absorbance α path length (*l)**concentration
$A = Ɛ*l*c$ (23)
Where:

- A is the absorbance, dimensionless number.

- Ɛ is the proportionality constant also known as absorption coefficient with units (litre/mole*cm)
- C is the concentration of dye in solution (mol/l)
- *l* is the thickness of absorbing layer of solution, or path length (cm).

2.9.4 Basic parts of spectrophotometer

There are seven basic parts that determine the functioning of the spectrophotometer.

- Radiation source
- Auxiliary optical system
- Dispersion system: optical prism or grating
- Slot diaphragm
- Cell with examined substance
- Radiation detector: photocell, photoelectric cell or photomultiplier
- Indicator or recording instrument [14].

The diagram bellow illustrates the schematic presentation of the spectrophotometer parts.

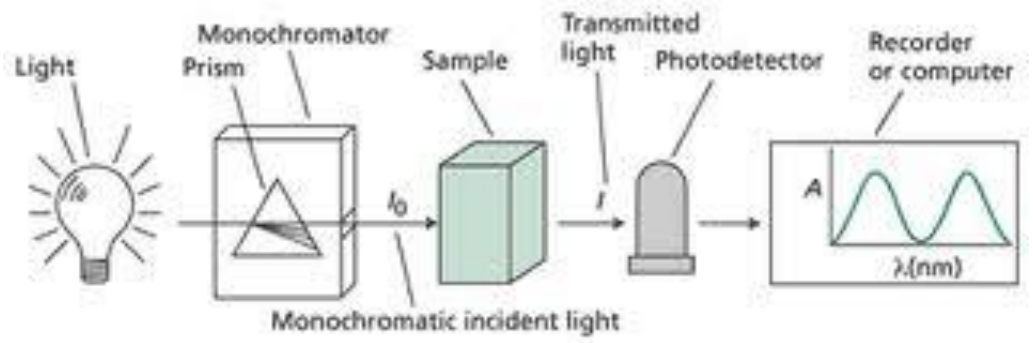

Figure 16: The spectrophotometer parts [14]

2.9.5 Performance of UV-VIS spectrophotometers

There are various factors that affect the performance and the reliability of the instruments; these will be discussed in details.

1. *Wavelength accuracy*

It is defined as the deviation of the wavelength reading at an absorption band or emission band from the known wavelength of the band. The wavelength deviation can cause errors in the qualitative and quantitative results of the UV-Vis measurement [17][12]. It is obvious that if the spectrometer is not able to maintain an accurate wavelength scale, the profile measured will be inaccurate such that the true λ_{max} of the analyte cannot be accurately characterized [17][12].

2. *Stray light*

This is defined as the detected light of any wavelength that is outside the bandwidth of the selected wavelength. The causes of this behavior are scattering, poor instrument design or higher order diffraction. As a result, there is a decrease in absorbance and the reduction of the linearity range of the instrument, higher absorbance measurements are more severely impacted by stray light [17].

3. *Resolution*

According to the Raleigh criteria, two peaks are normally taken into consideration to be resolved if the minimum between the peak of the detector output signal is lower than 80% of the maxima. The resolution of a UV-Vis spectrophotometer is related to its prectral band width (SBW). The finer resolutions result from the smaller spectral band width. The SBW is dependent on the slit width and the dispersive power of the monochromator [17][12].

4. *Noise*

It is mainly originating from the light source and electronic components of the instrument. It affects the accuracy at both ends of the absorbing scale during the measurement. Photon noise from the light source affects the accuracy of the measurements at low absorbance and electronic noise from electronic components affects the accuracy of the measurements at high absorbance. Thus high noise level will reduce the limit of detection and the instrument will be rendered less sensitive [17][12].

5. *Baseline flatness*

Most instruments have dual light sources, a deuterium lamp that is used for the UV range and a tungsten lamp that is used for the visible range. As a result, the intensity of the radiation produced from the light sources is not constant over the whole UV-Visible range. This also varies the response of the detector over the spectral range therefore a flat baseline demonstrates the ability of the instrument to normalize the output of the lamp and detector responses [17].

6. *Stability*

There is instrumental drift that results from variations in lamp intensity and electronic outputs between the measurements of I_0 and I. These changes can result to errors in the value of the measurements over a long period of time, these errors may be positive and negative. The stability test check is vital in order to maintain a steady state over time so that the effect of the drift on the accuracy of the measurement is insignificant [17].

7. *Photometric accuracy*

This is determined by the difference between the measured absorbance and the established standard value of absorbance. Most quantitative applications involve the measurement of the

standards and samples of comparable concentration in rapid succession on the same instrument. The absolute photometric accuracy may not be critical if the photometric measurements are reproducible and the response is linear over a defined range [17].

3. Experimental part

3.1 Objectives of the experiment

- To propose laboratory experiments that will test the sorption properties of nanofibers at different temperatures.
- The second main aim was to test and analyze sorption properties of three Acid dyes using polyamide 6 nanofibrous membrane, the effects of increasing temperature on the amount of the adsorbed dye or the dye that is recovered or removed from simulated dye solution.
- Last objective was to determine the effects of increasing the mass of the nanofibrous membrane on sorption capacity in order to propose the theoretical model of the observed sorption process.

3.2 Determination of the temperature difference between the dye solution and the membrane

The aim of this part of the experiment was to try and investigate the existing temperature difference between the solution to be filtered and the temperature of the nanofibrous membrane. This was done because it is a well understood fact that on an open system, external conditions in particular temperature has an effect on the system. As a result of temperature differences between the system and the environment and also the temperature difference between the glassware and the solutions, there is a decrease in the temperature on the surface of the membrane.

3.2.1 Apparatus and method

The electrospun polyamide 6 nanofibre membrane that was used as a sorbent during sorption nanofiltration was purchased from the company Elmarco s.r.o, with the areal density of $12 g/m^2$, this was used for all the experiments that were covered in this study [28]. The pieces of 30 mm x 30 mm were used for all the experiment such that the whole radial surface could fit within the dimension of the piece. The filtration unit that was used was the normal unit used for membrane filtration for laboratory scales.
Parts of the apparatus:

1. Filtration funnel
2. Sorbent (nanofibrous membrane of nylon 6)
3. Filter supporting unit
4. Vacuum pressure port
5. Vacuum flask

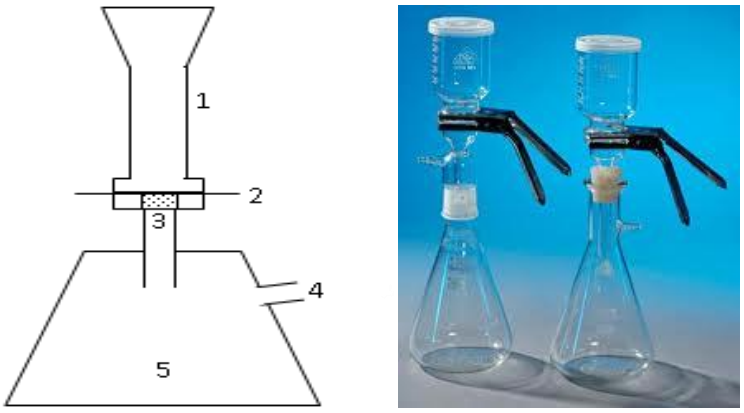

Figure 17: Filtration unit used during nanofitration [19][28]

For the purpose of this experiment mentioned above, water was used for temperature measurements, it was not necessary to use the dye solution because the aim was not to filter but to develop temperature difference relationship. The water was first heated to the initial temperature (i.e 40 $^{\circ}$C) using a glass beaker. The volume of 10 ml was transferred to the funnel which was preheated with water of the same temperature in order to warm the funnel. The water was filtered under vacuum and after filtration the temperature was immediately measured with the use of infrared thermometer. This thermometer was situated at the upper position of the funnel, the distance was long enough such that the crossing infrared lines could fit within the diameter of the funnel, and these lines could cross each other at the center of the membrane. After a period of 30 seconds, the other 10 ml volume of water with the same initial temperature was transferred into the funnel. The time of 30 seconds was essential in order to avoid further cooling of the funnel under elongated periods. This water was also filtered and after measuring the initial temperature of the membrane, the temperature of the membrane after filtration was also measured. This procedure was repeated for five or more times in order to work out the average temperature. The initial temperature of water was increased by the intervals of 5 ^{0}C till the temperature of 50 ^{0}C. It was then increased with the intervals of 10 ^{0}C from the temperature of 60 ^{0}C to 80 ^{0}C.
The following table shows the initial temperature of water and the final temperature of the nanofiber membrane after filtration.

Table 2 : The difference in temperatures of water and that of nanofiber membrane.

Temperature of water (°C)	20	40	45	50	60	70	80
Repetition / run	Membrane temp (°C)	Membrane temp (°C)	Membrane temp (°C)	Membrane temp (°C)	Membrane temp (°C)	Membrane temp (°C)	Membrane temp (°C)
1	20	37.2	36.5	46	53.3	62.1	57.1
2		37.2	36.4	44.1	52.6	58.9	60.4
3		37.5	38.1	43.3	52	55.4	61.9
4		37.6	38.4	41.4	51.7	55.2	60.4
5		35.6	38.1	41.2	52.5	51	59.8
6		36.1	39	40.9	51.9	50	60.9
7			38.9			52.2	
8						50	
Average membrane temp (°C)	20	36.9	37.9	42.8	52.3	54.4	60.1

The membrane temperature values were rounded off the nearest whole number and the graph of average membrane temperatures against the initial temperature of that was plotted in order to investigate the correlation between the actual temperature of the membrane and the exact temperature of water. Refer to the figure below.

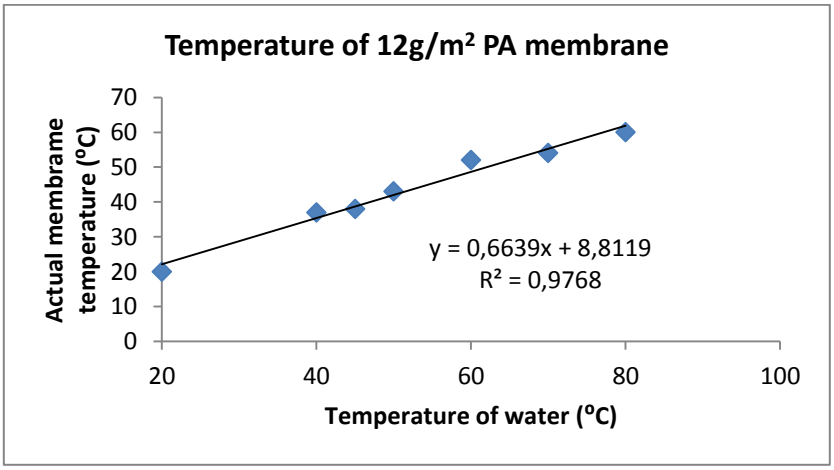

Figure 18: The relation between the membrane temperature and the actual temperature of water.

The equation obtained from the graph was:

$y = 0.6639x + 8.8119$

(24)

where:

y is the actual temperature of the membrane and *x* is the initial temperature of water. The above equation is a linear equation and it was then used for the determination of the initial water temperature that could be used in order to give the estimated membrane temperature. The table below shows the values of the water temperatures to be used, and also the practical measurable temperatures used initially. These are the temperatures that were used for simulated dye solutions throughout the experiment or investigation.

Table 3 : The predicted temperatures of the membrane and the actual measurable temperatures that could be measured initially.

Membrane temperature (°C)	Calculated solution temperature (°C)	Used temperature of liquor (°C)
30	31.92	32
35	39.45	40
40	46.98	47
45	54.51	55
50	62.04	62
55	69.57	70
60	77.10	77
65	84.64	85

3.3 Determination of effects of temperature on sorption filtration

3.3.1 Instrumental presetting

For the analysis, the spectrophotometer, spekol 11, zp100027, was used during this investigation, each of the wavelengths that were used could be selected from the adjustment screw of the wavelength setting. The accuracy of the instrument was up to three decimal places and in order to keep the instrument working properly it had to be switched on 15 minutes or more before the usage. Because of the very low concentrations that were used during the investigation (0.01g/l), cuvettes of larger dimensions were used other than the normal 1cm x 1 cm cuvette, the one that was used was 1 cm x 4.995 cm, this was necessary in order to increase the accuracy of the absorbance values obtained. As it was discussed above that the absorbance is directly proportional to the path length according to BEER-LAMBERT LAW. In order to investigate the operational wavelength of a certain dye, the wavelength was adjusted and the absorbance measured at different wavelengths till the

maximum value was obtained for each dye. Distilled water was used for zeroing the instrument during successive measurements. The wavelength that could result in a maximum absorbance value was taken as the working wavelength for that dye solution, for this purpose the stock solutions were used, namely the ones of 0.01 g/l.

3.3.2 Used materials and dyes

The electrospun polyamide 6 nanofibre membrane that was used as a sorbent during sorption nanofiltration was purchased from the company Elmarco s.r.o, with the areal density of 12g/m^2, this was used for all the experiments that were covered in this study [28]. The pieces of 30 mm x 30 mm were used for all the experiment such that the whole radial surface could fit within the dimensions of each piece. The filtration unit that was used was the normal unit used for membrane filtration for laboratory scales it is the same one as the one described before (figure 17 above).
The dyes that were used for this investigation were acid dyes for the reasons that have been mentioned under the topic "acid dyes and polyamide". Three dyes were used during the investigation namely acid dyes C.I Acid blue 41, C.I Acid blue 78 and C.I Acid yellow 42, they were received from Technical University of Liberec and their structures and scientific data are shown below. Acid dyes are so called because they possess acidic molecular group such as $-SO_3H$ and work in a low pH environment

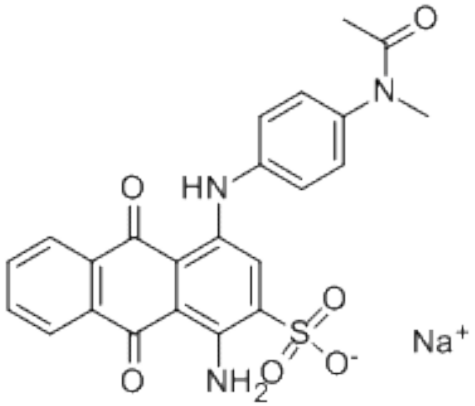

Figure 19: The chemical structure of dye C.I Acid blue 41[20]

Name: 2-Anthracenesulfonicacid, 4-[[4-(acetylmethylamino)phenyl]amino]-1-amino-9,10-dihydro-9,10-dioxo-,sodium salt (1:1)
Molecular weight: 487.46219 g/mol
Molecular formula: $C_{23}H_{18}N_3NaO_6S$

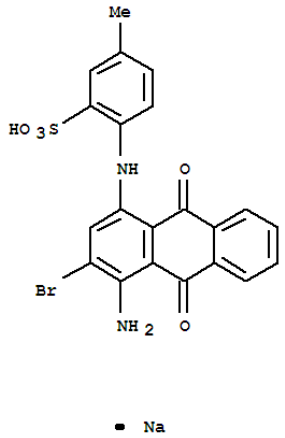

Figure 20: The chemical structure of dye C.I Acid blue 78[22]

Name: Benzenesulfonic acid,2-[(4-amino-3-bromo-9,10-dihydro-9,10-dioxo-1 anthracenyl)amino]-5-methyl-,sodium salt (1:1)

Molecular weight: 509.33 g/mol

Molecular formula: $C_{21}H_{15}BrN_2O_5SNa$

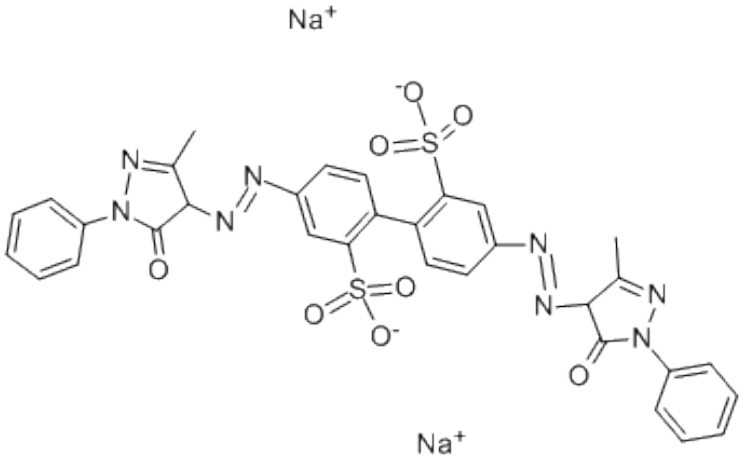

Figure 21: The chemical structure of dye C.I Acid yellow 42[16]

Name: oxo-1-phenyl-1H-pyrazol-4-yl)azo]-[1,1'-biphenyl]-2,2'-disulfonate
Molecular weight: 758.69 g/mol
Molecular formula: $C_{32}H_{24}N_8Na_2O_8S_2$

3.3.3 Preparation of dye solutions from powder

The stock solutions of each of the above dye samples were prepared by dissolving 0.5 g of dye powder in small amount of hot distilled water (about 30 ml) in order properly dissolve the dye, because otherwise the dye does not fully dissolve in cold water. This dissolved dye was then transferred into a 500 ml conical flask and filled up to the mark with cold distilled water, and the solution was shaken in order to achieve homogeneity. These were the solutions with a concentration of 0.1 g/l. The following equation was used in order to achieve this:

$C = m/V$ (C = concentration, m = mass and V = volume) (25)

For the dilution in order to achieve the concentration of 0.01 g/L, 5 mL of the above solution was pipetted and diluted to the final volume of 50 mL.
The following equations were used in order to achieve these values.
$C_1V_1 = C_2V_2$ (1 = initial solution and 2 = final solution)
$V_1 = C_2V_2/C_1$ (26)

These last solutions were used as the stock solutions for the rest of the experiments, all the dye solutions were prepared using this very same procedure these solutions were the ones used for the determination of the maximum wavelength for each of the used dyes, these are shown in the table below.

Table 4 : Dyes and the wavelengths used during the experiments.

Dye used	Wavelength used (nm)
C.I Acid blue 41	600
C.I Acid blue 78	590
C.I Acid yellow 42	410

3.4 Procedure

3.4.1 Determination of temperature effects on sorption

The following procedure was the same for all three dye solutions.
The solution was first heated to the initial temperature of the solution, for example, in order to achieve membrane temperature of 30 °C, the solution had to be heated to 32 °C as explained in the procedure of temperature determination above. The funnel was also heated to the same temperature using distilled water (dipped in distilled water). At this initial temperature the dye solution was immediately transferred to the funnel and the stopwatch was started at the same time of starting the pump, this time value was recorded. The filtrate was then transferred into the test tube for absorbance analysis. After a period of 30 seconds, the second solution was transferred into the funnel at the same initial temperature and the

time was measured during filtration. This procedure was repeated for a minimum of 20 times in order to achieve the equilibrium where the concentration of the dye before filtration is the same as the concentration of the dye after filtration. The same procedure was followed for the other temperatures i.e 40 °C, 50 °C and 60 °C while recording all the time values corresponding to each of the readings. The samples were then taken to the spectrophotometer for the determination of absorbance values that were further used for different calculations that will be discussed in details below in order to achieve the amount of dye removed from the original solution.

3.4.2 Determination of sorption capacity(Cs) and the theoretical model

From the study performed by S Ntaka, it was concluded that the equilibrium with the use of acid dyes and nanofibrous membrane could be reached at the period of 10 days. Therefore in this study, the period of 10 days was used in order to determine the sorption capacity, Cs and the theoretical model for sorption of the dyes at the temperature of 20 °C.

The same concentrations of dye solutions were used as in the above experiments for all three dyes (10 mg/L). The dimensions of the fibrous membrane used were 30mm x 30mm for each piece. Ten dye solutions of 10 mg/L, of the same volume of 100 ml were prepared such that in the first solution one piece of 30mm x 30mm was used, in the second solution, two pieces, the same was applied up to Ten pieces of membrane. After 10 days when the equilibrium was reached, the Absorbance of each of the ten solutions for each dye was determined using the spectrophotometer as in the above experiments.

Consider the sample calculations below that were applied in order to fill in the tables used for the determination of the dye that was removed or accumulated in the nanofibre membrane.

3.5 Sample calculations

The following equation was used in the calculation of the new concentration of the liquor after filtration.

<u>For the concentration after filtration</u>

$C_L = C_{L0}(A_t/A_0)$ (27)

Where

C_L = concentration of the filtrate

C_{L0} = the original concentration of before filtration (0.01g/l) in all the experiments studied.

A_t = Absorbance of the filtrate.

A_0 = Original absorbance of the dye solution before filtration.

Therefore, the results of the dye C.I Acid blue 41 will be used for the demonstration of all calculations and the same principles apply also for the other two dyes. (see table 5.1)

C_{L0} = 0.01g/l = 10 mg/l

$A_0 = 0.477$
$A_t = 0.152$ (in this case)
$C_L = C_{L0}(A_t/A_0)$
$= 10(0.152/0.477)$
$= 3.187$ mg/l

For the change in mass:

$\Delta m = m_0 – m_L$

(28)

Where Δm = change in mass (mg)
m_0 = original mass before filtration (0.1 mg)
m_L = mass after filtration = C_L* V

$\Delta m = m_0 – m_L$
$= 0.1 – (3.187*0.01)$
$= 0.0681$ mg

For the accumulated mass

It is the sum of the mass of dye accumulated in the membrane throughout the filtration. For example for the first two results in this case:

Accumulated mass = change in mass for the first reading + change in mass for the second one

$= \Delta m_1 + \Delta m_2$
$= 0.0681 + 0.035$
$= 0.1031$ mg.

For the accumulated volume

The same principle as for the accumulated mass is used here, the previous volume readings are summed up such that for 30 runs performed, there is a total volume of 300 ml used.

For the percentage of dye removed

$$\% \text{ dye removed } (\%E) = \frac{\text{(mass before filtration – mass after filtration)}}{\text{mass of dye before filtration}} \times 100 \quad (29)$$

$= ((m_0 – m_L)/m_0)*100$
$= ((0.1 – 3.187*.01)/0.1)*100$
$= 68.13\%$

4. RESULTS AND DISCUSSION

Below are the graphical presentations that show the relationship between accumulated mass of dye, change in mass of dye and also the concentration after filtration all against the number of runs in order to reflect the effect of the temperature of 20 °C on filtration during the investigation.

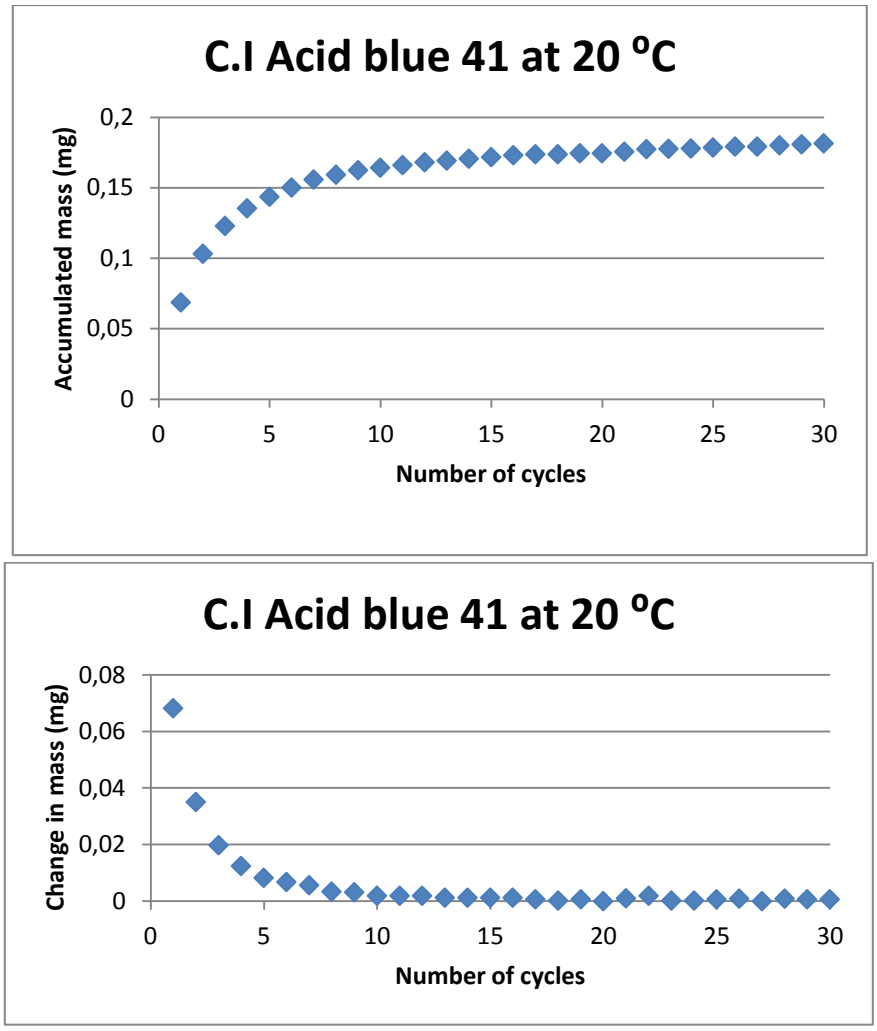

Figure 22.1 : The graphical representation of the effects of filtration on Acid Blue 41.

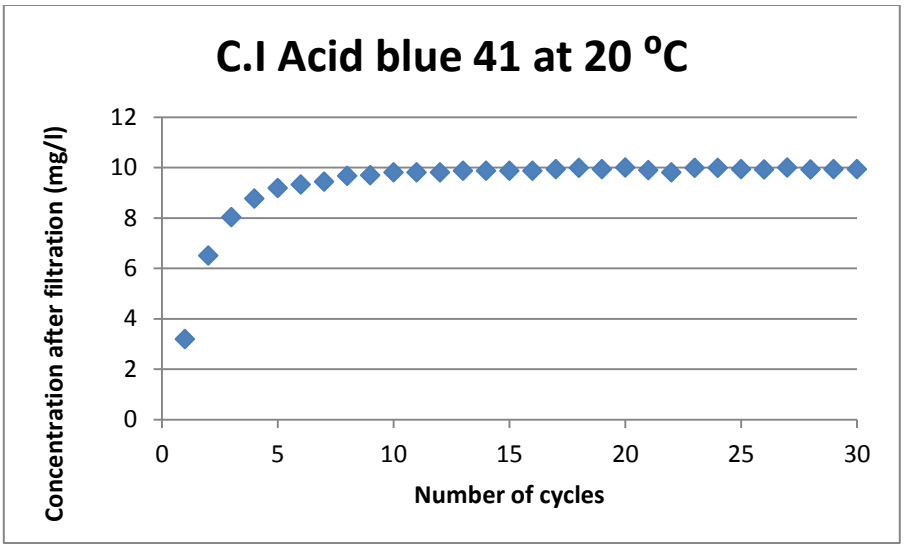

Figure 22.1 : The graphical representation of the effects of filtration on Acid Blue 41.

The table that was used for the construction of these graphs was table 5.1 (**in appendixA**). Tables 5.2 to 5.5 were used for the construction of figure 22.2 to figure 22.5 for C.I Acid Blue 41 dye solutions between temperatures of 20 to 60 °C.

The following graph gives the summary of the effect of increasing temperature on the amount of dye that is accumulated on the membrane, it is an overview of the total effect of all the temperature used, also reflects the behavior of the accumulation of dye at each temperature (the shape of the graph).

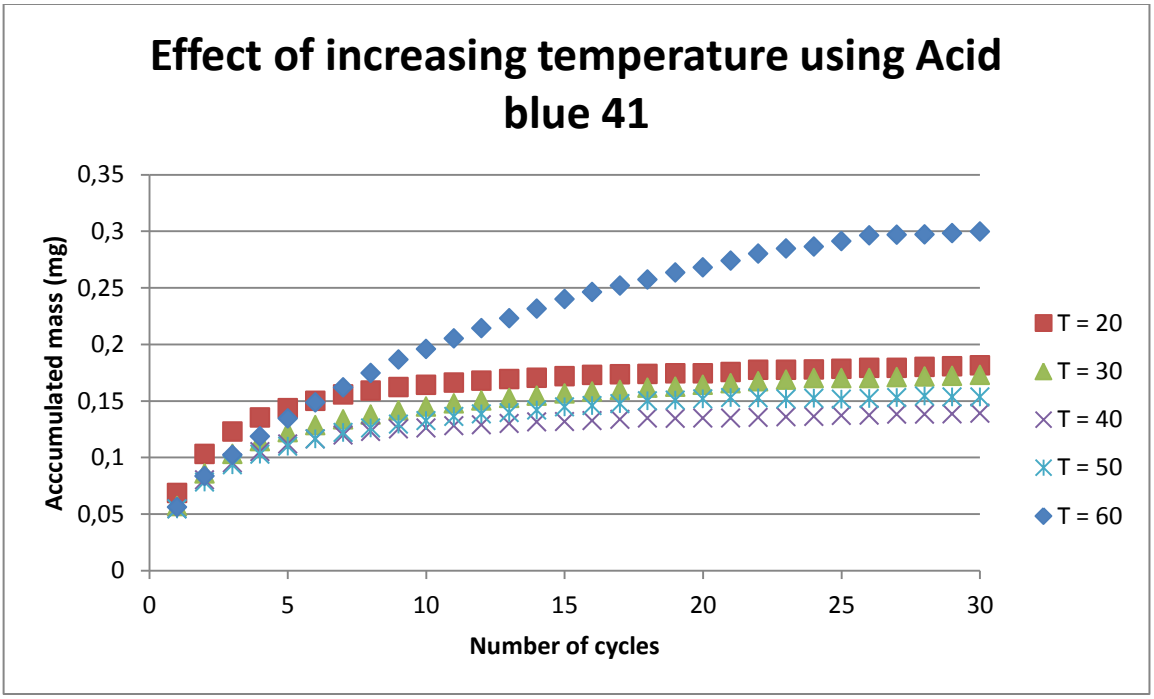

Figure 22.6: The summary of the effects of temperature on Acid blue 41

The following results were obtained when the solution prepared from dye C.I acid yellow 42 was used. The tables corresponding to the data start from table 6.1 to table 6.5 (in appendix A) and the graphs corresponding to the tables start from figure 23.1 to figure 23.5 (appendix B) The same procedure as discussed above was used, the calculation used are also exactly the same as above.

The following graph gives the summary of the effect of increasing temperature on the amount of dye that is accumulated in the membrane, it is an overview of the total effect of all the temperature used, also reflects the behavior of the accumulation of dye at each temperature (the shape of the graph), for Acid Yellow 42.

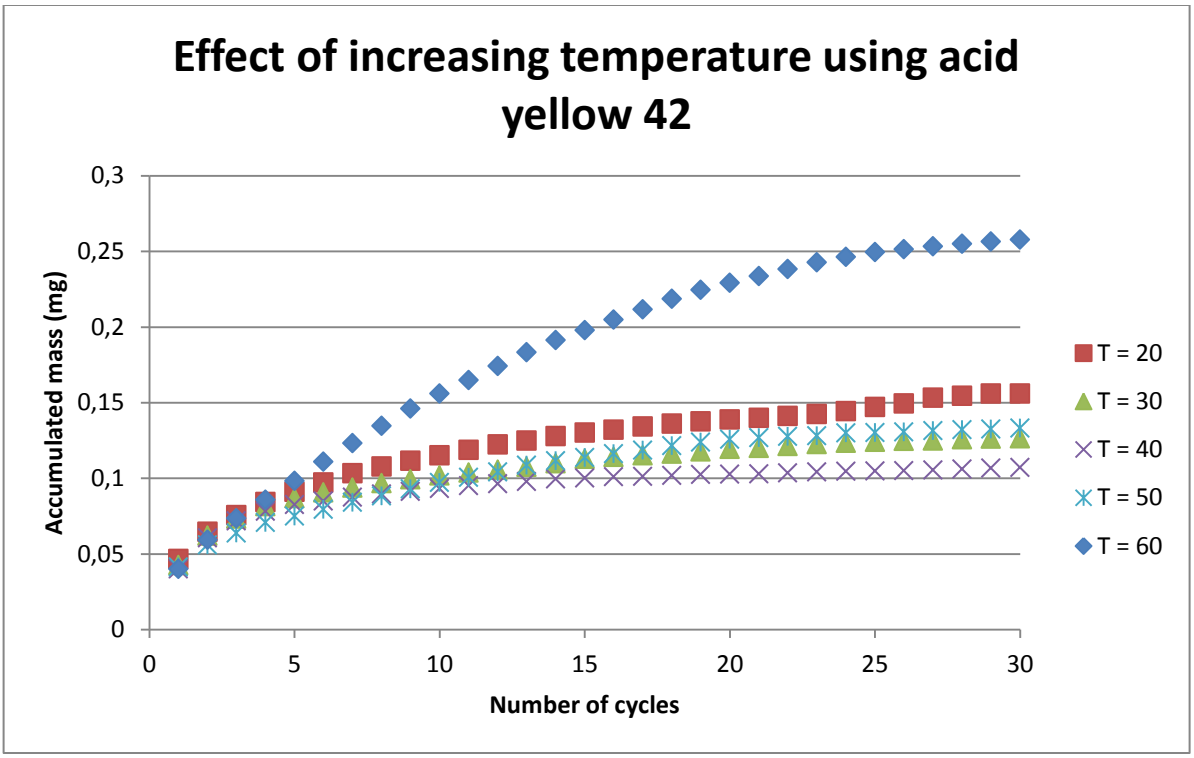

Figure 23.6: Shows the summary of the effects of temperature on Acid Yellow 42.

The following results were obtained when the solution prepared from dye C.I acid Blue 78 was used. The tables corresponding to the data start from table 7.1 to table 7.5 (in appendix A) and the graphs corresponding to the tables start from figure 24.1 to figure 24.5 (appendix B) The same procedure as discussed above was used, the calculation used are also exactly the same as above.

The following graph gives the summary of the effect of increasing temperature on the amount of dye that is accumulated in the membrane, it is an overview of the total effect of all the temperature used, also reflects the behavior of the accumulation of dye at each temperature (the shape of the graph), for Acid Blue 78.

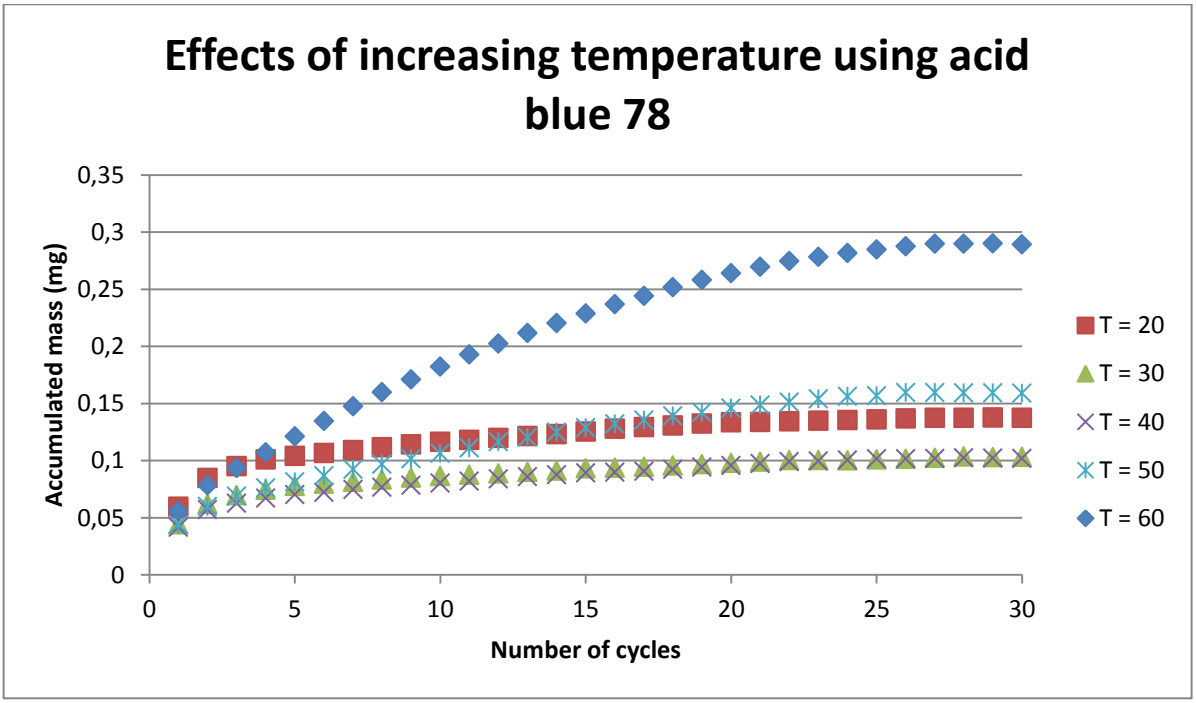

Figure 24.6: Shows the summary of the effects of temperature for Acid Blue 78.

The other dyes were also tried but the problem was that, these could not reach the equilibrium after 30 cycles so it was decided that the results could be discarded.

4.1 Percentage dye removal and molecular mass

All the results obtained from all the three dyes used namely, C.I Acid blue 41, C.I Acid yellow 42 and C.I Acid blue 78 were all presented in tabular and graphical form. The results show that from the temperature of 20 °C to the temperature of 60 °C, in all the cases the percentage of removed dye is higher for dye C.I Acid blue 41 (68% at 20 °C and 56% at 60 °C), both for the first run, followed by dye C.I Acid blue 78 and lastly dye C.I Acid yellow 42 except for the temperature of 60 °C. These results are in good agreement with the molar masses of the dyes C.I Acid blue 41 has the smallest molar mass (487.46 g/mol), followed by C.I Acid blue 78 (509.33 g/mol) and lastly is C.I Acid Yellow 42 (758.69 g/mol). The molar mass values show that less grams of C.I Acid Blue 41 are needed for every mole as opposed to more grams of C.I Acid yellow 42 needed per mole. The molar mass values could be a good indication to reflect that there is a high possibility of the dye C.I Acid blue 41 having larger molecules or particles compared to the other two and also that dye C.I Acid yellow 42 had smallest particles than all other investigated dyes. No solid observations could be deducted based on the values of accumulated masses at equilibrium because all the

three dyes could not reach equilibrium with exactly the same number of runs, therefore could not be compared for each temperature.

4.2 Overall effect of temperature on filtration

The effect of temperature increase on sorption in this study is better discussed using the accumulated mass of the dye on the sorbent for each temperature in equilibrium, this value is also known as sorption capacity. This is the point where by the concentration of the initial concentration before filtration is close enough to that of the filtrate after filtration, which is a reflection of that, no further sorption or filtration is taking place. Figure 22.6, Figure 23.6 and Figure 24.6 above for C.I Acid blue 41, C.I Acid yellow 42 and C.I Acid blue 78 reflect the effects of temperature on these solutions of the dyes. All the figures show that accumulated mass of the dye decreases as the temperature increases. For the dye C.I Acid blue 41 and C.I Acid yellow 42, the accumulated mass decreases from the temperature of 20 °C to the temperature of 40 °C. After this temperature there is a turn over point such that the accumulated mass is higher at 50 °C but below the one at 20 °C (see figure 22.6 and figure 23.6). For C.I Acid blue 78, the accumulated mass only decreases between 20 °C and 30 °C and the turn over point is at 40 °C, the accumulated mass at 50 °C is much higher than the one at 20 °C (see figure 24.6) as opposed to the other two dyes. For all the dyes the accumulated mass of the dye in the sorbent is much higher when the filtration was performed at the temperature of 60 °C than the filtration at the temperature of 20 °C. When the ratio of the accumulated mass of dyes per mass of fibre was calculated (see below) for each temperature, it was deduced that C.I Acid blue 41 had higher values followed by Acid yellow 42 in all the cases except for the temperature of 50 °C where C.I Acid blue 78 value is higher than the other two values.

4.3 For the mass of dye per mass of fibre

From the above results, it was then proposed that the determination of the amount of each dye that could be accumulated per mass of fibre for each temperature could result in a good conclusion in terms of comparison amongst the three dyes.

Consider the following calculations.

Area of funnel

$A_f = \pi d^2/4$

(30)

A_f is the area of the funnel, d is the diameter of the funnel = 17 mm

$A_f = \pi d^2/4$

$= \pi(17 \times 10^{-3})^2/4$

$= 2 \times 10^{-4}\ m^2$

This is the same as the area of fibers that will be covered by the circumference of the funnel of the filter.

For the total mass of fibers (m_f) that is covered by this area.

$m_f = \rho_f * A_f$

(31)

ρ_f is the areal density of fibres.

$m_f = \rho_f * A_f$

$= 12 * 2x10^{-4}$

$= 3x10^{-3}$ g

For the average values of the accumulated mass of each dye at equilibrium, the average values of accumulated mass of dye were determined using four of five values at equilibrium. The average values were then divided by the mass of the fibres for each dye at different temperatures and these values were presented graphically.

$C_s = m_d/mf$

C_s is the ratio of the mass of dye to that of fibre, m_d is the mass of accumulated dye

For example for C.I Acid yellow 42 at 20 °C (refer to the table below for the average mass)

$C_s = m_d/mf$ (32)

$= 0.155/3x10^{-3}$

$= 51.66$ mg/g

The results for each dye were calculated using the above calculations and these were presented in the table below.

Table 8: The average accumulated masses of three dyes on the mass of fibre

Temp (°C)	Average accumulated mass of Acid blue 41 (mg)	Mass of dye / mass of fibre (mg/g)	Average accumulated mass of Acid yellow 42 (mg)	Mass of dye / mass of fibre (mg/g)	Average accumulated mass of Acid blue 78 (mg	Mass of dye / mass of fibre (mg/g)
20	0.180	60.0	0.155	51.7	0.138	45.9
30	0.172	57.2	0.126	41.9	0.103	34.4
40	0.138	46.1	0.106	35.3	0.102	34.0
50	0.153	51.1	0.132	44.0	0.159	53.1
60	0.298	99.2	0.255	84.9	0.289	96.5

The results in the table above were used to plot the graphs of ratios of mass of dye per mass of dye versus the temperature for each dye investigated.

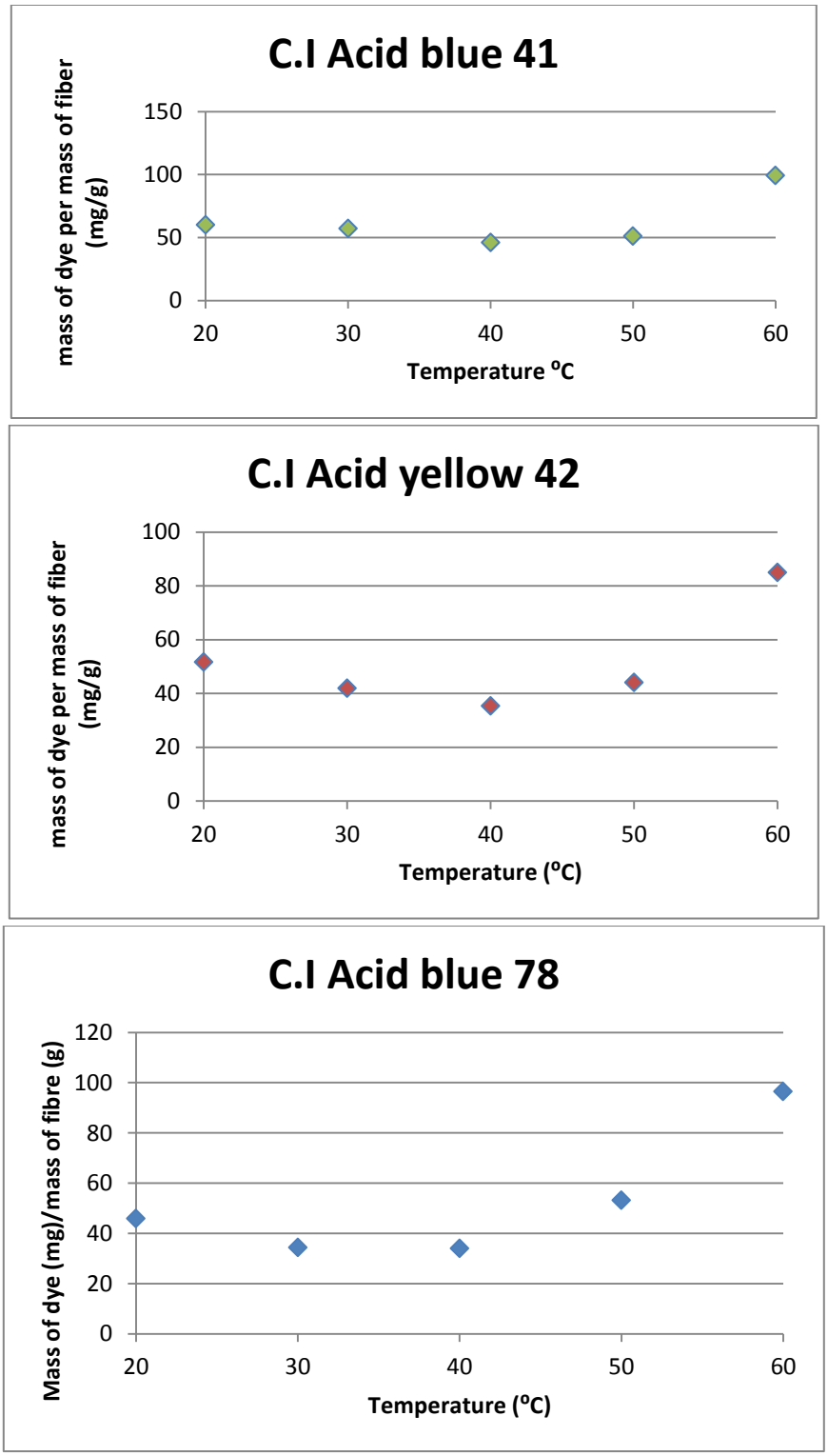

Figure 25: The mass of dye per mass of fibre for each dye

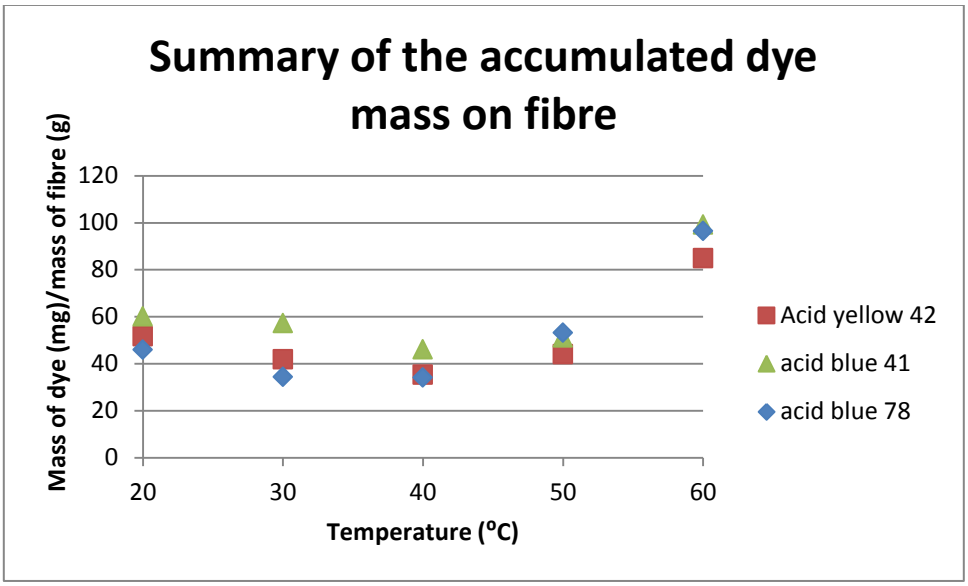

Figure 26: The comparison of the three dyes using the above graphs

There are reasons for the above behavior of the polyamide 6 nanofiltration membrane, theoretically because of the fact that filtration reactions are exothermic, there is also a decrease in the accumulation of dye in the polymer till the critical temperature is reached. The critical temperature of the polymer in this case is referred to as a glass transition temperature of the polymer (T_g). Below T_g the increase of temperature in the solution filtered results in the decrease of retention, due to the fact that the kinetic energy of the molecules is increased at elevated temperatures and this provides them with enough energy to pass easily through the membrane [24][26]. T_g for polyamide is 47 ^{0}C, this means that any increase of temperature but below T_g results in the decrease of retention, due to that increase in temperature, there is also an increase in flux and the decrease in accumulated dye mass as the temperature increases. However, when the operational temperatures are higher than T_g, there is a sharp increase mobility of the molecule segments in the polymer that is observed. Under these conditions the polyamide is now above its glass-transition temperature and it is highly in an elastic state [26]. As a result there is swelling of the fibres within the membrane that implies a decrease in fiber pores and also inter-spaces in-between the fibres [24][26]. Because of this swelling, there is high percentage of dye molecules that do not make it through the membrane, thus resulting in the accumulation at higher temperatures much higher than the one of lower temperatures. These reasons provide a good explanation of the behavior that was observed with this investigation.

4.4 Determination of sorption capacity at equilibrium and Proposed Sorption isotherm

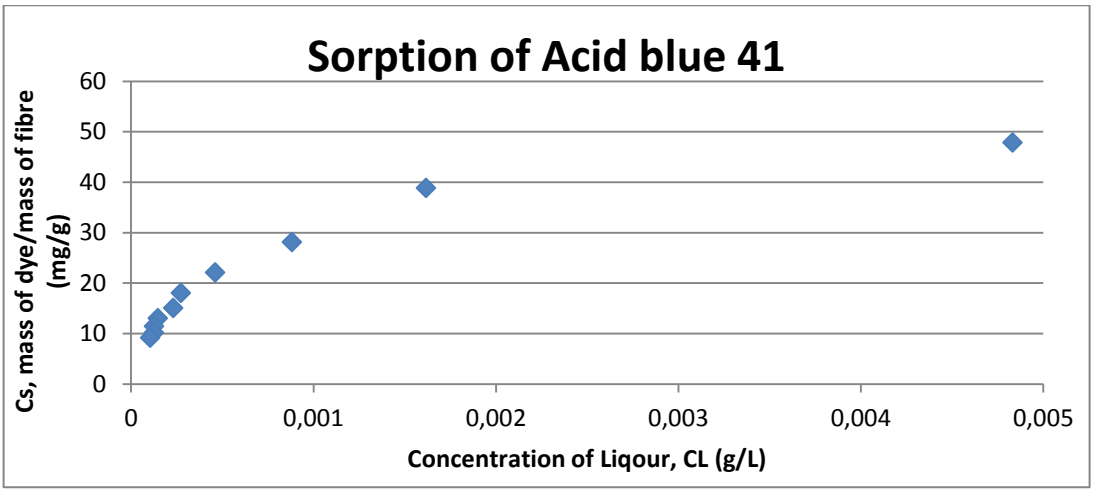

Figure 27: Sorption capacity (Cs) and the concentration of the filtrate at equilibrium.

The above graph was constructed using the values from table 9 from appendix A, the results corresponded to C.I Acid blue 41. The same calculations and processing was done for Acid Blue 78, on table 10 (appendix A) and figure 28 (appendix B), and for Acid Yellow 42, on table 11 (appendix A) and figure 29 (appendix B). The results from the tables and graphs were used for the determination of the sorption isotherm, which in this case was the Langmuir isotherm in order to best describe the results scientifically. Using equations:

(number 6 and 8 above): $C_S = \frac{K*CL*S}{(1+K*CL)}$ (where Cs is the sorption capacity of mass of dye per mass of fibre (mg/g), K is the affinity between sorbate and sorbent (L/g), C_L is the concentration in liquor (g/L), S is the maximum amount of dye that can be adsorbed (mg/g). The linear form of the equation was used to determine the constants S and K from the intercept and the slope from the graph of : $\frac{1}{C_S} = \frac{1}{C_L} * \frac{1}{K.S} + \frac{1}{S}$

Table 12: The Results of constants of different dyes using linear graphs of each dye

Dye/constant	S (mg/g)	K (L/g)
Acid Blue 41	43.860	2533.333
Acid Blue 78	20.080	16600.27
Acid Yellow 42	24.213	6883.333

The following straight line graph was obtained for Acid Blue 41 for the determination of the constants.

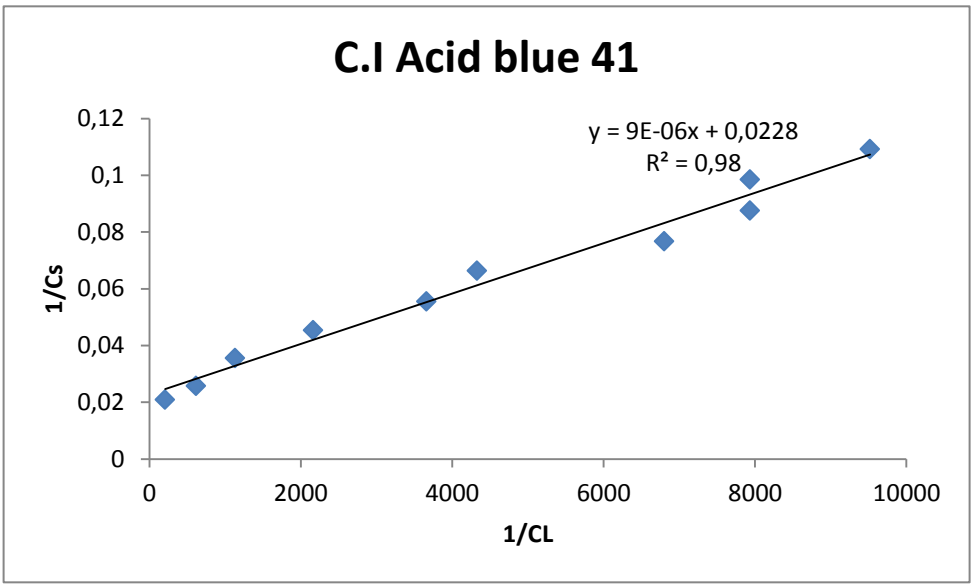

Figure 30: Determination of constants S and K for Acid Blue 41 used for Langmuir curve.

The same approach was used for the other Dyes, and their curves are represented in appendix B as Figure 31 and figure 35. The above values on table 12 were then used for the construction of the Langmuir curve which was then compared to the experimental curve for each of the three dyes used and these are shown below

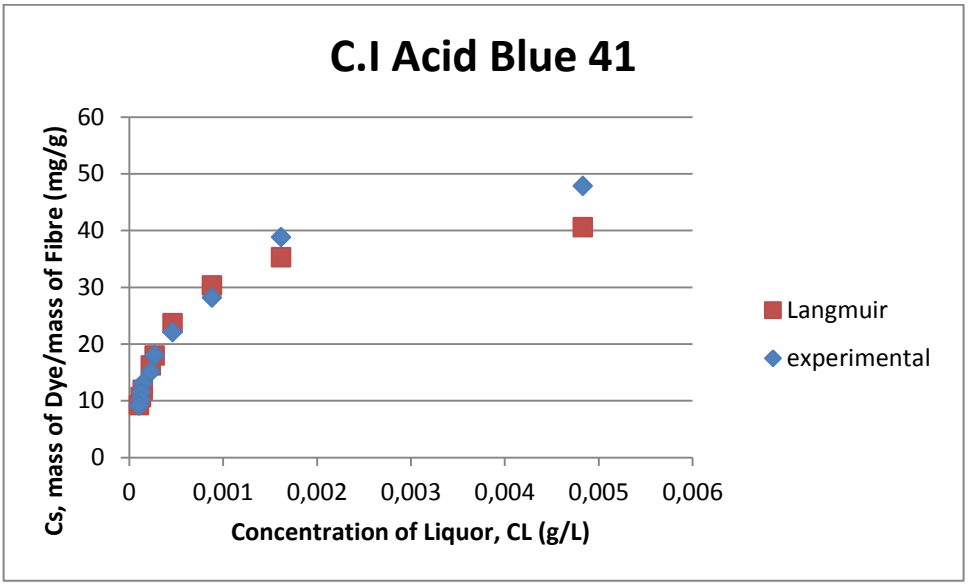

Figure 36: Experimental results and Langmuir sorption isotherm for Acid Blue 41

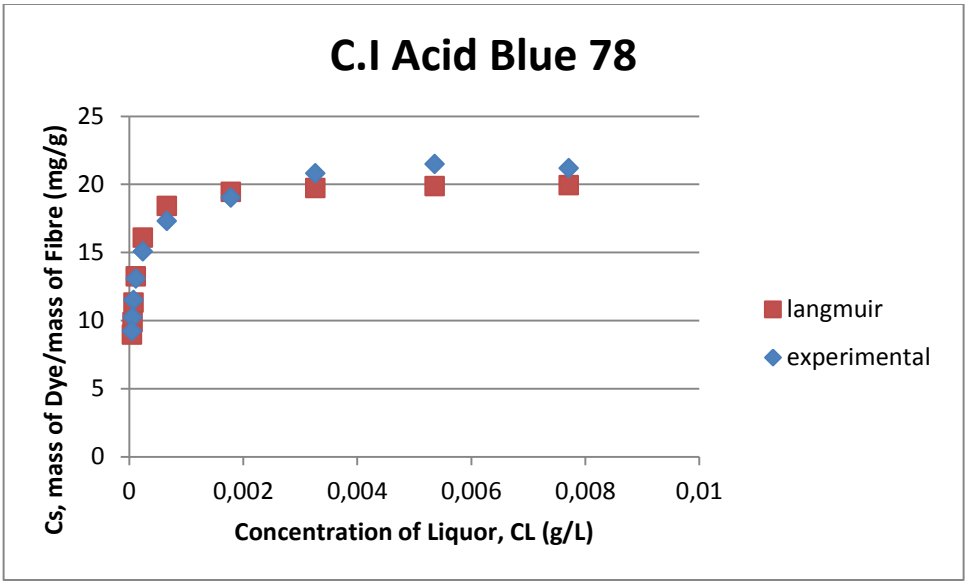

Figure 37: Experimental results and Langmuir sorption isotherm for Acid Blue 78

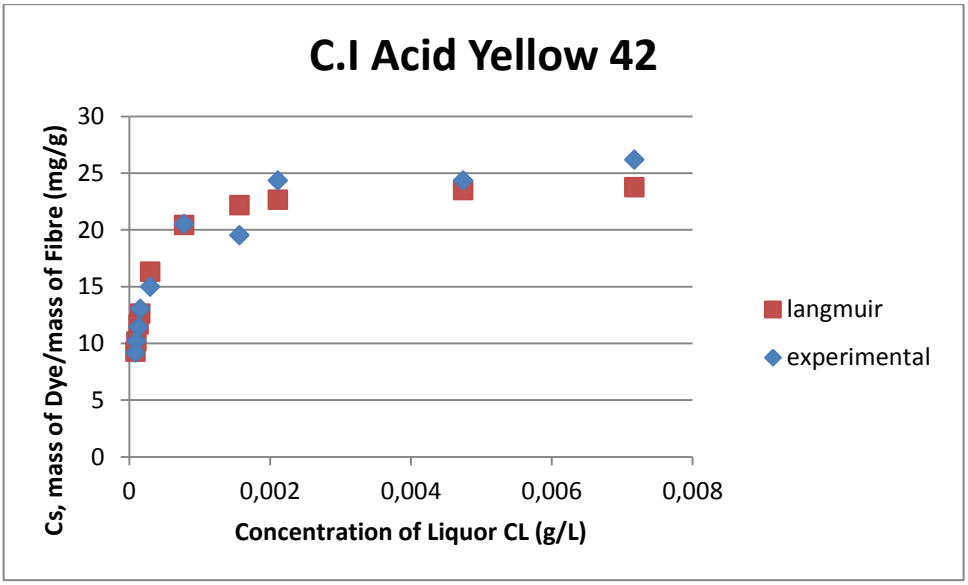

Figure 38: Experimental results and Langmuir sorption isotherm for Acid Yellow 42.

The results in table 12, obtained from the straight line version of Langmuir isotherm showed that the constant S (maximum amount of dye that can be adsorbed) was the highest for Acid Blue 41 and the other two dyes had almost half of the value of Acid Blue 41, this is the

reflection of that in almost all cases the Dye Acid Blue 41 will always have higher values of Sorption capacity, as this is directly proportional to the S values, thus more percentage of Acid Blue 41 is exhausted than for the other two dye. The table also shows the values of K, Acid Blue 78 had the highest value followed by Acid yellow 42 and then Acid Blue 41. Even though these dyes had highest affinity but they had lower S values.

The graphs from figure 36 to figure 38 show the experimental results and the results for the theoretical model. All the graphs were in close agreement with the values and the shapes of the Langmuir isotherm, with very small or ignorable differences that could not be detected at times. Acid Blue 41 had highest Cs values at equilibrium of about 50 mg/g followed by Acid yellow 42 with values of about 26 mg/g and lastly Acid Blue 78 with values of about 22 mg/g. These results were in good agreement with S values following exactly the same trend as the sorption capacity values (Cs), the main reason for this observation is that the two terms are directly proportional to each other according to the relationship by Langmuir isotherm. See below.

$$C_S = \frac{K * CL * S}{(1 + \mathrm{K} * CL)}$$

$$C_s \, \alpha \, S$$

4.5 Images from scanning electron microscope

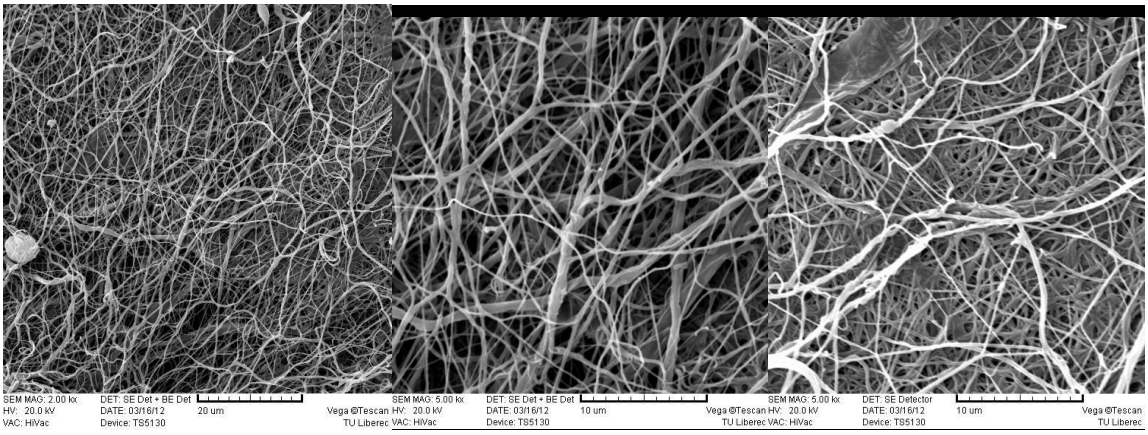

Figure 32: Unused nanofiltration membrane from the scanning electron microscope (SEM)

The above images show the porosity in the nanofiltration membrane and the magnification, the porosity within the single fibres could not be detected using this kind of microscope so it could not be deduced whether it had an effect on the results or not, therefore only the porosity within the fibres was taken into consideration in this study.

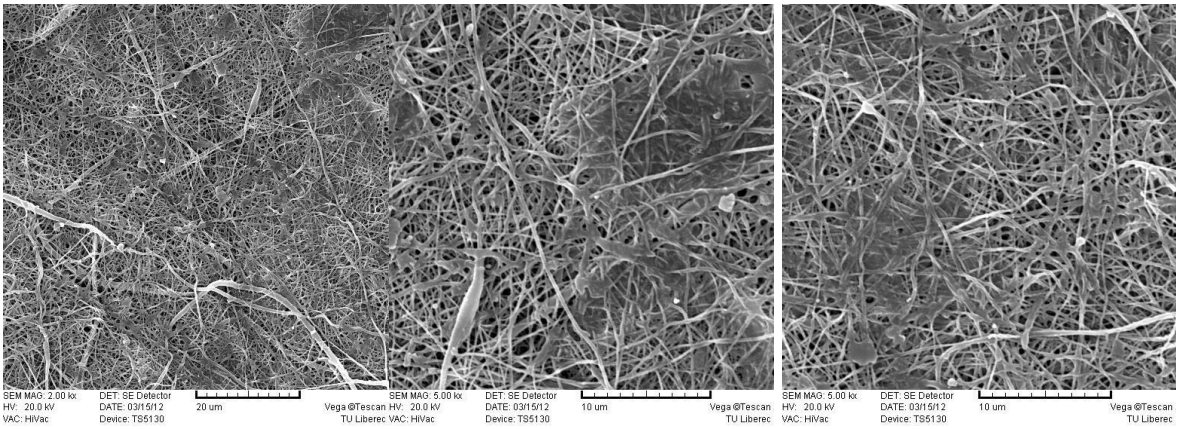

Figure 33: Used nanofiltration membrane from the scanning electron microscope (SEM).

The above figure illustrates the deposition of dye on the surface of the membrane, the only dye that could diffuse through the membrane was the one consisting the particles smaller than the porosity of the membrane, and most of the dye particles could be entrapped at the surface of the membrane.

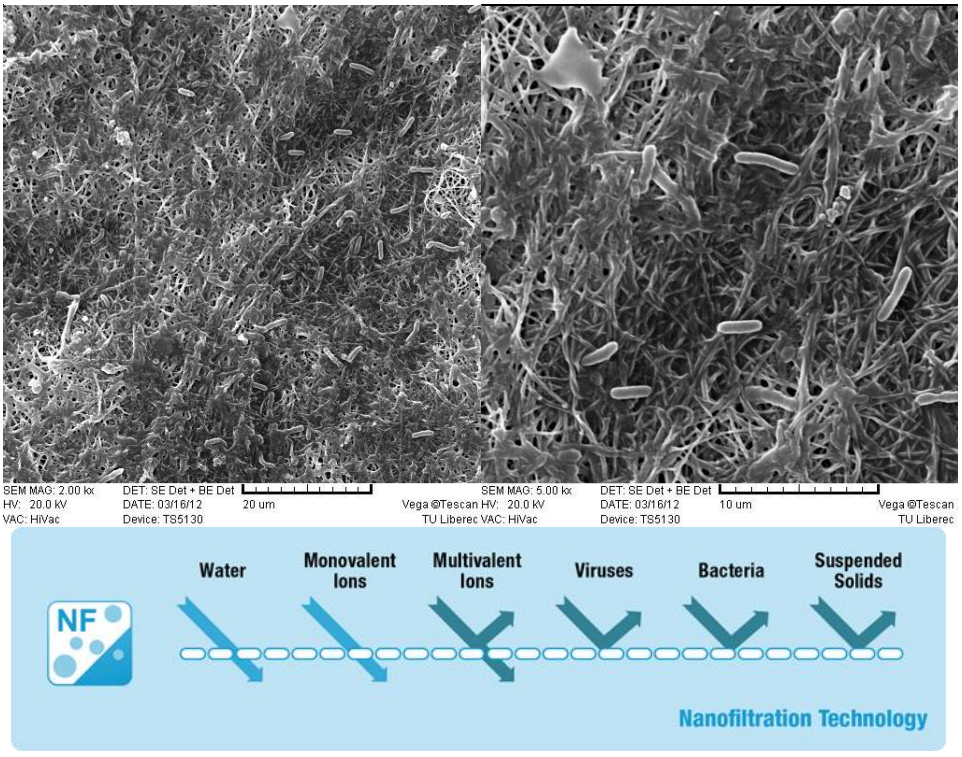

Figure 34: Bacteria entrapped on the membrane surface and also the number of substance that could be filtered using nanofiltration.

In the above figure the bacteria species are entrapped on the surface of the membrane, even though searching the filtration was not aim of the study, the bacteria was captured by

accident. The pore size of the nanofiltration membrane ranges from 0.001µm to 0.01 µm (1 nm to 10 nm) and the smallest bacteria species known as *Mycoplasma Genitalium* has the size of 200 nm to 300 nm, big enough not to make it through the membrane and this was the case during this experiment. Even though the nature of the bacteria itself cannot be identified because it was an accident but no bacteria could pass though the nanofiltration membrane because of the size difference between the two.

5. Conclusion

In conclusion, after the analysis of results of the determination of temperature effects on sorption using three dyes, it was obtained that C.I Acid Blue 41 solution had a high percentage of dye removal, or accumulated on the membrane, followed by C.I Acid Blue 78 and then lastly C.I Acid Yellow 42. This behaviour was observed in almost all temperatures during the study, from a temperature of 20 °C to 60 °C. These results were in good agreement with the molar masses of the dyes, C.I Acid blue 41 has the smallest molar mass, followed by C.I Acid blue 78 and lastly was C.I Acid Yellow 42. The molar mass values could be a good indication to reflect that there is an implication of the dye C.I Acid blue 41 having larger molecules or particles compared to the other two and also that dye C.I Acid yellow 42 had smallest particles than all other investigated dyes.

All the figures showed that accumulated mass of the dye decreases as the temperature increases, till the temperature of about 40 °C such that at higher temperature there is a turn over point such that the accumulated mass is higher at 50 °C but below the one at 20 °C. At the temperature of 60 °C, the accumulated mass was higher than all other temperatures. The reason for this was that above the glass transition temperatures of Polyamide 6 (47°C), there was swelling of the membrane making the pores even smaller for dyes to diffuse. All the dyes tested could follow the Langmuir isotherm of sorption such that the curves for the experiments and the ones for Langmuir isotherm cold be comparable with very small differences. The results also showed that C.I Acid Blue 41 had the highest values of sorption capacity compared to Acid Blue 78 and Acid Yellow 42, this was because of the highest saturation value (S) compared to the other two. The diagrams from the scanning electron microscope (SEM) also showed that large portion of adsorption could occur at the pores between the fibres, according to the results pores decreased in size at temperatures higher than Tg due to swelling.

If the research could be taken further, it would be advisable to do the same experiments at different pH values because it has an effect on the surface charge of the polyamide. Other conditions that could be changed could be the number of fibre layers used, also the equilibrium at different temperature could be tested with the use of the closed system.

6. References

1. Ahmed M. et al. *Effect of structural properties of acid dyes on their adsorption behaviour from aqueous solutions by amine modified silica*, Journal of Hazardous Materials, 161, 1544 – 1550, 2009.
2. Akbari, A. et al. *Treatment of textile dye effluent using a polyamide-based nanofiltration membrane*, Chemical Engineering and Processing, 41, 601 – 609, 2002.
3. Andrady, A.L. *SCIENCE AND TECHNOLOGY OF POLYMER NANOFIBER*, A JOHN WILEY AND SONS, INC., 1 – 100, 2008.
4. BAZBOUZ, M.B. et al. *The Tensile Properties of Electrospun Nylon 6 Single Nanofibers*, Journal of Polymer Science, 48, 1719 – 1731, 2010.
5. Chakraborty, S. et al. *Nanofiltration of textile plant effluent for color removal and reduction in COD*, Separation and Purification Technology, 31, 141 – 151, 2003.
6. Eda, G., Liu, J. et al. *Solvent effects on jet evolution during electrospinning of semi-dilute polystyrene solutions*, European Polymer Journal 43, 1154 – 1167, 2007.
7. Fujihara, K.; Teo, W. et al. *An Introduction to Electrospinning and Nanofibers*, World Scientific Publishing Co. Pte. Ltd, 5 – 100, 2005.
8. Guceri, S. et al. *Nanoengineered Nanofibrous materials*, Kluwer Academic Publishers, 69, 5 – 20, 2003.
9. He, J. Liu, Y. et al. *Electrospun Nanofibres and Their Applications*, Smithers, 1 – 62, 2008.
10. HENCHMAN, R.H. *Diffusion of Small Molecules in Amorphous Glassy Polymers*, DEPARTMENT OF THEORETICAL CHEMISTRY UNIVERSITY OF SYDNEY, 1 – 68, 1995.
11. http://cpe.njit.edu/dlnotes/CHE685/Cls11-1.pdf (12/12/11)
12. http://employees.oneonta.edu/kotzjc/LAB/Spec_intro.pdf (31/01/12)
13. http://pslc.ws/macrog/nysix.htm (29/11/11)
14. http://ulb.upol.cz/tutorial/spectrophotometryold.pdf. (02/02/12).
15. http://www.cee.vt.edu/ewr/environmental/teach/gwprimer/sorp/sorp.html (28/01/12).
16. http://www.chemicalbook.com/ProductChemicalPropertiesCB7719987_EN.htm (02/02/12)
17. http://www.cvg.ca/images/Performance_UV_Vis.pdf (31/01/12)
18. http://www.dharmatrading.com/html/eng/9332935-AA.shtml (28/01/12)
19. http://www.google.cz/search?hl=cs&q=infrared+thermometer&rlz=1R2ACAW_en&gs_sm=c&gs_upl=2122l7067l0l10905l12l9l0l3l3l0l172l1184l1.8l12l0&bav=on.2,or.r_gc.r_pw.,cf. (02/02/12)
20. http://www.google.cz/search?pq=acid+blue+41&hl=cs&cp=12&gs_id=b&xhr=t&q=acid+blue+78&rlz=1R2ACAW_en&gs_upl=&bav=on.2,or.r_gc. (02/02/12)
21. http://www.hoki.ibp.fhg.de/wufi/grundl_poros_e.html (25/01/12)
22. http://www.lookchem.com/C-I-Acid-blue-78/ (02/02/12).
23. http://www.norit.com/norit%20products/activated%20carbon (22/12/11)

24. Mänttäri, M. et al. *Effect of temperature and membrane pre-treatment by pressure on the filtration properties of nanofiltration membranes*, Desalination, 145, 81 – 86, 2002.
25. Maria van Dijk, A.J. *6-aminocapronitrile as analternative monomer for the nylon 6 synthesis*, Technische Universiteit Eindhoven, 297, 1 – 121, 6 June 2006.
26. Nedkova, M. et al. *THE INFLUENCE OF ACID DYES UPON SOME STRUCTURAL AND PHYSICO-MECHANICAL INDICES OF POLYAMIDE FIBRES,* AUTEX Research Journal, vol 5, 1 – 14, 2005.
27. Nilsson, M. et al. *Performance, energy and cost evaluation of a nanofiltration plant operated at elevated temperatures*, Separation and Purification Technology, 60, 36-45, 2007.
28. Ntaka, S., Šašková, J., Wiener, J. *Sorption processes in nanofibers*, 1 – 89, 2011.
29. Robinson, T. et al. *Remediation of dyes in textile e.uent: a critical review on current treatment technologies with a proposed alternative*, Bioresource Technology, 77, 1 – 9, 2001.
30. Sheindof,C.H. et al. *A Freudlich-type multicomponent Isotherm*, Department of chemical engineering, 1 – 7, 1980.
31. WALTER J. WEBER *JR. Adsorption processes*, The University of Michigan, 1 – 18.
32. www.npg6.com/internet/en/html/algemeen/aboutnylon6/aboutnpg6.pshe#10LG1M4CB4442S2A3BDE. (29/11/11).

7. APPENDIX A

Table 5.1: Shows the results that were obtained experimentally and also calculated for the dye C.I Acid blue 41, for the temperature of 20 °C. $A_0 = 0.477$

Number of runs	Time (s)	Absorbance	Conc. After filtration (mg/L)	Change in mass (mg)	Accumulated mass (mg)	Accumulated volume (ml)	% of dye removed
1	14	0.152	3.187	0.0681	0.069	10	68.1
2	15	0.31	6.499	0.0350	0.103	20	35.0
3	15	0.383	8.029	0.0197	0.123	30	19.7
4	15	0.418	8.763	0.0124	0.135	40	12.4
5	16	0.438	9.182	0.0082	0.143	50	8.2
6	16	0.445	9.329	0.0067	0.150	60	6.7
7	17	0.45	9.434	0.0057	0.156	70	5.7
8	16	0.461	9.665	0.0034	0.159	80	3.4
9	16	0.462	9.686	0.0031	0.162	90	3.1
10	17	0.468	9.811	0.0019	0.164	100	1.9
11	17	0.468	9.811	0.0019	0.166	110	1.9
12	18	0.468	9.811	0.0019	0.168	120	1.9
13	18	0.471	9.874	0.0013	0.169	130	1.3
14	18	0.471	9.874	0.0013	0.170	140	1.3
15	19	0.471	9.874	0.0013	0.172	150	1.3
16	19	0.471	9.874	0.0013	0.173	160	1.3
17	20	0.474	9.937	0.0006	0.174	170	0.6
18	20	0.476	9.979	0.0002	0.174	180	0.2
19	20	0.474	9.937	0.0006	0.174	190	0.6
20	20	0.477	10.000	0.0000	0.174	200	0.0
21	21	0.472	9.895	0.0010	0.175	210	1.0
22	20	0.468	9.811	0.0019	0.177	220	1.9
23	20	0.476	9.979	0.0002	0.178	230	0.2
24	21	0.476	9.979	0.0002	0.178	240	0.2
25	22	0.474	9.937	0.0006	0.178	250	0.6
26	22	0.473	9.916	0.0008	0.179	260	0.8
27	23	0.477	10.000	0.0000	0.179	270	0.0
28	23	0.473	9.916	0.0008	0.180	280	0.8
29	23	0.474	9.937	0.0006	0.181	290	0.6
30	23	0.474	9.937	0.0006	0.181	300	0.6

Table 5.2; Shows the results that were obtained experimentally and also calculated for the dye C.I Acid blue 41, for the temperature of 30 °C. $A_0 = 0.49$

Number of runs	Time (s)	Absorbance	Conc. After filtration (mg/L)	Change in mass (mg)	Accumulated mass (mg)	Accumulated volume (ml)	% of dye removed
1	12	0.211	4.306	0.0569	0.057	10	56.9
2	14	0.348	7.102	0.0290	0.086	20	29.0
3	15	0.406	8.286	0.0171	0.103	30	17.1
4	16	0.435	8.878	0.0112	0.114	40	11.2
5	17	0.45	9.184	0.0082	0.122	50	8.2
6	18	0.46	9.388	0.0061	0.129	60	6.1
7	18	0.465	9.490	0.0051	0.134	70	5.1
8	19	0.47	9.592	0.0041	0.138	80	4.1
9	20	0.471	9.612	0.0039	0.142	90	3.9
10	20	0.474	9.673	0.0033	0.145	100	3.3
11	22	0.476	9.714	0.0029	0.148	110	2.9
12	22	0.478	9.755	0.0024	0.150	120	2.4
13	22	0.478	9.755	0.0024	0.153	130	2.4
14	23	0.48	9.796	0.0020	0.155	140	2.0
15	25	0.481	9.816	0.0018	0.157	150	1.8
16	25	0.482	9.837	0.0016	0.158	160	1.6
17	25	0.482	9.837	0.0016	0.160	170	1.6
18	27	0.481	9.816	0.0018	0.162	180	1.8
19	26	0.486	9.918	0.0008	0.162	190	0.8
20	26	0.482	9.837	0.0016	0.164	200	1.6
21	27	0.482	9.837	0.0016	0.166	210	1.6
22	28	0.482	9.837	0.0016	0.167	220	1.6
23	29	0.484	9.878	0.0012	0.169	230	1.2
24	29	0.482	9.837	0.0016	0.170	240	1.6
25	29	0.49	10.000	0.0000	0.170	250	0.0
26	30	0.49	10.000	0.0000	0.170	260	0.0
27	30	0.486	9.918	0.0008	0.171	270	0.8
28	31	0.487	9.939	0.0006	0.172	280	0.6
29	31	0.487	9.939	0.0006	0.172	290	0.6
30	32	0.487	9.939	0.0006	0.173	300	0.6

Table 5.3: Shows the results that were obtained experimentally and also calculated for the dye C.I Acid blue 41, for the temperature of 40 °C. $A_0 = 0.488$

Number of runs	Time (s)	Absorbance	Conc. After filtration (mg/L)	Change in mass (mg)	Accumulated mass (mg)	Accumulated volume (ml)	% of dye removed
1	10	0.227	4.652	0.0535	0.0547	10	53.5
2	11	0.358	7.336	0.0266	0.0801	20	26.6
3	13	0.414	8.484	0.0152	0.0953	30	15.2
4	13	0.44	9.016	0.0098	0.105	40	9.8
5	14	0.455	9.324	0.0068	0.112	50	6.8
6	16	0.466	9.549	0.0045	0.116	60	4.5
7	17	0.471	9.652	0.0035	0.120	70	3.5
8	18	0.473	9.693	0.0031	0.123	80	3.1
9	18	0.478	9.795	0.0020	0.125	90	2.0
10	19	0.483	9.898	0.0010	0.126	100	1.0
11	20	0.479	9.816	0.0018	0.128	110	1.8
12	22	0.484	9.918	0.0008	0.129	120	0.8
13	23	0.482	9.877	0.0012	0.130	130	1.2
14	24	0.481	9.857	0.0014	0.131	140	1.4
15	24	0.487	9.980	0.0002	0.132	150	0.2
16	26	0.484	9.918	0.0008	0.132	160	0.8
17	27	0.482	9.877	0.0012	0.134	170	1.2
18	28	0.483	9.898	0.0010	0.135	180	1.0
19	28	0.489	10.020	-0.0002	0.134	190	-0.2
20	30	0.487	9.980	0.0002	0.135	200	0.2
21	30	0.488	10.000	0.0000	0.135	210	0.0
22	31	0.484	9.918	0.0008	0.136	220	0.8
23	32	0.486	9.959	0.0004	0.136	230	0.4
24	32	0.486	9.959	0.0004	0.136	240	0.4
25	34	0.484	9.918	0.0008	0.137	250	0.8
26	35	0.487	9.980	0.0002	0.137	260	0.2
27	35	0.484	9.918	0.0008	0.138	270	0.8
28	36	0.488	10.000	0.0000	0.138	280	0.0
29	37	0.486	9.959	0.0004	0.139	290	0.4
30	38	0.485	9.939	0.0006	0.139	300	0.6

Table 5.4: Shows the results that were obtained experimentally and also calculated for the dye C.I Acid blue 41, for the temperature of 50 °C. A_0 = 0.506

Number of runs	Time (s)	Absorbance	Conc. After filtration (mg/L)	Change in mass (mg)	Accumulated mass (mg)	Accumulated volume (ml)	% of dye removed
1	9	0.233	4.605	0.0540	0.0543	10	54.0
2	12	0.383	7.569	0.0243	0.0783	20	24.3
3	10	0.429	8.478	0.0152	0.0935	30	15.2
4	11	0.459	9.071	0.0093	0.103	40	9.3
5	11	0.47	9.289	0.0071	0.120	50	7.1
6	13	0.473	9.348	0.0065	0.116	60	6.5
7	13	0.478	9.447	0.0055	0.122	70	5.5
8	14	0.485	9.585	0.0042	0.126	80	4.2
9	14	0.49	9.684	0.0032	0.129	90	3.2
10	14	0.49	9.684	0.0032	0.132	100	3.2
11	14	0.487	9.625	0.0038	0.136	110	3.8
12	15	0.494	9.763	0.0024	0.139	120	2.4
13	16	0.501	9.901	0.0010	0.139	130	1.0
14	17	0.494	9.763	0.0024	0.142	140	2.4
15	18	0.492	9.723	0.0028	0.145	150	2.8
16	18	0.501	9.901	0.0010	0.146	160	1.0
17	19	0.497	9.822	0.0018	0.147	170	1.8
18	19	0.493	9.743	0.0026	0.150	180	2.6
19	19	0.503	9.941	0.0006	0.151	190	0.6
20	20	0.5	9.881	0.0012	0.151	200	1.2
21	20	0.501	9.901	0.0010	0.153	210	1.0
22	20	0.507	10.020	-0.0002	0.153	220	-0.2
23	20	0.51	10.079	-0.0008	0.152	230	-0.8
24	20	0.504	9.960	0.0004	0.152	240	0.4
25	20	0.509	10.059	-0.0006	0.152	250	-0.6
26	20	0.504	9.960	0.0004	0.152	260	0.4
27	20	0.501	9.901	0.0010	0.153	270	1.0
28	20	0.5	9.881	0.0012	0.154	280	1.2
29	19	0.509	10.059	-0.0006	0.154	290	-0.6
30	19	0.507	10.020	-0.0002	0.153	300	-0.2

Table 5.5: Shows the results that were obtained experimentally and also calculated for the dye C.I Acid blue 41, for the temperature of 60 °C. $A_0 = 0.587$

Number of runs	Time (s)	Absorbance	Conc. After filtration (mg/L)	Change in mass (mg)	Accumulated mass (mg)	Accumulated volume (ml)	% of dye removed
1	10	0.257	4.378	0.0562	0.0562	10	56.2
2	19	0.427	7.274	0.0273	0.0835	20	27.3
3	35	0.477	8.126	0.0187	0.102	30	18.7
4	50	0.49	8.348	0.0165	0.119	40	16.5
5	59	0.494	8.416	0.0158	0.135	50	15.8
6	68	0.505	8.603	0.0140	0.149	60	14.0
7	68	0.508	8.654	0.0135	0.162	70	13.5
8	67	0.513	8.739	0.0126	0.175	80	12.6
9	62	0.517	8.807	0.0119	0.187	90	11.9
10	62	0.532	9.063	0.0094	0.196	100	9.4
11	55	0.532	9.063	0.0094	0.205	110	9.4
12	51	0.535	9.114	0.0089	0.214	120	8.9
13	47	0.535	9.114	0.0089	0.223	130	8.9
14	46	0.537	9.148	0.0085	0.232	140	8.5
15	38	0.537	9.148	0.0085	0.240	150	8.5
16	36	0.551	9.387	0.0061	0.246	160	6.1
17	32	0.553	9.421	0.0058	0.252	170	5.8
18	29	0.555	9.455	0.0055	0.257	180	5.5
19	25	0.551	9.387	0.0061	0.264	190	6.1
20	25	0.561	9.557	0.0044	0.268	200	4.4
21	23	0.552	9.404	0.0060	0.274	210	6.0
22	23	0.55	9.370	0.0063	0.280	220	6.3
23	21	0.561	9.557	0.0044	0.285	230	4.4
24	21	0.577	9.830	0.0017	0.286	240	1.7
25	19	0.558	9.506	0.0049	0.291	250	4.9
26	19	0.5574	9.496	0.0050	0.296	260	5.0
27	19	0.584	9.949	0.0005	0.297	270	0.5
28	19	0.585	9.966	0.0003	0.297	280	0.3
29	19	0.58	9.881	0.0012	0.298	290	1.2
30	19	0.58	9.881	0.0012	0.300	300	1.2

Table 6.1: Shows the results that were obtained experimentally and also calculated for the dye C.I Acid yellow 42, for the temperature of 20 ºC. A_0 = 1.373

Number of runs	Time (s)	Absorbance	Conc. After filtration (mg/L)	Change in mass (mg)	Accumulated mass (mg)	Accumulated volume (ml)	% of dye removed
1	13	0.733	5.339	0.0466	0.0466	10	46.6
2	14	1.126	8.201	0.0180	0.0646	20	18.0
3	15	1.222	8.900	0.0110	0.0756	30	11.0
4	16	1.255	9.141	0.0086	0.0842	40	8.6
5	17	1.28	9.323	0.0068	0.0910	50	6.8
6	18	1.287	9.374	0.0063	0.0972	60	6.3
7	20	1.29	9.395	0.0060	0.103	70	6.0
8	21	1.312	9.556	0.0044	0.108	80	4.4
9	24	1.32	9.614	0.0039	0.112	90	3.9
10	25	1.323	9.636	0.0036	0.115	100	3.6
11	28	1.324	9.643	0.0036	0.119	110	3.6
12	31	1.325	9.650	0.0035	0.122	120	3.5
13	34	1.336	9.731	0.0027	0.125	130	2.7
14	37	1.334	9.716	0.0028	0.128	140	2.8
15	42	1.341	9.767	0.0023	0.130	150	2.3
16	48	1.345	9.796	0.0020	0.132	160	2.0
17	54	1.346	9.803	0.0020	0.134	170	2.0
18	60	1.345	9.796	0.0020	0.136	180	2.0
19	68	1.355	9.869	0.0013	0.138	190	1.3
20	78	1.355	9.869	0.0013	0.139	200	1.3
21	89	1.357	9.883	0.0012	0.140	210	1.2
22	100	1.355	9.869	0.0013	0.141	220	1.3
23	115	1.358	9.891	0.0011	0.142	230	1.1
24	133	1.347	9.811	0.0019	0.144	240	1.9
25	144	1.335	9.723	0.0028	0.147	250	2.8
26	153	1.34	9.760	0.0024	0.150	260	2.4
27	158	1.32	9.614	0.0039	0.153	270	3.9
28	189	1.356	9.876	0.0012	0.155	280	1.2
29	207	1.354	9.862	0.0014	0.156	290	1.4
30	231	1.371	9.985	0.0001	0.156	300	0.1

Table 6.2: Shows the results that were obtained experimentally and also calculated for the dye C.I Acid yellow 42, for the temperature of 30 °C. A_0 = 1.383

Number of runs	Time (s)	Absorbance	Conc. After filtration (mg/L)	Change in mass (mg)	Accumulated mass (mg)	Accumulated volume (ml)	% of dye removed
1	11	0.793	5.734	0.0427	0.0427	10	42.7
2	12	1.115	8.062	0.0194	0.0620	20	19.4
3	13	1.228	8.879	0.0112	0.0732	30	11.2
4	14	1.267	9.161	0.0084	0.0816	40	8.4
5	15	1.312	9.487	0.0051	0.0868	50	5.1
6	16	1.33	9.617	0.0038	0.0906	60	3.8
7	18	1.339	9.682	0.0032	0.0938	70	3.2
8	19	1.343	9.711	0.0029	0.0967	80	2.9
9	21	1.346	9.732	0.0027	0.0993	90	2.7
10	22	1.348	9.747	0.0025	0.102	100	2.5
11	23	1.358	9.819	0.0018	0.104	110	1.8
12	25	1.357	9.812	0.0019	0.106	120	1.9
13	28	1.354	9.790	0.0021	0.108	130	2.1
14	31	1.353	9.783	0.0022	0.110	140	2.2
15	34	1.34	9.689	0.0031	0.113	150	3.1
16	34	1.366	9.877	0.0012	0.114	160	1.2
17	39	1.369	9.899	0.0010	0.115	170	1.0
18	45	1.367	9.884	0.0012	0.116	180	1.2
19	48	1.365	9.870	0.0013	0.118	190	1.3
20	53	1.359	9.826	0.0017	0.119	200	1.7
21	62	1.375	9.942	0.0006	0.120	210	0.6
22	65	1.365	9.870	0.0013	0.121	220	1.3
23	75	1.366	9.877	0.0012	0.123	230	1.2
24	77	1.369	9.899	0.0010	0.124	240	1.0
25	84	1.374	9.935	0.0007	0.124	250	0.7
26	99	1.376	9.949	0.0005	0.125	260	0.5
27	115	1.378	9.964	0.0004	0.125	270	0.4
28	129	1.374	9.935	0.0007	0.126	280	0.7
29	139	1.377	9.957	0.0004	0.126	290	0.4
30	157	1.379	9.971	0.0003	0.126	300	0.3

Table 6.3: Shows the results that were obtained experimentally and also calculated for the dye C.I Acid yellow 42, for the temperature of 40 °C. A_0 = 1.383

Number of runs	Time (s)	Absorbance	Conc. After filtration (mg/L)	Change in mass (mg)	Accumulated mass (mg)	Accumulated volume (ml)	% of dye removed
1	10	0.829	5.994	0.0401	0.0402	10	40.1
2	12	1.099	7.946	0.0205	0.0606	20	20.5
3	15	1.229	8.886	0.0111	0.0717	30	11.1
4	17	1.295	9.364	0.0064	0.0781	40	6.4
5	20	1.322	9.559	0.0044	0.0825	50	4.4
6	24	1.348	9.747	0.0025	0.0850	60	2.5
7	28	1.35	9.761	0.0024	0.0874	70	2.4
8	33	1.353	9.783	0.0022	0.0896	80	2.2
9	38	1.361	9.841	0.0016	0.0912	90	1.6
10	44	1.354	9.790	0.0021	0.0933	100	2.1
11	50	1.359	9.826	0.0017	0.0950	110	1.7
12	54	1.363	9.855	0.0014	0.0965	120	1.4
13	61	1.364	9.863	0.0014	0.0978	130	1.4
14	67	1.36	9.834	0.0017	0.0995	140	1.7
15	70	1.374	9.935	0.0007	0.100	150	0.7
16	75	1.372	9.920	0.0008	0.101	160	0.8
17	75	1.378	9.964	0.0004	0.101	170	0.4
18	79	1.374	9.935	0.0007	0.102	180	0.7
19	82	1.376	9.949	0.0005	0.103	190	0.5
20	78	1.379	9.971	0.0003	0.103	200	0.3
21	84	1.38	9.978	0.0002	0.103	210	0.2
22	80	1.376	9.949	0.0005	0.104	220	0.5
23	80	1.372	9.920	0.0008	0.104	230	0.8
24	85	1.378	9.964	0.0004	0.105	240	0.4
25	82	1.379	9.971	0.0003	0.105	250	0.3
26	79	1.38	9.978	0.0002	0.105	260	0.2
27	86	1.379	9.971	0.0003	0.105	270	0.3
28	98	1.375	9.942	0.0006	0.106	280	0.6
29	102	1.372	9.920	0.0008	0.107	290	0.8
30	105	1.377	9.957	0.0004	0.107	300	0.4

Table 6.4: Shows the results that were obtained experimentally and also calculated for the dye C.I Acid yellow 42, for the temperature of 50 °C. A_0 = 1.455

Number of runs	Time (s)	Absorbance	Conc. After filtration (mg/L)	Change in mass (mg)	Accumulated mass (mg)	Accumulated volume (ml)	% of dye removed
1	10	0.859	5.904	0.0410	0.0414	10	41.0
2	12	1.236	8.495	0.0151	0.0560	20	15.1
3	16	1.343	9.230	0.0077	0.0637	30	7.7
4	20	1.353	9.299	0.0070	0.0707	40	7.0
5	28	1.392	9.567	0.0043	0.0751	50	4.3
6	36	1.39	9.553	0.0045	0.0795	60	4.5
7	49	1.39	9.553	0.0045	0.0840	70	4.5
8	58	1.391	9.560	0.0044	0.0884	80	4.4
9	68	1.389	9.546	0.0045	0.0929	90	4.5
10	73	1.393	9.574	0.0043	0.0972	100	4.3
11	81	1.404	9.649	0.0035	0.101	110	3.5
12	88	1.403	9.643	0.0036	0.104	120	3.6
13	75	1.393	9.574	0.0043	0.109	130	4.3
14	81	1.409	9.684	0.0032	0.112	140	3.2
15	81	1.426	9.801	0.0020	0.114	150	2.0
16	82	1.417	9.739	0.0026	0.116	160	2.6
17	86	1.421	9.766	0.0023	0.119	170	2.3
18	85	1.412	9.704	0.0030	0.122	180	3.0
19	81	1.423	9.780	0.0022	0.124	190	2.2
20	80	1.427	9.808	0.0019	0.126	200	1.9
21	82	1.439	9.890	0.0011	0.127	210	1.1
22	77	1.441	9.904	0.0010	0.128	220	1.0
23	72	1.45	9.966	0.0003	0.128	230	0.3
24	77	1.429	9.821	0.0018	0.130	240	1.8
25	77	1.45	9.966	0.0003	0.130	250	0.3
26	83	1.449	9.959	0.0004	0.131	260	0.4
27	83	1.443	9.918	0.0008	0.132	270	0.8
28	81	1.446	9.938	0.0006	0.132	280	0.6
29	73	1.448	9.952	0.0005	0.133	290	0.5
30	70	1.446	9.938	0.0006	0.133	300	0.6

Table 6.5: Shows the results that were obtained experimentally and also calculated for the dye C.I Acid yellow 42, for the temperature of 60 °C. A_0 = 1.672

Number of runs	Time (s)	Absorbance	Conc. After filtration (mg/L)	Change in mass (mg)	Accumulated mass (mg)	Accumulated volume (ml)	% of dye removed
1	10	1.002	5.993	0.0401	0.0401	10	40.1
2	18	1.35	8.074	0.0193	0.0593	20	19.3
3	37	1.435	8.583	0.0142	0.0735	30	14.2
4	52	1.465	8.762	0.0124	0.0859	40	12.4
5	62	1.466	8.768	0.0123	0.0982	50	12.3
6	68	1.46	8.732	0.0127	0.111	60	12.7
7	69	1.464	8.756	0.0124	0.123	70	12.4
8	69	1.484	8.876	0.0112	0.135	80	11.2
9	71	1.481	8.858	0.0114	0.146	90	11.4
10	64	1.506	9.007	0.0099	0.156	100	9.9
11	59	1.522	9.103	0.0090	0.165	110	9.0
12	59	1.518	9.079	0.0092	0.174	120	9.2
13	54	1.518	9.079	0.0092	0.183	130	9.2
14	48	1.539	9.205	0.0080	0.191	140	8.0
15	47	1.56	9.330	0.0067	0.198	150	6.7
16	44	1.558	9.318	0.0068	0.205	160	6.8
17	39	1.559	9.324	0.0068	0.212	170	6.8
18	39	1.553	9.288	0.0071	0.219	180	7.1
19	37	1.573	9.408	0.0059	0.225	190	5.9
20	36	1.595	9.539	0.0046	0.229	200	4.6
21	34	1.596	9.545	0.0045	0.234	210	4.5
22	33	1.596	9.545	0.0045	0.238	220	4.5
23	33	1.599	9.563	0.0044	0.243	230	4.4
24	31	1.61	9.629	0.0037	0.246	240	3.7
25	28	1.62	9.689	0.0031	0.250	250	3.1
26	29	1.64	9.809	0.0019	0.251	260	1.9
27	29	1.64	9.809	0.0019	0.253	270	1.9
28	28	1.643	9.827	0.0017	0.255	280	1.7
29	25	1.649	9.862	0.0014	0.256	290	1.4
30	25	1.65	9.868	0.0013	0.258	300	1.3

Table 7.1: Shows the results that were obtained experimentally and also calculated for the dye C.I Acid blue 78 , for the temperature of 20 °C. A_0 =1.003

Number of runs	Time (s)	Absorbance	Conc. After filtration (mg/L)	Change in mass (mg)	Accumulated mass (mg)	Accumulated volume (ml)	% of dye removed
1	14	0.412	4.108	0.0589	0.0597	10	58.9
2	14	0.744	7.418	0.0258	0.0847	20	25.8
3	15	0.898	8.953	0.0105	0.0952	30	10.5
4	15	0.944	9.412	0.0059	0.101	40	5.9
5	15	0.972	9.691	0.0031	0.104	50	3.1
6	16	0.978	9.751	0.0025	0.107	60	2.5
7	15	0.977	9.741	0.0026	0.109	70	2.6
8	15	0.978	9.751	0.0025	0.112	80	2.5
9	16	0.977	9.741	0.0026	0.114	90	2.6
10	16	0.982	9.791	0.0021	0.117	100	2.1
11	16	0.986	9.831	0.0017	0.118	110	1.7
12	16	0.985	9.821	0.0018	0.120	120	1.8
13	17	0.988	9.850	0.0015	0.121	130	1.5
14	17	0.985	9.821	0.0018	0.123	140	1.8
15	17	0.98	9.771	0.0023	0.126	150	2.3
16	17	0.98	9.771	0.0023	0.128	160	2.3
17	17	0.988	9.850	0.0015	0.129	170	1.5
18	17	0.989	9.860	0.0014	0.131	180	1.4
19	18	0.987	9.840	0.0016	0.132	190	1.6
20	18	0.99	9.870	0.0013	0.134	200	1.3
21	18	1.001	9.980	0.0002	0.134	210	0.2
22	18	0.997	9.940	0.0006	0.134	220	0.6
23	19	0.997	9.940	0.0006	0.135	230	0.6
24	19	0.999	9.960	0.0004	0.135	240	0.4
25	19	0.996	9.930	0.0007	0.136	250	0.7
26	20	0.994	9.910	0.0009	0.137	260	0.9
27	20	0.999	9.960	0.0004	0.137	270	0.4
28	20	1.001	9.980	0.0002	0.138	280	0.2
29	21	1	9.970	0.0003	0.138	290	0.3
30	21	1.008	10.050	-0.0005	0.137	300	-0.5

Table 7.2: Shows the results that were obtained experimentally and also calculated for the dye C.I Acid blue 78 , for the temperature of 30 °C. A_0 = 1.019

Number of runs	Time (s)	Absorbance	Conc. After filtration (mg/L)	Change in mass (mg)	Accumulated mass (mg)	Accumulated volume (ml)	% of dye removed
1	11	0.569	5.584	0.0442	0.0442	10	44.2
2	12	0.837	8.214	0.0179	0.0620	20	17.9
3	13	0.942	9.244	0.0076	0.0696	30	7.6
4	14	0.97	9.519	0.0048	0.0744	40	4.8
5	13	0.985	9.666	0.0033	0.0777	50	3.3
6	14	0.998	9.794	0.0021	0.0798	60	2.1
7	14	1.001	9.823	0.0018	0.0816	70	1.8
8	14	1.001	9.823	0.0018	0.0833	80	1.8
9	15	1.002	9.833	0.0017	0.0850	90	1.7
10	16	1.003	9.843	0.0016	0.0866	100	1.6
11	16	1.009	9.902	0.0010	0.0875	110	1.0
12	17	1.006	9.872	0.0013	0.0888	120	1.3
13	17	1.006	9.872	0.0013	0.0901	130	1.3
14	19	1.008	9.892	0.0011	0.0912	140	1.1
15	20	0.999	9.804	0.0020	0.0931	150	2.0
16	20	1.013	9.941	0.0006	0.0937	160	0.6
17	23	1.011	9.921	0.0008	0.0945	170	0.8
18	25	1.006	9.872	0.0013	0.0958	180	1.3
19	28	1.009	9.902	0.0010	0.0968	190	1.0
20	32	1.008	9.892	0.0011	0.0978	200	1.1
21	37	1.007	9.882	0.0012	0.0990	210	1.2
22	42	1.005	9.863	0.0014	0.100	220	1.4
23	48	1.019	10.000	0.0000	0.100	230	0.0
24	56	1.02	10.010	-0.0001	0.100	240	-0.1
25	65	1.01	9.912	0.0009	0.101	250	0.9
26	76	1.015	9.961	0.0004	0.102	260	0.4
27	85	1.009	9.902	0.0010	0.103	270	1.0
28	94	1.009	9.902	0.0010	0.104	280	1.0
29	104	1.024	10.049	-0.0005	0.103	290	-0.5
30	112	1.015	9.961	0.0004	0.103	300	0.4

Table 7.3: Shows the results that were obtained experimentally and also calculated for the dye C.I Acid blue 78 , for the temperature of 40 °C. A_0 = 1.046

Number of runs	Time (s)	Absorbance	Conc. After filtration (mg/L)	Change in mass (mg)	Accumulated mass (mg)	Accumulated volume (ml)	% of dye removed
1	10	0.609	5.822	0.0418	0.0418	10	41.8
2	12	0.886	8.470	0.0153	0.0571	20	15.3
3	12	0.986	9.426	0.0057	0.0628	30	5.7
4	12	0.999	9.551	0.0045	0.0673	40	4.5
5	13	1.015	9.704	0.0030	0.0703	50	3.0
6	14	1.026	9.809	0.0019	0.0722	60	1.9
7	16	1.02	9.751	0.0025	0.0747	70	2.5
8	14	1.024	9.790	0.0021	0.0768	80	2.1
9	15	1.03	9.847	0.0015	0.0783	90	1.5
10	20	1.026	9.809	0.0019	0.0802	100	1.9
11	21	1.027	9.818	0.0018	0.0820	110	1.8
12	24	1.025	9.799	0.0020	0.0840	120	2.0
13	25	1.025	9.799	0.0020	0.0860	130	2.0
14	26	1.029	9.837	0.0016	0.0877	140	1.6
15	29	1.029	9.837	0.0016	0.0893	150	1.6
16	31	1.039	9.933	0.0007	0.0900	160	0.7
17	33	1.039	9.933	0.0007	0.0906	170	0.7
18	36	1.027	9.818	0.0018	0.0924	180	1.8
19	39	1.027	9.818	0.0018	0.0943	190	1.8
20	43	1.03	9.847	0.0015	0.0958	200	1.5
21	49	1.029	9.837	0.0016	0.0974	210	1.6
22	50	1.029	9.837	0.0016	0.0990	220	1.6
23	51	1.039	9.933	0.0007	0.0997	230	0.7
24	55	1.038	9.924	0.0008	0.101	240	0.8
25	61	1.035	9.895	0.0011	0.102	250	1.1
26	59	1.045	9.990	0.0001	0.102	260	0.1
27	61	1.044	9.981	0.0002	0.102	270	0.2
28	62	1.039	9.933	0.0007	0.103	280	0.7
29	62	1.049	10.029	-0.0003	0.102	290	-0.3
30	59	1.049	10.029	-0.0003	0.102	300	-0.3

Table 7.4: Shows the results that were obtained experimentally and also calculated for the dye C.I Acid blue 78 , for the temperature of 50 °C. A_0 = 1.102

Number of runs	Time (s)	Absorbance	Conc. After filtration (mg/L)	Change in mass (mg)	Accumulated mass (mg)	Accumulated volume (ml)	% of dye removed
1	9	0.619	5.617	0.0438	0.0438	10	43.8
2	9	0.925	8.394	0.0161	0.0599	20	16.1
3	10	1.003	9.102	0.0090	0.0689	30	9.0
4	11	1.023	9.283	0.0072	0.0760	40	7.2
5	11	1.042	9.456	0.0054	0.0815	50	5.4
6	13	1.045	9.483	0.0052	0.0867	60	5.2
7	15	1.04	9.437	0.0056	0.0923	70	5.6
8	14	1.051	9.537	0.0046	0.0969	80	4.6
9	19	1.05	9.528	0.0047	0.102	90	4.7
10	21	1.049	9.519	0.0048	0.106	100	4.8
11	23	1.051	9.537	0.0046	0.111	110	4.6
12	26	1.043	9.465	0.0054	0.116	120	5.4
13	31	1.057	9.592	0.0041	0.121	130	4.1
14	36	1.054	9.564	0.0044	0.125	140	4.4
15	44	1.06	9.619	0.0038	0.129	150	3.8
16	53	1.064	9.655	0.0034	0.132	160	3.4
17	64	1.064	9.655	0.0034	0.136	170	3.4
18	77	1.062	9.637	0.0036	0.139	180	3.6
19	84	1.069	9.701	0.0030	0.142	190	3.0
20	84	1.06	9.619	0.0038	0.146	200	3.8
21	86	1.073	9.737	0.0026	0.149	210	2.6
22	85	1.073	9.737	0.0026	0.151	220	2.6
23	82	1.071	9.719	0.0028	0.154	230	2.8
24	83	1.079	9.791	0.0021	0.156	240	2.1
25	61	1.094	9.927	0.0007	0.157	250	0.7
26	61	1.071	9.719	0.0028	0.160	260	2.8
27	61	1.103	10.009	-0.0001	0.160	270	-0.1
28	62	1.106	10.036	-0.0004	0.160	280	-0.4
29	59	1.102	10.000	0.0000	0.160	290	0.0
30	55	1.104	10.018	-0.0002	0.159	300	-0.2

Table 7.5: Shows the results that were obtained experimentally and also calculated for the dye C.I Acid blue 78 , for the temperature of 60 °C. A_0 = 1.209

Number of runs	Time (s)	Absorbance	Conc. After filtration (mg/L)	Change in mass (mg)	Accumulated mass (mg)	Accumulated volume (ml)	% of dye removed
1	9	0.535	4.425	0.0557	0.0557	10	55.7
2	15	0.936	7.742	0.0226	0.0783	20	22.6
3	28	1.025	8.478	0.0152	0.0935	30	15.2
4	40	1.043	8.627	0.0137	0.107	40	13.7
5	48	1.04	8.602	0.0140	0.121	50	14.0
6	50	1.048	8.668	0.0133	0.135	60	13.3
7	51	1.051	8.693	0.0131	0.148	70	13.1
8	51	1.06	8.768	0.0123	0.160	80	12.3
9	54	1.073	8.875	0.0112	0.171	90	11.2
10	52	1.076	8.900	0.0110	0.182	100	11.0
11	50	1.081	8.941	0.0106	0.193	110	10.6
12	47	1.091	9.024	0.0098	0.203	120	9.8
13	44	1.098	9.082	0.0092	0.212	130	9.2
14	44	1.106	9.148	0.0085	0.220	140	8.5
15	40	1.105	9.140	0.0086	0.229	150	8.6
16	39	1.113	9.206	0.0079	0.237	160	7.9
17	35	1.118	9.247	0.0075	0.244	170	7.5
18	35	1.12	9.264	0.0074	0.252	180	7.4
19	33	1.13	9.347	0.0065	0.258	190	6.5
20	30	1.137	9.404	0.0060	0.264	200	6.0
21	28	1.144	9.462	0.0054	0.270	210	5.4
22	25	1.147	9.487	0.0051	0.275	220	5.1
23	25	1.164	9.628	0.0037	0.278	230	3.7
24	24	1.17	9.677	0.0032	0.282	240	3.2
25	22	1.169	9.669	0.0033	0.285	250	3.3
26	22	1.177	9.735	0.0026	0.288	260	2.6
27	19	1.18	9.760	0.0024	0.290	270	2.4
28	20	1.209	10.000	0.0000	0.290	280	0.0
29	19	1.208	9.992	0.0001	0.290	290	0.1
30	19	1.217	10.066	-0.0007	0.289	300	-0.7

Table 9: The determination of sorption capacity of nanofibrous membrane using Acid blue 41, $A_0 = 0.476$.

mass of nanofibers (g)	absorbance	conc of filtrate (g/L)	% Exhaustion	mass of Dye in Fibre (g)	m_d/m_f Cs mg/g
0.0108	0.23	0.00483	51.681	0.000517	47.852
0.0216	0.077	0.00162	83.824	0.000838	38.807
0.0324	0.042	0.00088	91.176	0.000912	28.141
0.0432	0.022	0.00046	95.378	0.000954	22.078
0.054	0.013	0.00027	97.269	0.000973	18.013
0.0648	0.011	0.00023	97.689	0.000977	15.075
0.0756	0.007	0.00015	98.529	0.000985	13.033
0.0864	0.006	0.00013	98.739	0.000987	11.428
0.0972	0.006	0.00013	98.739	0.000987	10.158
0.108	0.005	0.00011	98.950	0.000989	9.162

Table 10: The determination of sorption capacity of nanofibrous membrane using Acid blue 78, $A_0 = 1.032$. (corresponds to figure 28)

mass of nanofibers (g)	absorbance	conc of filtrate (g/L)	% Exhaustion	mass of dye in Fibre (g)	m_d/m_f, Cs mg/g
0.0108	0.796	0.0077	22.868	0.000229	21.174
0.0216	0.553	0.0054	46.415	0.000464	21.488
0.0324	0.337	0.0033	67.345	0.000673	20.785
0.0432	0.184	0.0018	82.171	0.000822	19.021
0.054	0.068	0.0007	93.411	0.000934	17.298
0.0648	0.025	0.0002	97.578	0.000976	15.058
0.0756	0.012	0.0001	98.837	0.000988	13.074
0.0864	0.008	0.0001	99.225	0.000992	11.484
0.0972	0.006	0.0001	99.419	0.000994	10.228
0.108	0.005	0.0000	99.516	0.000995	9.214

Table 11: The determination of sorption capacity of nanofibrous membrane using Acid Yellow 42, A_0 = 1.334. (Corresponds to figure 29)

mass of nanofibers (g)	absorbance	conc of filtrate (g/L)	% Exhaustion	mass of dye in F (g)	m_d/m_f, Cs (mg/g)
0.0108	0.957	0.007	28.261	0.000283	26.167
0.0216	0.633	0.005	52.549	0.000525	24.328
0.0324	0.282	0.002	78.861	0.000789	24.340
0.0432	0.209	0.002	84.333	0.000843	19.521
0.045	0.104	0.001	92.204	0.000922	20.490
0.0648	0.04	0.000	97.001	0.000970	14.969
0.0756	0.021	0.000	98.426	0.000984	13.019
0.0864	0.018	0.000	98.651	0.000987	11.418
0.0972	0.014	0.000	98.951	0.000990	10.180
0.108	0.012	0.000	99.100	0.000991	9.176

APPENDIX B

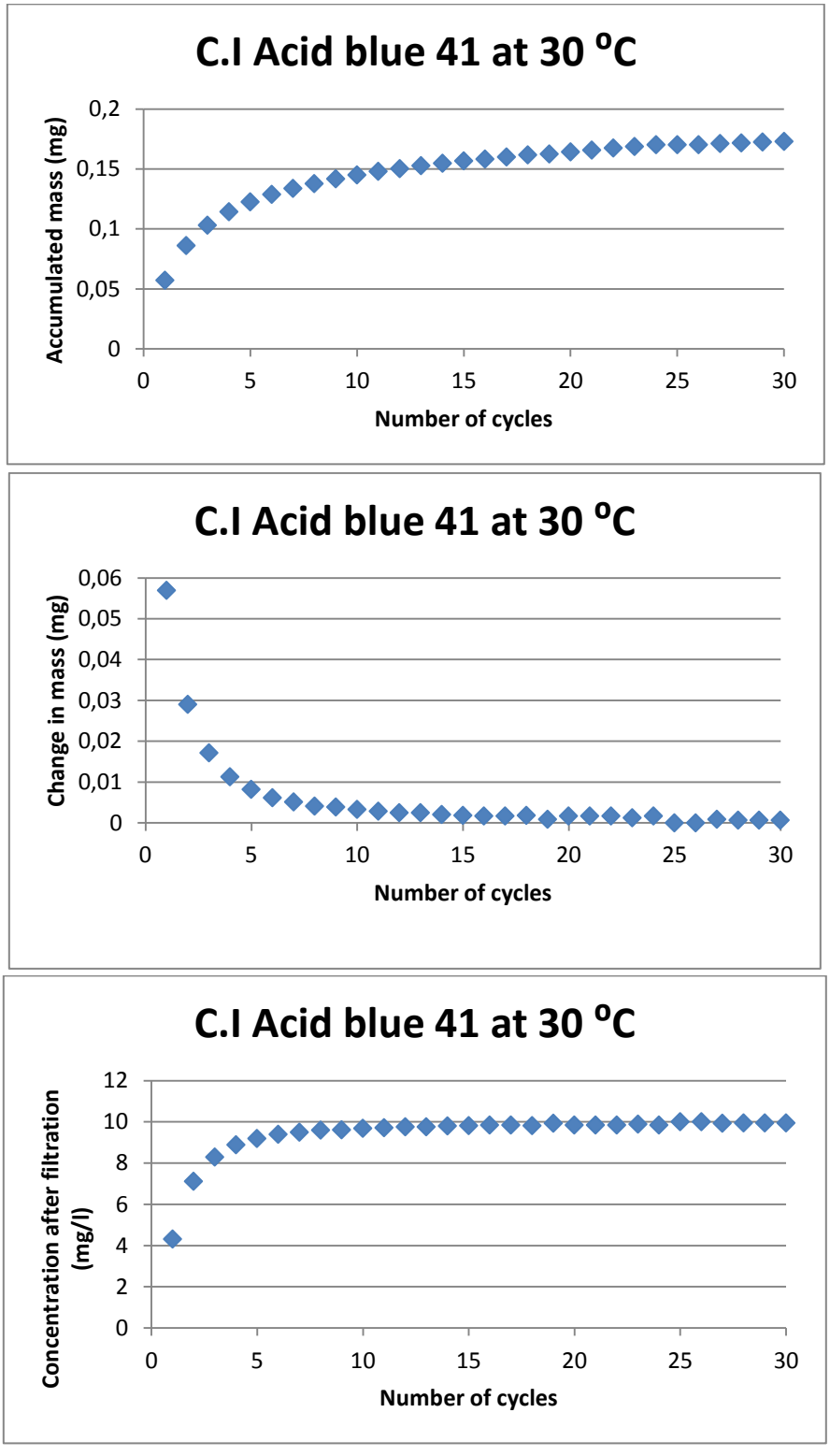

Figure 22.2: Shows the graphical representation of the effects of filtration

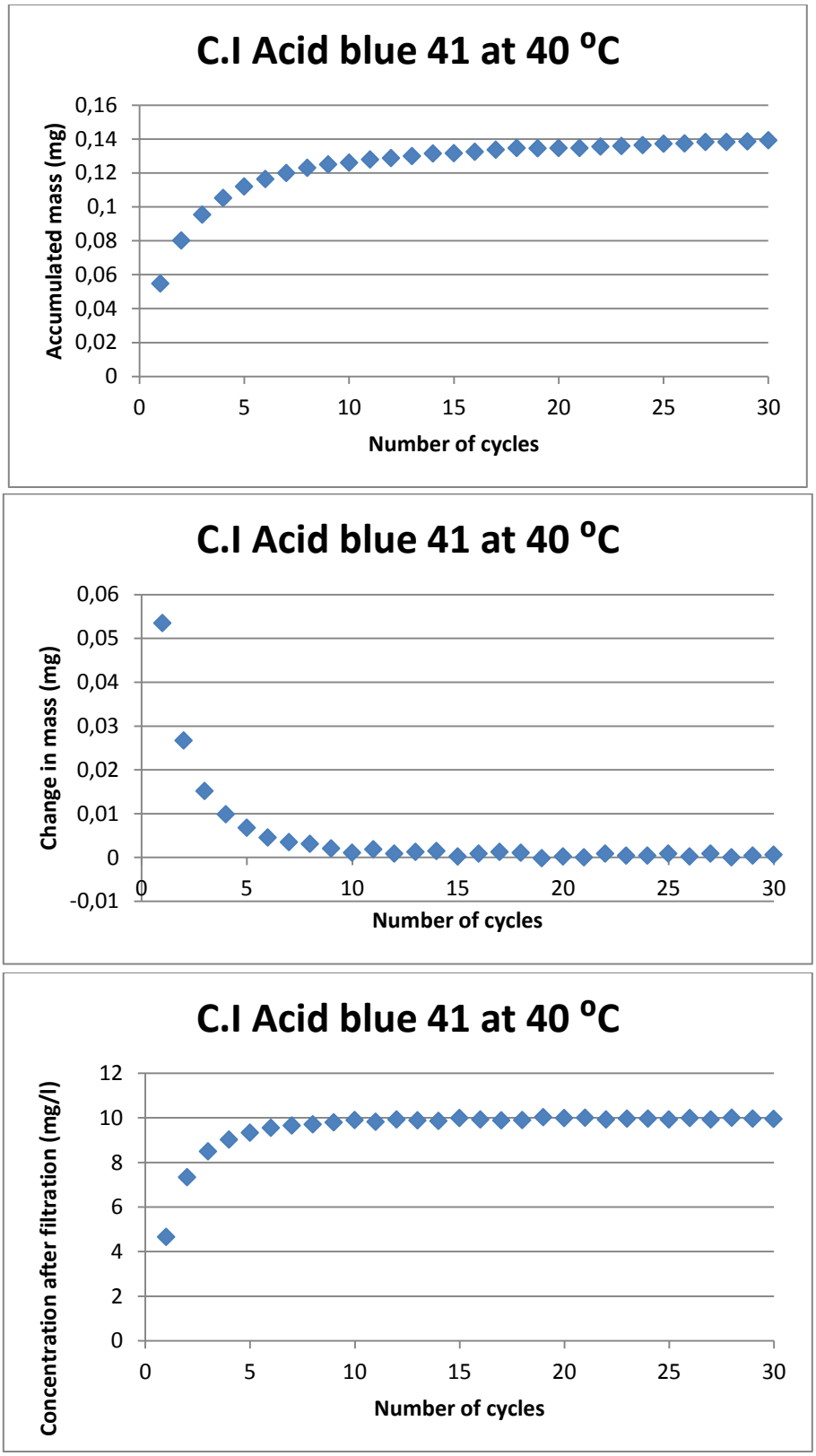

Figure 22.3: Shows the graphical representation of the effects of filtration

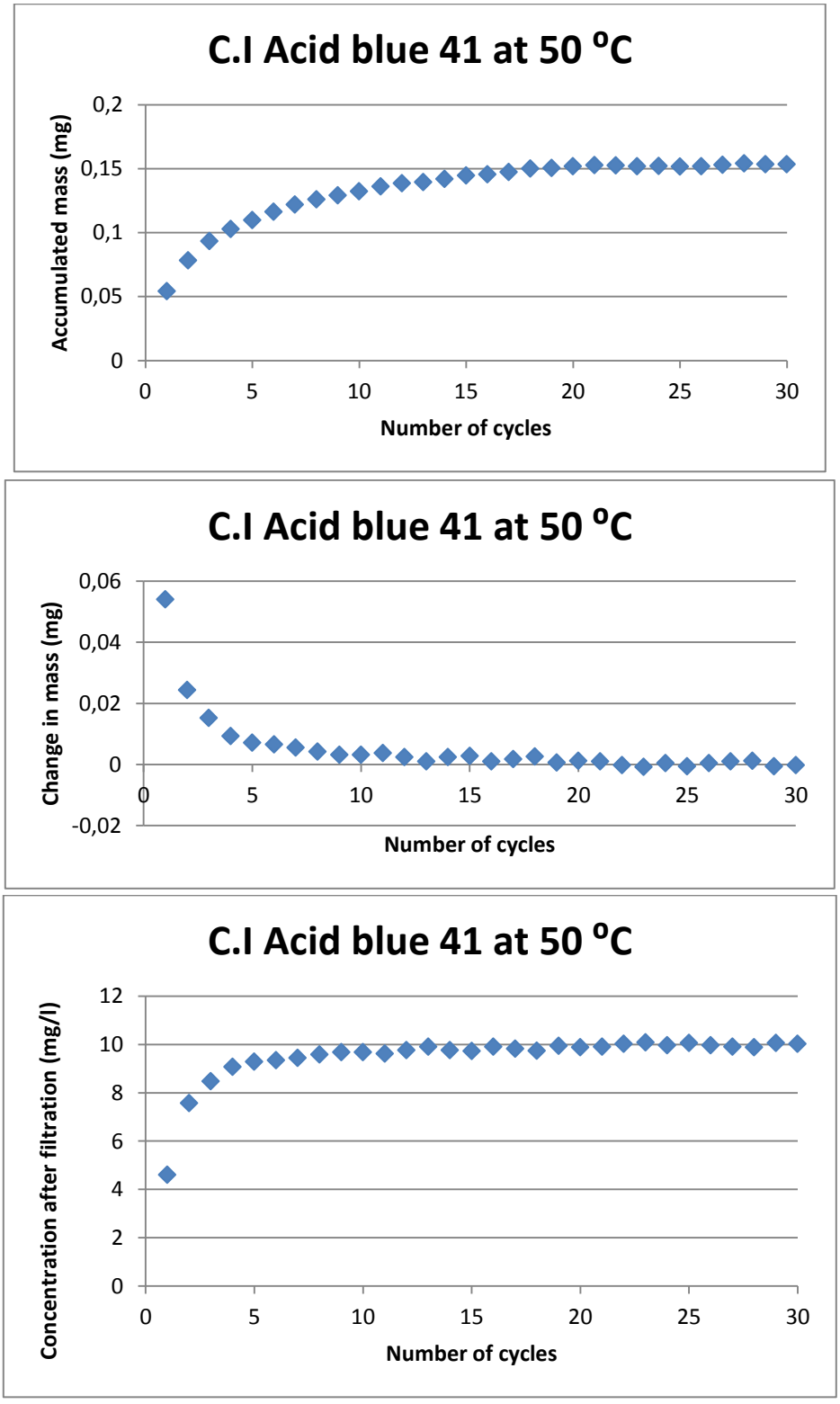

Figure 22.4: Shows the graphical representation of the effects of filtration

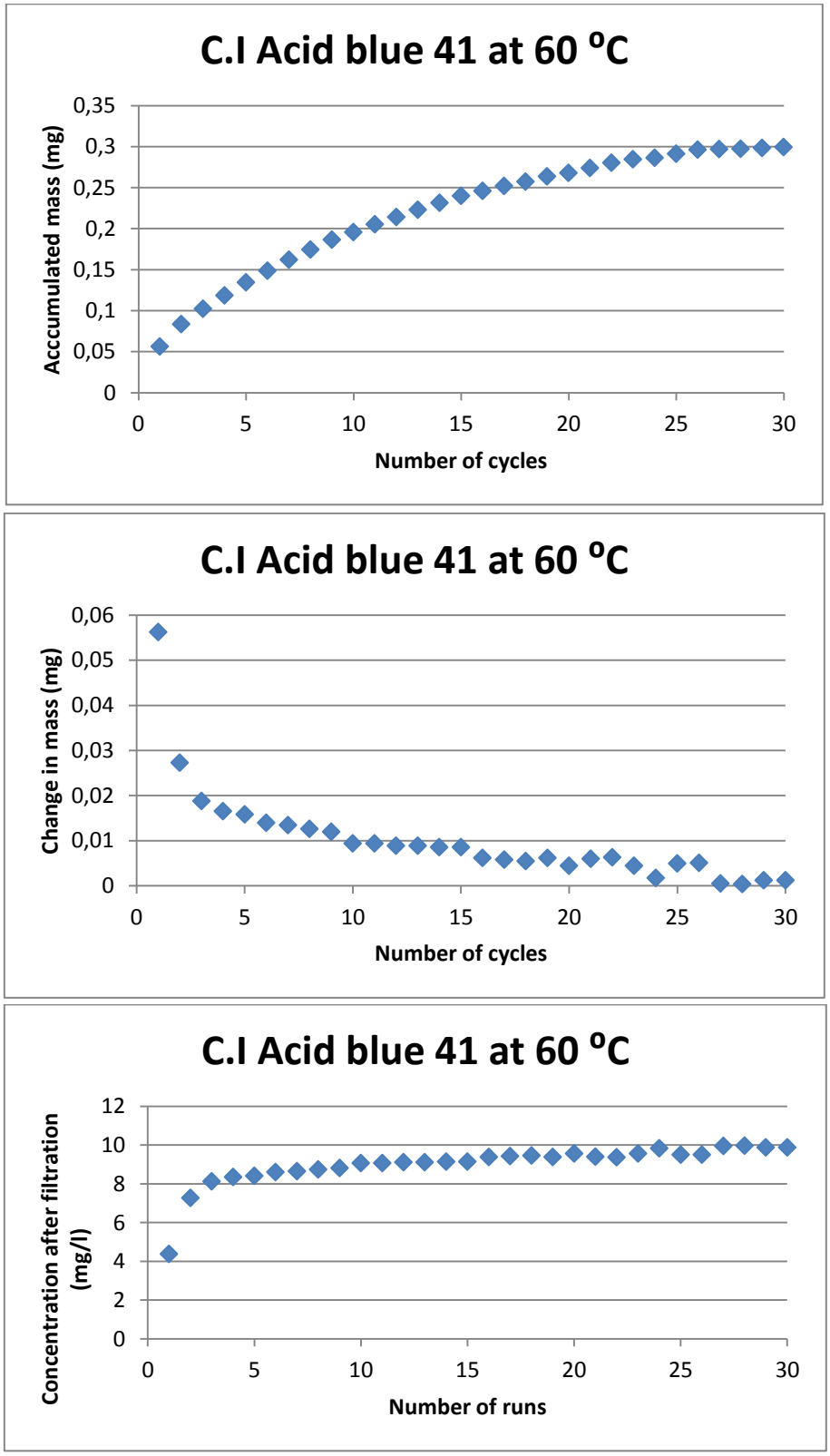

Figure 22.5 : Shows the graphical representation of the effects of filtration

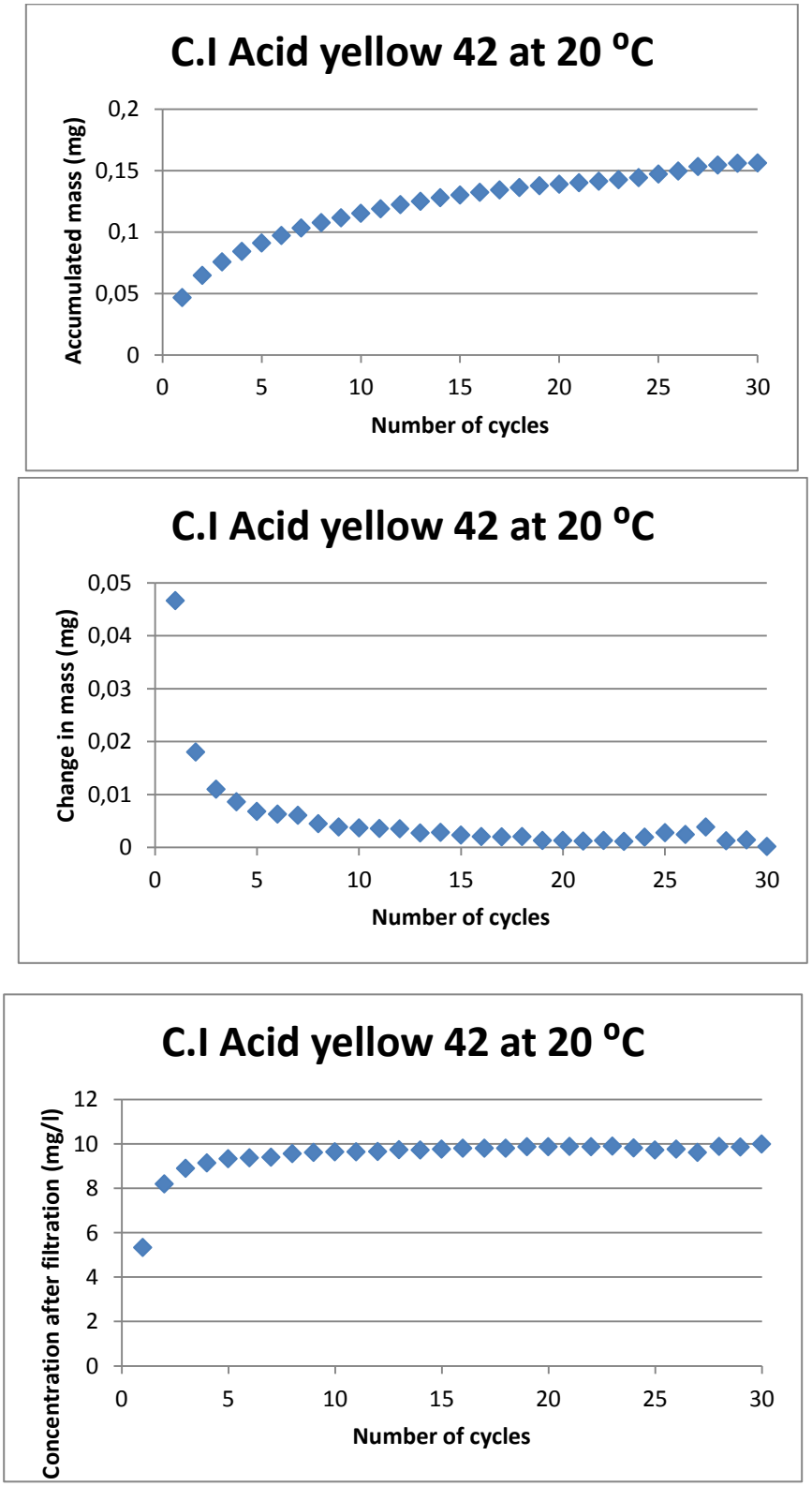

Figure 23.1: Shows the graphical representation of the effects of filtration

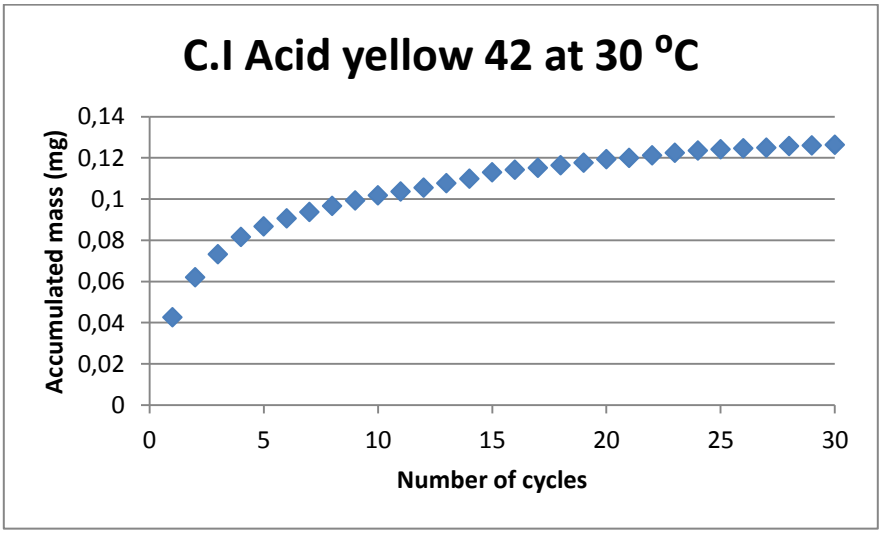

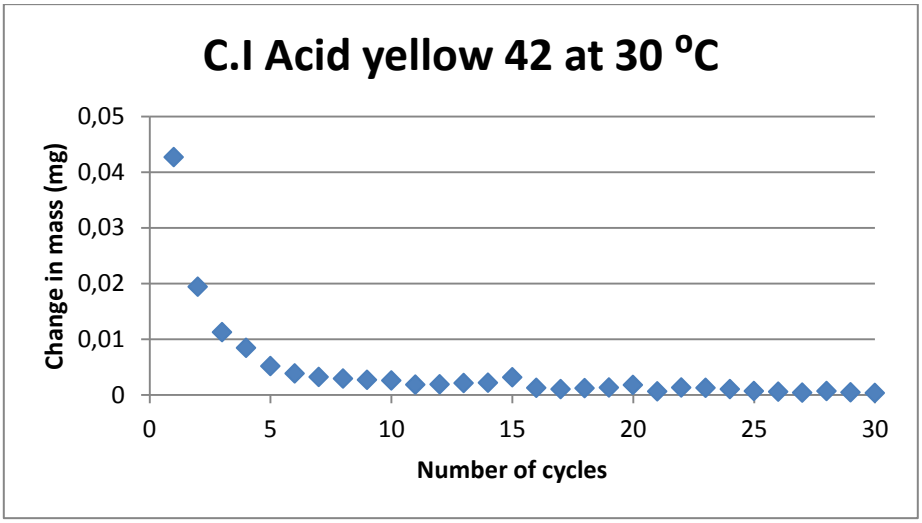

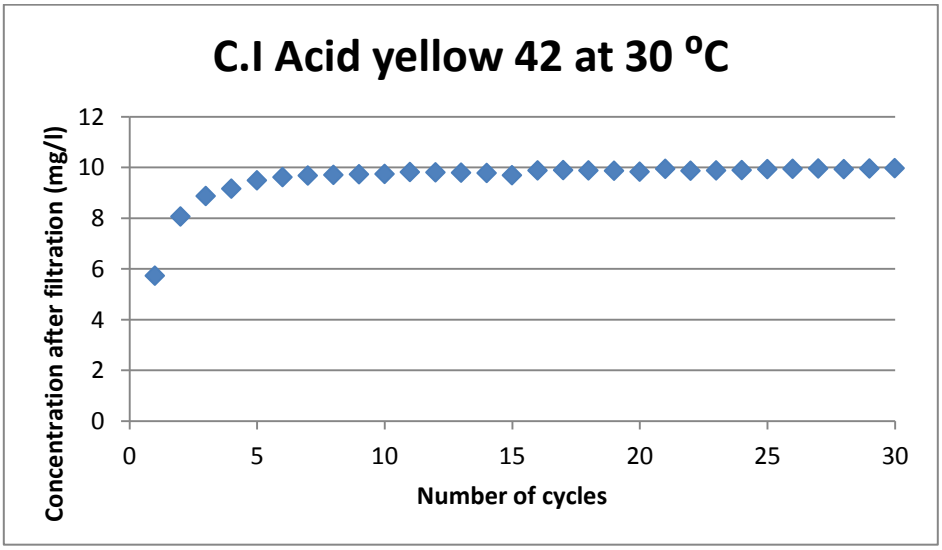

Figure 23.2: Shows the graphical representation of the effects of filtration

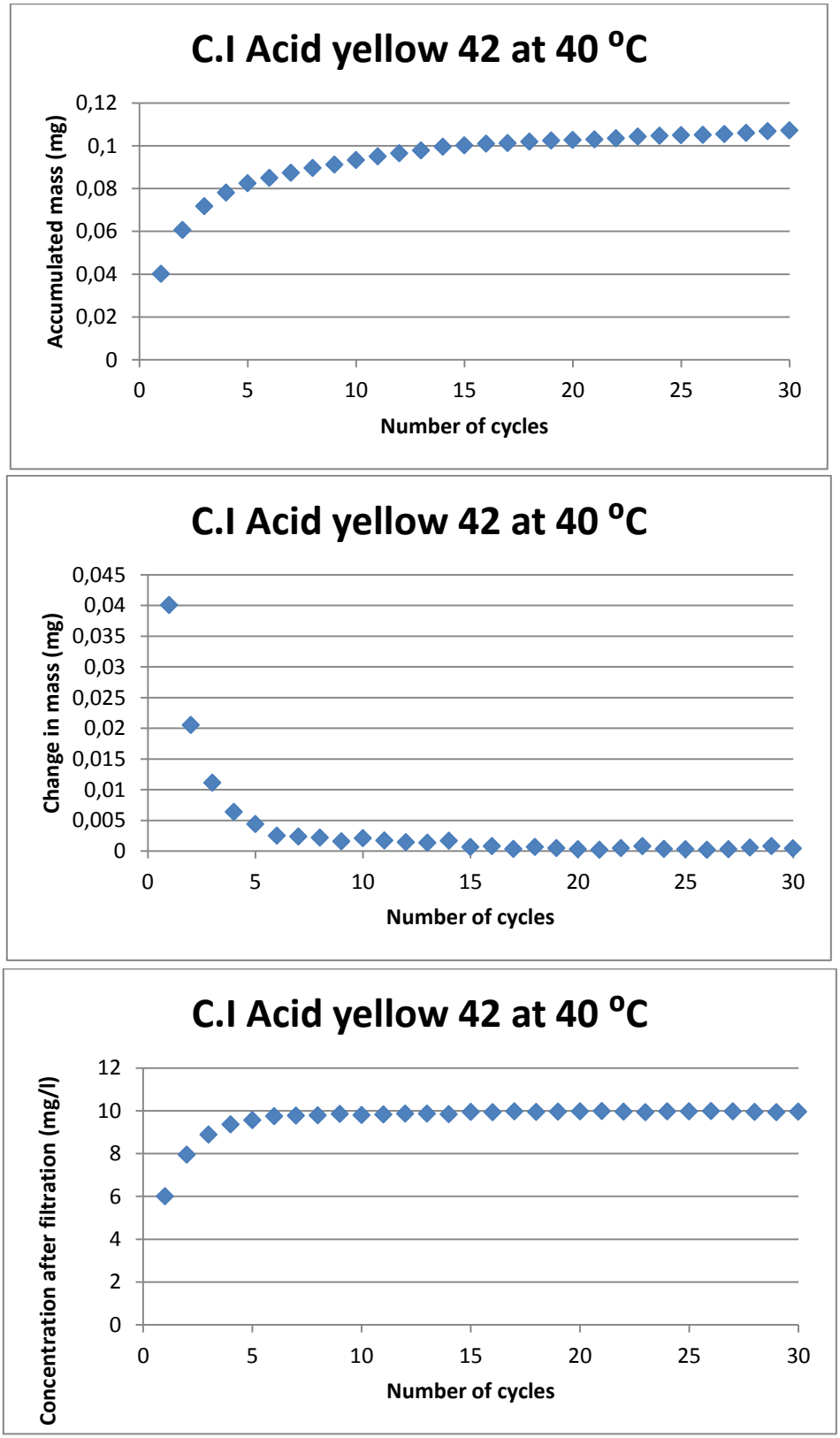

Figure 23.3: Shows the graphical representation of the effects of filtrati

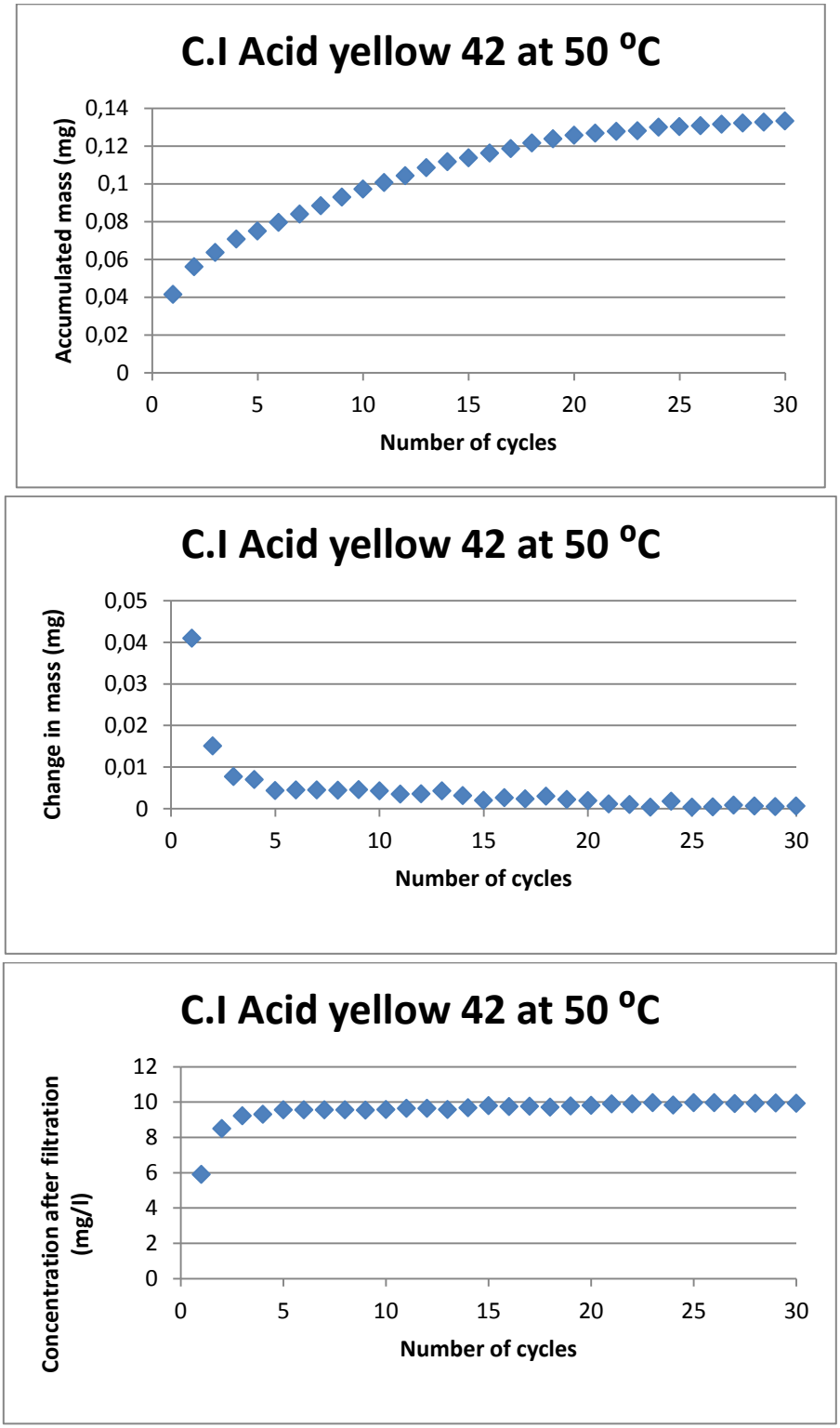

Figure 23.4: Shows the graphical representation of the effects of filtration

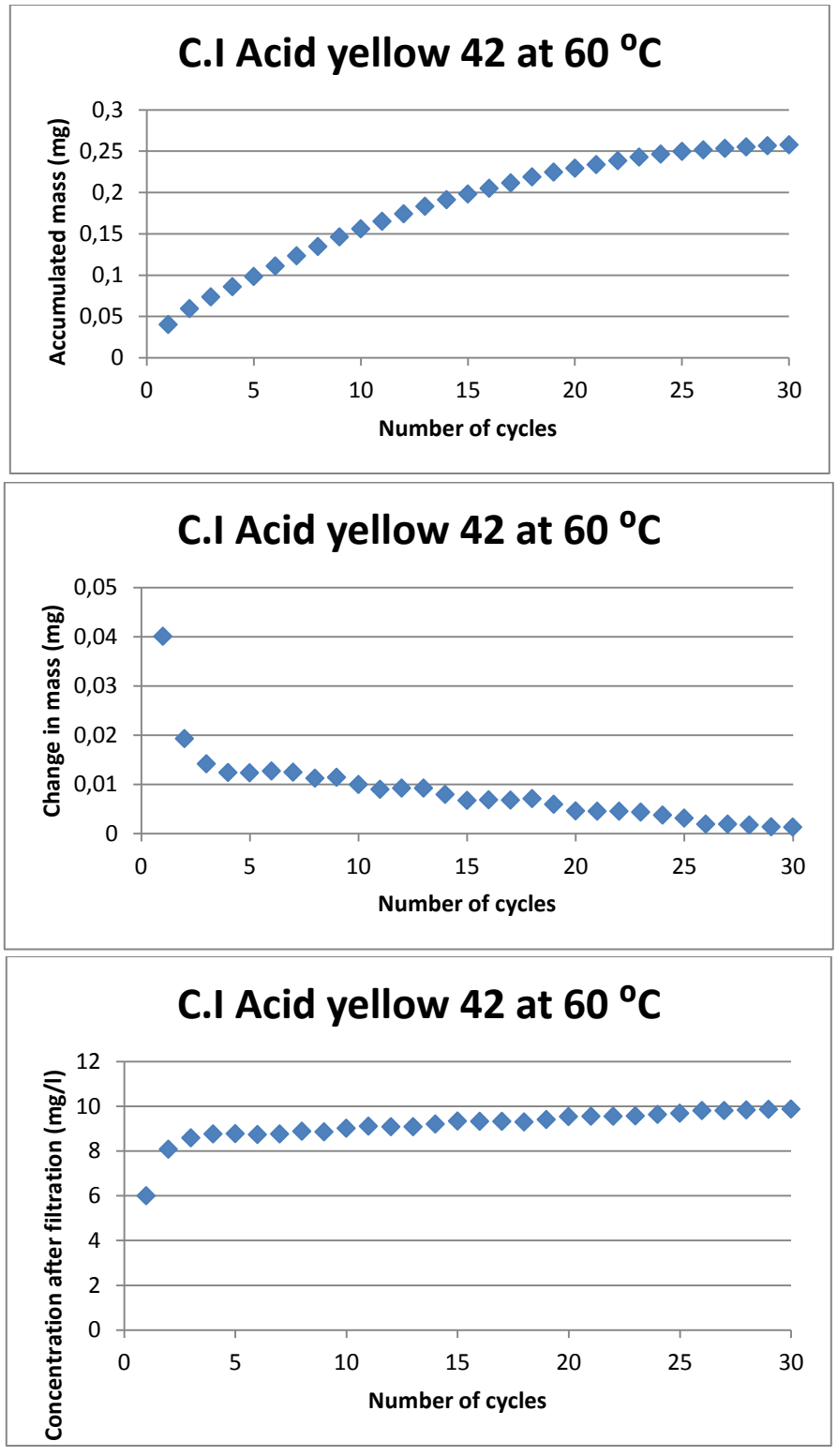

Figure 23.5: Shows the graphical representation of the effects of filtration

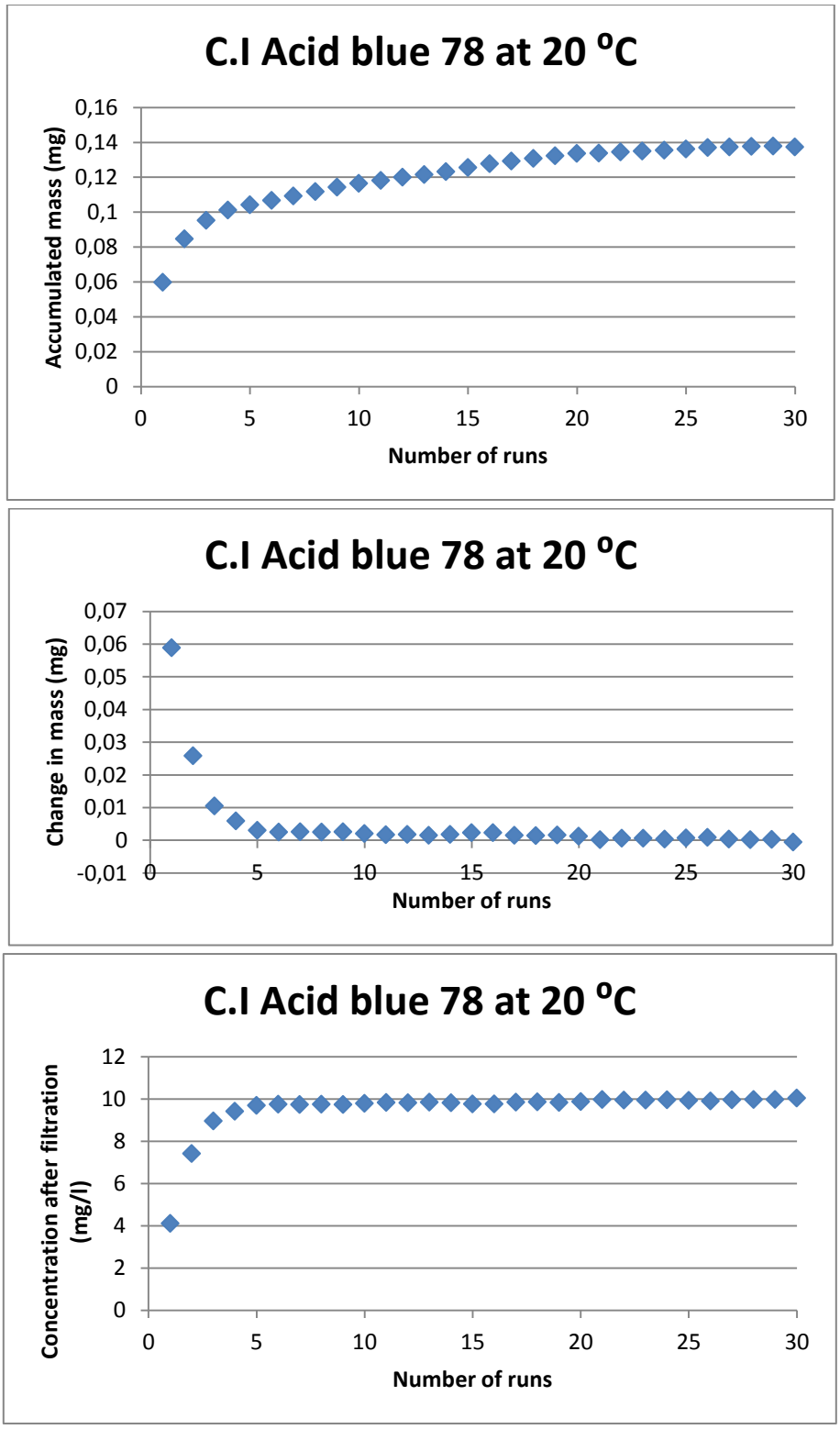

Figure 24.1: Shows the graphical representation of the effects of filtratio

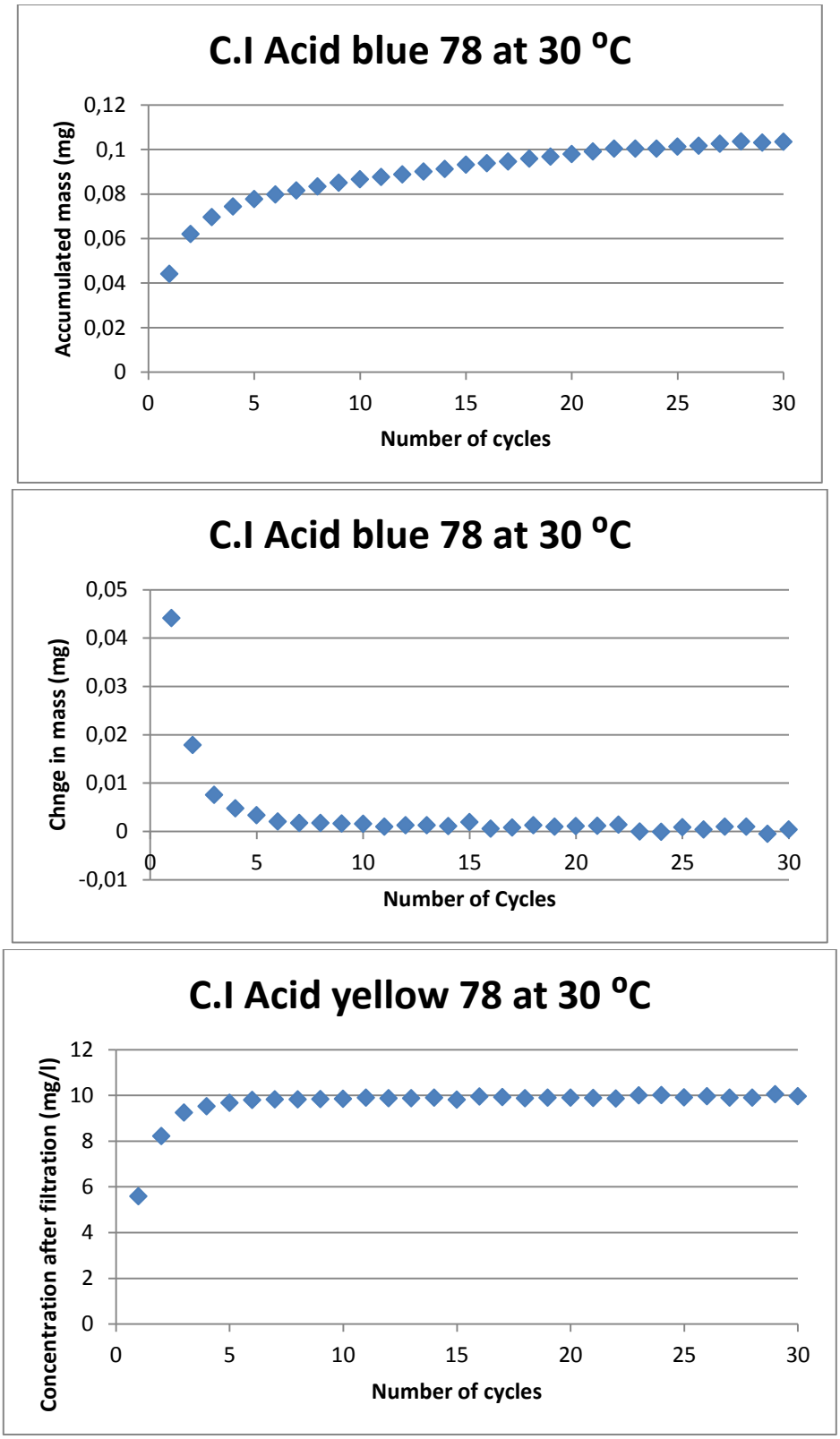

Figure 24.2: Shows the graphical representation of the effects of filtration

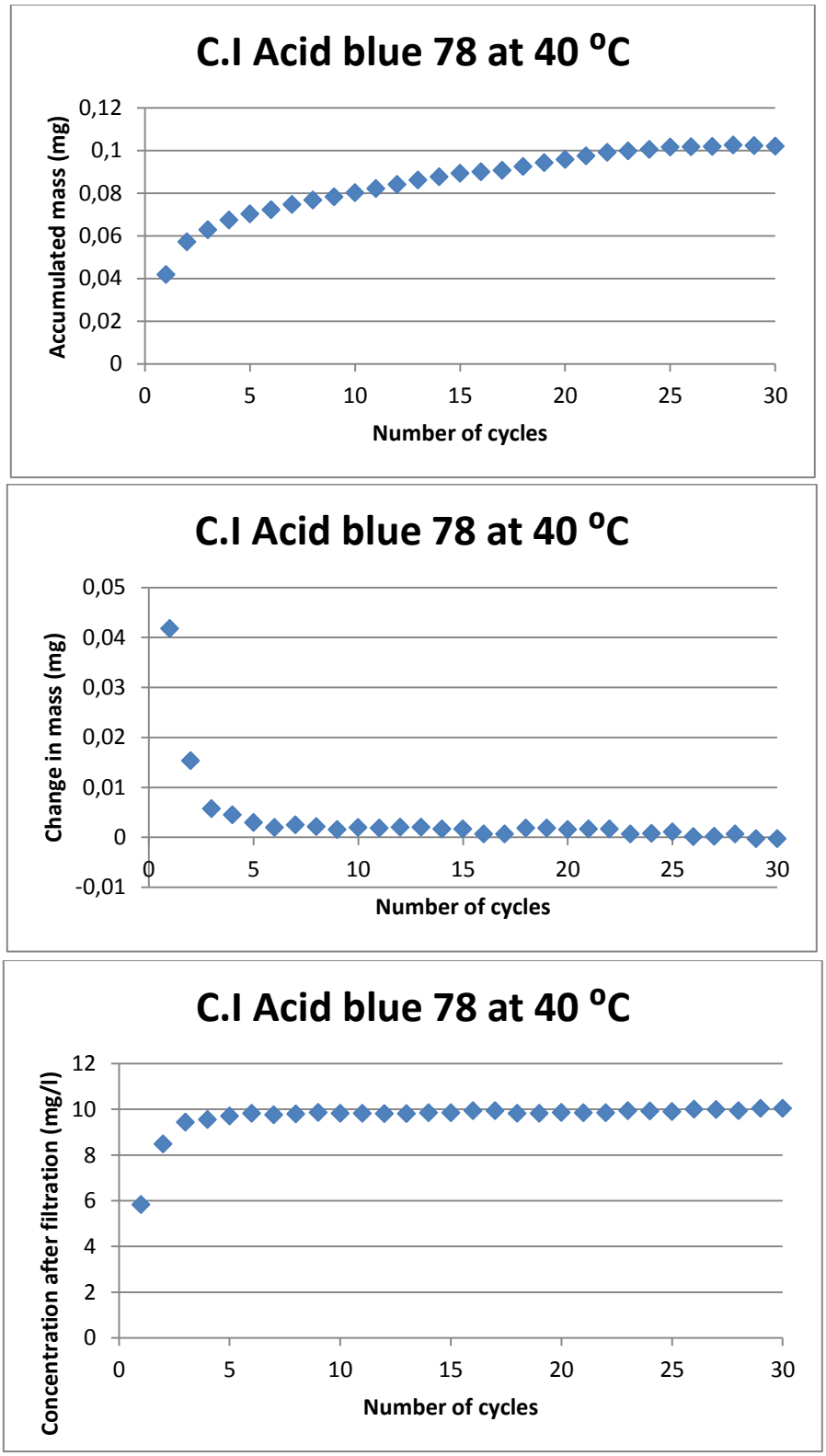

Figure 24.3: Shows the graphical representation of the effects of filtration

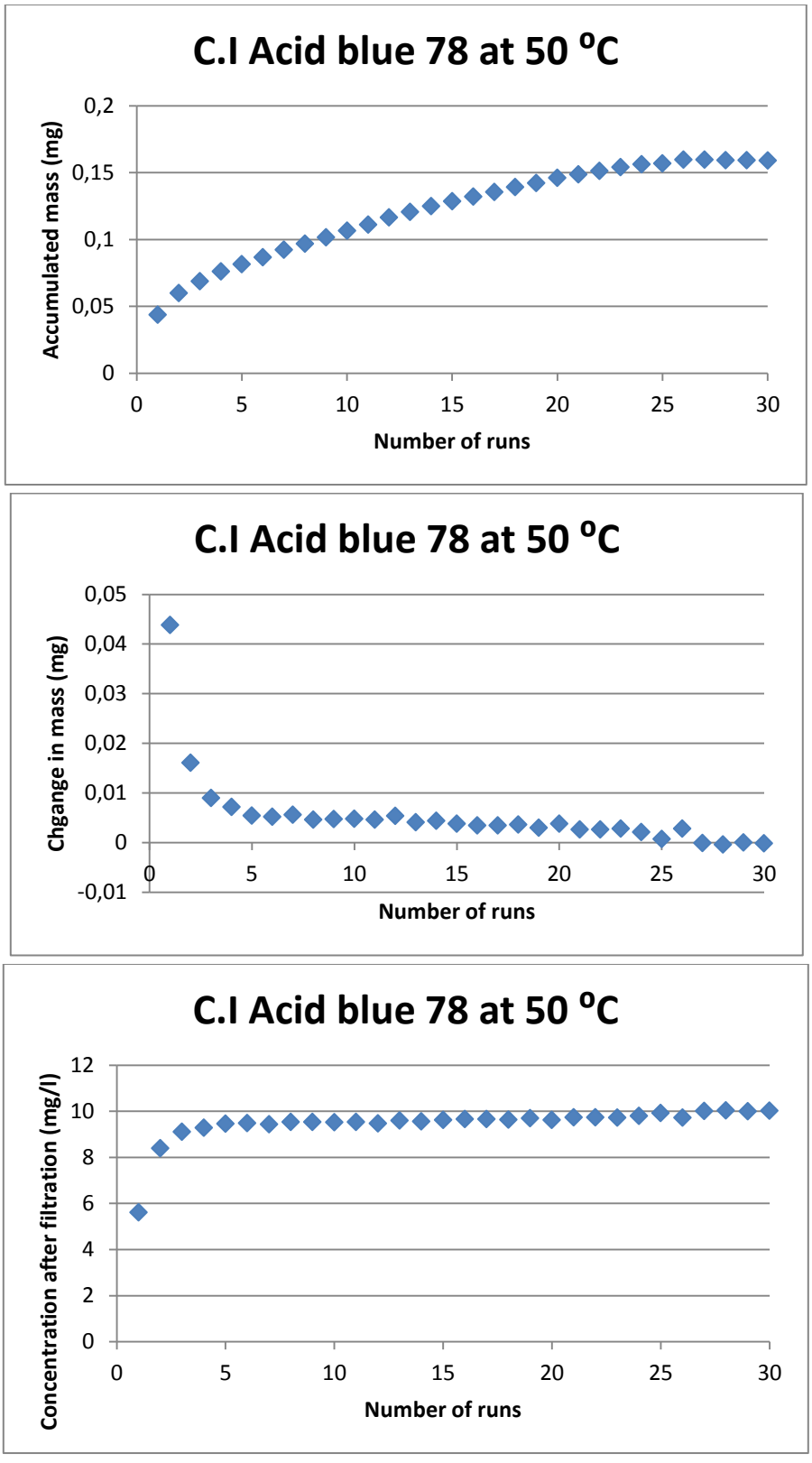

Figure 24.4 : Shows the graphical representation of the effects of filtration

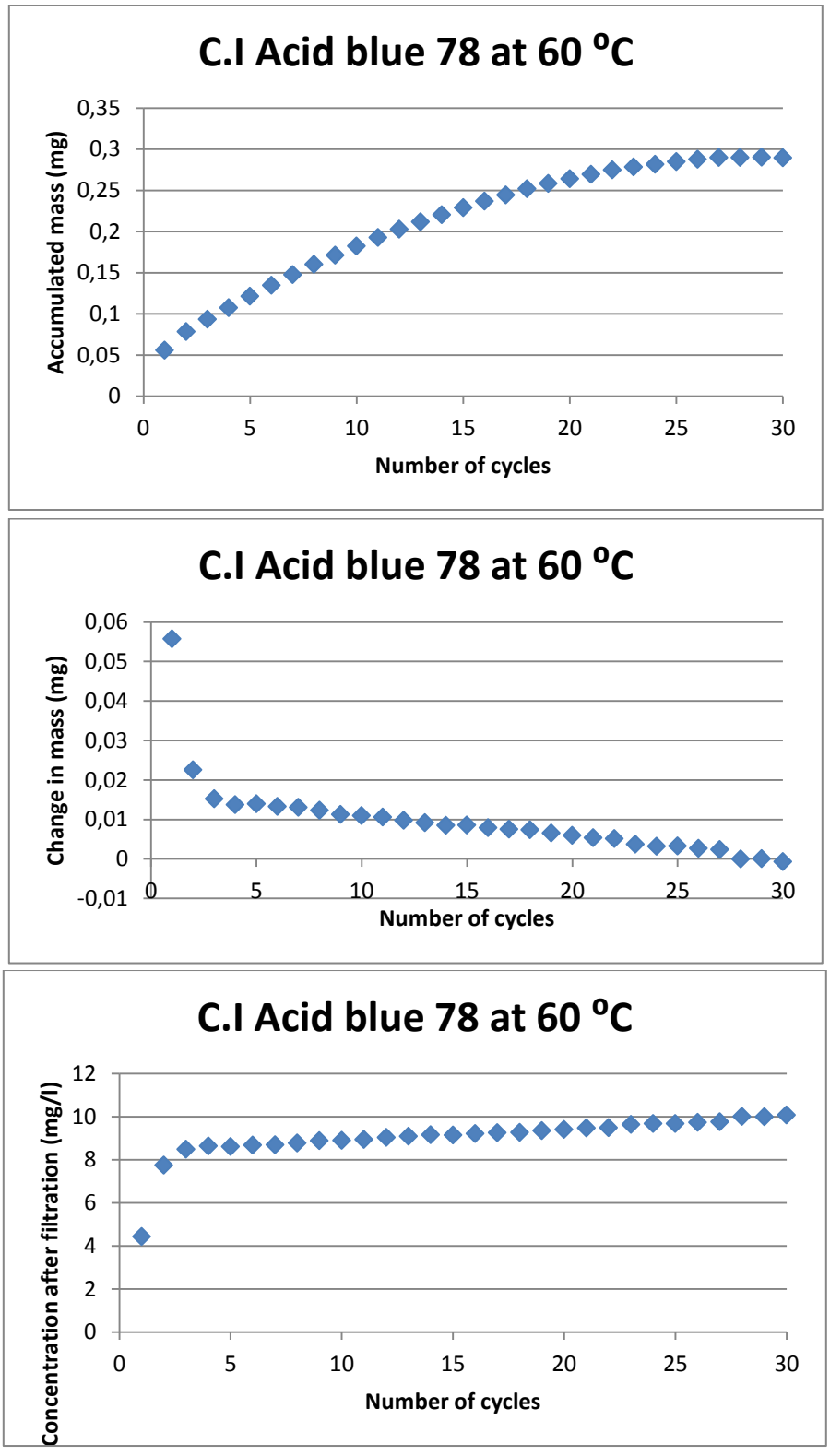

Figure 24.5: Shows the graphical representation of the effects of filtration

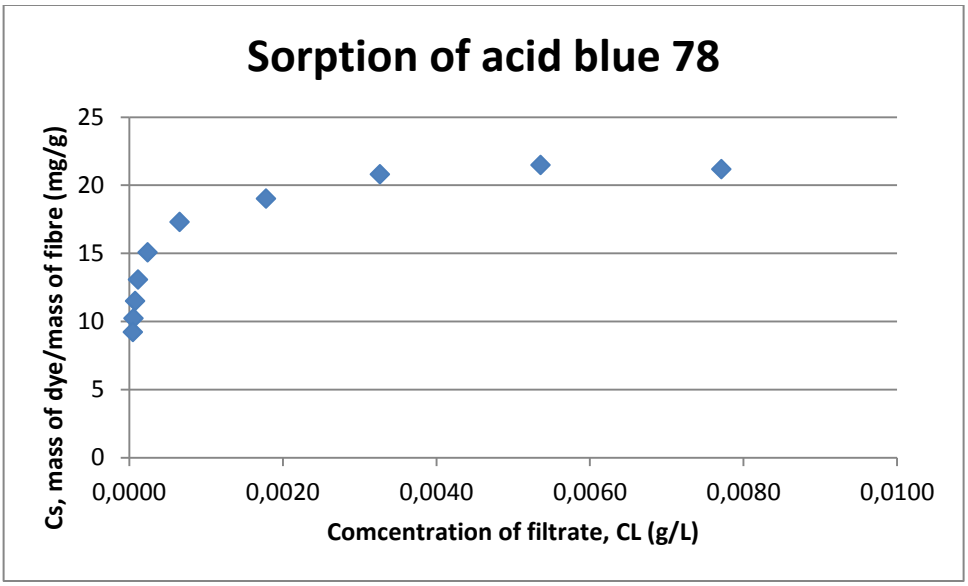

Figure 28: The relationship between sorption capacity (Cs) and the concentration of the filtrate at equilibrium.

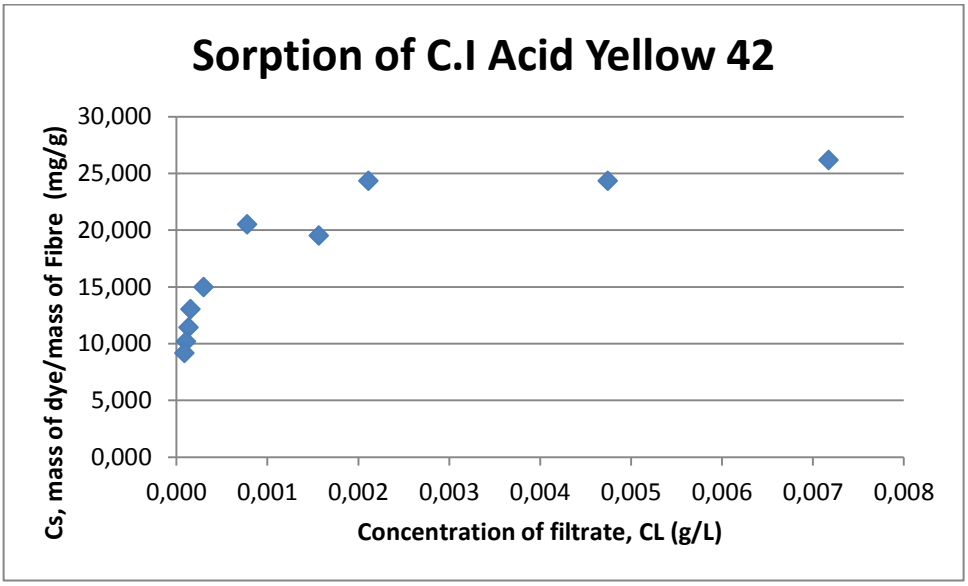

Figure 29: The relationship between sorption capacity (Cs) and the concentration of the filtrate at equilibrium.

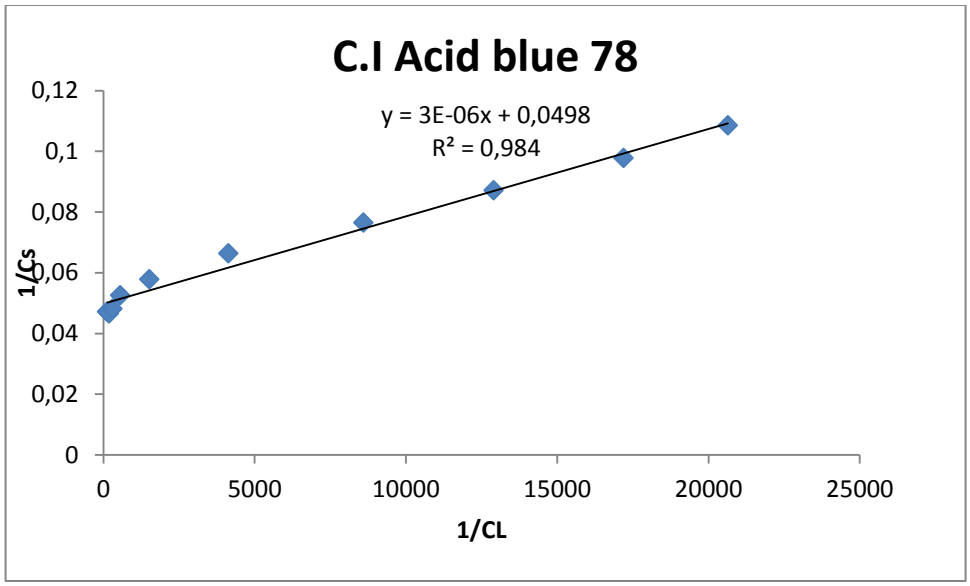

Figure 31: Linear graph used for the determination of constants S and K for Acid Blue 78 used for Langmuir curve.

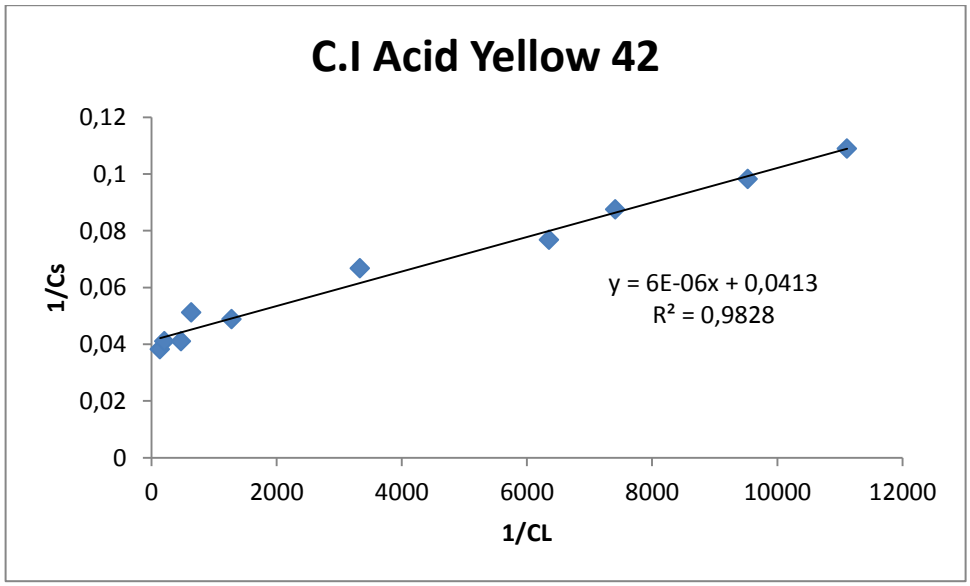

Figure 35: Linear graph used for the determination of constants S and K for Acid Yellow 42 used for Langmuir curve.